

Infocommunications Journal

A PUBLICATION OF THE SCIENTIFIC ASSOCIATION FOR INFOCOMMUNICATIONS (HTE)

December 2015

Volume VII

Number 4

ISSN 2061-2079

SPECIAL ISSUE ON ADVANCED WIRELESS AND MOBILE TECHNOLOGIES AND SERVICES, PART II

Guest Editorial *H. Charaf and S. Imre* 1

PAPERS OF THE SPECIAL ISSUE

Network Coding as a Software *D. Szabó, A. Csoma, P. Megyesi, A. Gulyás, and F. H.P. Fitzek* 2

Increasing energy efficiency in WSNs using wakeup signal length
optimization combined with payload aggregation and FEC
..... *Á. Milánkovich, G. Ill, K. Lendvai, S. Imre and S. Szabó* 12

PAPERS FROM OPEN CALL

Modeling and Simulation of Mode Filtered Radio over
Multimode Fiber Links *T. Cseh and T. Bercei* 20

Fault-Tolerance Algorithm in Wireless Sensor Networks *N. Al-Qadami and A. Koucheryavy* 28

On Measuring the Geographic Diversity of Internet Routes
..... *A. Csoma, A. Gulyás and L. Toka* 34

CALL FOR PAPERS / PARTICIPATION

39th International Conference on Telecommunications and Signal Processing (TSP) –
2016, Vienna, Austria 41

18th International Conference on Speech and Computer – SPECOM 2016, Budapest 42

European Signal Processing Conference – EUSIPCO 2016, Budapest 43

MISCELLANEOUS

Our reviewers in 2015 40

ADDITIONAL

Guidelines for our Authors 44

Technically Co-Sponsored by



Editorial Board

Editor-in-Chief: CSABA A. SZABO, Budapest University of Technology and Economics (BME), Hungary

Associate Editor-in-Chief: ROLLAND VIDA, Budapest University of Technology and Economics (BME), Hungary

- | | |
|---|---|
| ÖZGÜR B. AKAN
Koc University, Istanbul, Turkey | LEVENTE KOVÁCS
Óbuda University, Budapest, Hungary |
| JAVIER ARACIL
Universidad Autónoma de Madrid, Spain | MAJA MATIJASEVIC
University of Zagreb, Croatia |
| LUIGI ATZORI
University of Cagliari, Italy | VACLAV MATYAS
Masaryk University, Brno, Czech Republic |
| LÁSZLÓ BACSÁRDI
University of West Hungary | OSCAR MAYORA
Create-Net, Trento, Italy |
| JÓZSEF BIRÓ
Budapest University of Technology and Economics, Hungary | MIKLÓS MOLNÁR
University of Montpellier, France |
| STEFANO BREGNI
Politecnico di Milano, Italy | SZILVIA NAGY
Széchenyi István University of Győr, Hungary |
| VESNA CRNOJEVIĆ-BENGIN
University of Novi Sad, Serbia | PÉTER ODRY
VTS Subotica, Serbia |
| KÁROLY FARKAS
Budapest University of Technology and Economics, Hungary | JAUELICE DE OLIVEIRA
Drexel University, USA |
| VIKTORIA FODOR
Royal Technical University, Stockholm | MICHAL PIORO
Warsaw University of Technology, Poland |
| EROL GELENBE
Imperial College London, UK | ROBERTO SARACCO
Trento Rise, Italy |
| CHRISTIAN GÜTL
Graz University of Technology, Austria | GHEORGHE SEBESTYÉN
Technical University Cluj-Napoca, Romania |
| ANDRÁS HAJDU
University of Debrecen, Hungary | BURKHARD STILLER
University of Zürich, Switzerland |
| LAJOS HANZO
University of Southampton, UK | LÁSZLÓ ZSOLT SZABÓ
Sapientia University, Tirgu Mures, Romania |
| THOMAS HEISTRACHER
Salzburg University of Applied Sciences, Austria | TAMÁS SZIRÁNYI
Institute for Computer Science and Control, Budapest, Hungary |
| JUKKA HUHTAMÄKI
Tampere University of Technology, Finland | JÁNOS SZTRIK
University of Debrecen, Hungary |
| SÁNDOR IMRE
Budapest University of Technology and Economics, Hungary | DAMLA TURGUT
University of Central Florida, USA |
| ANDRZEJ JAJSZCZYK
AGH University of Science and Technology, Krakow, Poland | ESZTER UDVARY
Budapest University of Technology and Economics, Hungary |
| FRANTISEK JAKAB
Technical University Kosice, Slovakia | SCOTT VALCOURT
University of New Hampshire, USA |
| KLIMO MARTIN
University of Zilina, Slovakia | JINSONG WU
Bell Labs Shanghai, China |
| DUSAN KOCUR
Technical University Kosice, Slovakia | GERGELY ZÁRUBA
University of Texas at Arlington, USA |
| ANDREY KOUCHERYAVY
St. Petersburg State University of Telecommunications, Russia | |

Indexing information

Infocommunications Journal is covered by Inspec, Compendex and Scopus.

Infocommunications Journal

Technically co-sponsored by IEEE Communications Society and IEEE Hungary Section

Supporters

FERENC VÁGUJHELYI – president, National Council for Telecommunications and Informatics (NHIT)

GÁBOR MAGYAR – president, Scientific Association for Infocommunications (HTE)

Editorial Office (Subscription and Advertisements):
Scientific Association for Infocommunications
H-1051 Budapest, Bajcsy-Zsilinszky str. 12, Room: 502
Phone: +36 1 353 1027, Fax: +36 1 353 0451
E-mail: info@hte.hu • Web: www.hte.hu

Articles can be sent also to the following address:
Budapest University of Technology and Economics
Department of Networked Systems and Services
Te l.: +36 1 463 3261, Fax: +36 1 463 3263
E-mail: szabo@hit.bme.hu

Subscription rates for foreign subscribers: 4 issues 50 USD, single copies 15 USD + postage

Publisher: PÉTER NAGY • Manager: ANDRÁS DANKÓ

HU ISSN 2061-2079 • Layout: PLAZMA DS • Printed by: FOM Media

Special Issue on Advanced Wireless and Mobile Technologies and Services/Part II – Guest Editorial

Hassan Charaf and Sándor Imre

We have been witnessing a rapid development of wireless and mobile technologies and services during the past two decades. 4G mobile services are penetrating, mobile access is becoming an increasingly important way for accessing the Internet, and it is expected to become the dominant one. The progress continues as 5G mobile systems are underway. Although many of the new technologies have already been incorporated in practical systems, there is still enough room for research and experimentation, in particular in the areas of cognitive radio, self-organizing networks, M2M communications, or cross-layer optimization, just to name a few.

The 21th European Wireless (EW) Conference was held in Budapest, Hungary, on 22-25 May 2015 and has been organized by the Budapest University of Technology and Economics (BME). On the EW 2015 conference, there were more than **140 participants** from **30 different countries**. Among them 7 papers were selected for the European Wireless Special Issue which consists of two parts. The following 2 papers belong to Part II and are published in this issue while further 5 papers appeared in the 2015/3 issue as Part I.

The first paper focuses on Network Coding (NC) showing great potential in various communication scenarios through changing the packet forwarding principles of current networks. NC can improve not only throughput, latency, reliability and security but also alleviates the need of coordination in many cases. The paper explains how it can improve the performance of the network, provides how Software Defined Networking (SDN) can resolve the crucial problems of deployment and orchestration of NC elements, and finally presents a prototype architecture with measurement results on the performance.

Energy efficiency in wireless sensor networks is vital although there are several possibilities to achieve longer battery life in such devices. Our second paper investigates delaytolerant wireless sensor networks with battery-operated nodes and use data aggregation to lower the size of transmitted data overhead caused by packet headers. The presented results and graphs are based on the investigation of an existing system thus they can be applied to arbitrary packetbased wireless protocols and radio modules supporting wakeup signal listening.

We hope this careful selection will satisfy our readers' expectations and please have a look at Part I of this Special Issue in our No 3, 2015 Issue.



HASSAN CHARAF received his PhD in 1998. He is an Associate Professor and fellow at the Department of Automation and Applied Informatics at the Budapest University of Technology and Economics. He is the head of the IT group. As an outstanding figure in teaching, research and development, he holds key positions at several organizations at the university. His research fields are: distributed systems, cloud computing, multiplatform application development methods, software modeling and data technologies.



SÁNDOR IMRE [M'93] is Professor and Head of Dept. of Networked Systems and Services at the Budapest University of Technology (BME). He obtained his Dr. Univ. degree in probability theory and statistics in 1996, Ph.D. degree in 1999, and D.Sc. degree from the Hungarian Academy of Sciences in 2007. He is Chairman of the Telecommunication Scientific Committee of the Hungarian Academy of Sciences. He participates on the Editorial Board of two journals: Infocommunications Journal and Hungarian Telecommunications. He was invited to join the Mobile Innovation Centre as R&D director in 2005. His research interests include mobile and wireless systems, quantum computing and communications. He has contributions especially on different wireless access technologies, mobility protocols, security and privacy, reconfigurable systems, quantum computing based algorithms and protocols.

Network Coding as a Service

Dávid Szabó¹, Attila Csoma¹, Péter Megyesi¹, András Gulyás^{1 2}, Frank H.P. Fitzek^{3 4}

Abstract—Network Coding (NC) shows great potential in various communication scenarios through changing the packet forwarding principles of current networks. It can improve not only throughput, latency, reliability and security but also alleviates the need of coordination in many cases. However, it is still controversial due to widespread misunderstandings on how to exploit the advantages of it. The aim of the paper is to facilitate the usage of NC by (i) explaining how it can improve the performance of the network (regardless the existence of any butterfly in the network), (ii) showing how Software Defined Networking (SDN) can resolve the crucial problems of deployment and orchestration of NC elements, and (iii) providing a prototype architecture with measurement results on the performance of our network coding capable software router implementation compared by fountain codes.

Index Terms—Network Coding; SDN; Click; VNF

I. INTRODUCTION

According to the traditional concept of packet switched networks independent data flows may share network devices but the information itself remains separated. NC breaks up this principle as it treats these flows as algebraically combinable information, thereby when two flows f_1, f_2 enter a node Kirchoff’s law doesn’t hold any more; the output appears not as $f_1 + f_2$ but $F(f_1, f_2)$.

In the seminal paper [1] Ahlswede et al. show a butterfly topology for illustrating that even a simple bitwise XOR, i.e. $F(f_1, f_2) = f_1 \text{ XOR } f_2$, used at the proper node of the network can lead to a considerable throughput gain. Unfortunately this nice example also caused confusion as many people mistakenly think that NC can only be used in such a far-fetched, artificial situation. This misunderstanding often appears in literature [2] and overshadows its intense evolution during the last decade.

Nowadays NC is not only about butterflies and XOR operations but instead creating linear combinations in a distributed way using random number generators, known as “random linear network code” (RLNC) [3]. RLNC also introduces *recoding*, i.e. to recombine the flows without first decoding them thus fundamentally changes nodes’ behaviour since it replaces the *store-and-forward* approach with *compute-and-forward*. This is ground breaking to all other coding strategies that are only end-to-end based (Reed-Solomon, Raptor, etc.)

and leads to gain not only for throughput, but for latency, security and complexity as well, furthermore it is feasible for any topology.

However, for the efficient use of RLNC we have to deploy *encoder*, *decoder* and *recoder* elements in the network and we have to take care of steering the traffic properly over them. At this point Software Defined Networking with Network Function Virtualization (NFV) can be the “door opener” technologies for RLNC, since they enable to implement RLNC specific features as Virtualized Network Functions (VNFs) [4] that can be connected, or chained, to create communication services. These VNFs then can easily be orchestrated by the control layer of SDN.

The integration of network coding into SDN has already been proposed. [5] and [6] discuss the possibilities of using XOR type network coding through the extension of OpenFlow protocol [7] and functions of switches. In [8] authors investigate the delay bounds in survivable routing with network coding in SDN. In this paper we extend our prior works [9], [10] that is orthogonal to the aforementioned ones as we investigate the usability of RLNC through NFV in SDNs, that doesn’t require to modify existing devices or protocols (e.g. OpenFlow), and also provide a proof of concept.

In the following we give an overview about RLNC and also highlight its features that make it fundamentally different from the generally used block codes (Section II), then we describe our SDN prototype architecture - with implementation details - that enables the definition, configuration and automated deployment of RLNC specific VNFs (Section III), finally we provide an extensive comparison about the performance of RLNC and block codes with analytical and measurement results side-by-side (Section IV). Section V concludes the paper with future work.

II. RANDOM LINEAR NETWORK CODING

A. Fundamentals

RLNC treats data in the form of generations and symbols. A symbol \vec{s} is a vector of Galois Field (GF) elements that represent some data depending on the number of elements n and the size of the GF f according to $|\vec{s}| = n \cdot \log_2(f)$ [byte]. For example 8 elements in GF(2) can represent 1 byte. A generation G comprises g symbols of size $|\vec{s}|$, so it can represent $g \cdot |\vec{s}|$ bytes of data and it is arranged into a matrix $\mathbf{M} = [s_1^T, s_2^T, \dots, s_g^T]$.

In order to create a coded symbol \vec{s}_c a coding vector \vec{v} is required, that contains a coefficient – which is an element of GF – for each symbol in the generation. To encode a new symbol \vec{s}_c from a generation at the source \mathbf{M} is multiplied with a randomly generated coding vector \vec{v} of length g , $\vec{s}_c = \mathbf{M} \cdot \vec{v}^T$.

Manuscript received: August 27, 2015. Revised: November 23, 2015.

¹Budapest University of Technology and Economics, Hungary

¹HSNLab, Dept. of Telecommunications and Media Informatics

²MTA-BME Information systems research group

³Technische Universität Dresden, Germany

⁴5G Lab Germany

Email: {szabod,csoma,megyesi,gulyas}@tmit.bme.hu
frank.fitzek@tu-dresden.de

In this way we can produce $g+e$ coded symbols, where $e \in \mathbb{Z}$ is the number of extra symbols as RLNC is a rate-less code.

When a coded symbol is transmitted on the network it is accompanied by its coding vector, and together they form a coded packet $p_c = \{\vec{v}, \vec{s}_c\}$. In order to successfully decode a generation the decoder has to receive g linearly independent symbols and coding vectors from that generation. All received symbols are placed in the matrix $\mathbf{S}_c = [\vec{s}_{c1}^\top, \vec{s}_{c2}^\top, \dots, \vec{s}_{cg}^\top]$ and all coding vectors are placed in the matrix $\mathbf{V} = [\vec{v}_1^\top, \vec{v}_2^\top, \dots, \vec{v}_g^\top]$. The original data then can be decoded as $\mathbf{M} = \mathbf{S}_c \cdot \mathbf{V}^{-1}$.

In practice approximately any g coded symbols are enough for a successful decoding of generation G . Certainly it is possible to receive a linearly dependent symbol but the chances of this is negligible by using at least GF(8), furthermore, sending another randomly coded symbol is a much looser constraint compared to when no coding is used, where exactly all g unique, original symbols have to be collected.

However, the most important feature of RLNC is recoding. Any node that received at least $g' \in [2, g]$ linearly independent symbols from a generation and its rank is equal to the rank of \mathbf{V} , can recode. All received symbols are placed in the matrix $\mathbf{S}_c = [\vec{s}_{c1}^\top, \vec{s}_{c2}^\top, \dots, \vec{s}_{cg'}^\top]$ and all coding vectors in the matrix $\mathbf{V} = [\vec{v}_1^\top, \vec{v}_2^\top, \dots, \vec{v}_{g'}^\top]$. To recode a symbol these matrices are multiplied with a randomly generated vector \vec{w} of length g' , $\vec{v} = \mathbf{V} \cdot \vec{w}^\top$, $\vec{s}_c = \mathbf{S}_c \cdot \vec{w}^\top$. In practice this means that a node that have received more than one symbol can recombine those symbols into recoded symbols, similar to the way coded symbols are constructed at the source, but without having to wait for the whole generation. In other words, a node can change its behaviour from *store-and-forward* to *compute-and-forward*.

B. Insights of the benefits of RLNC

In order to shed some more light on this conceptual change we take a closer look on three different coding schemes that are carried out on a *single path - multihop* channel. This restriction may seem strange at first glance but we have two good reasons for doing this: (i) packet forwarding on the Internet is mostly carried out in this way, and (ii) we would like to dispel the common misunderstanding that NC cannot be used in any other case than multicast.

Accordingly we assume an encoder E that delivers a message comprises G packets to a decoder D . Along the path packets forwarded by multiple relay nodes (X s) and we also assume error prone links with loss probability $0 \leq \epsilon \leq 1$ (Fig. 1). We consider the following three cases:

Block codes in end-to-end manner (E2E): In this scheme encoding and decoding are performed only once by E and D , respectively. The relay nodes only *store-and-forward* each successfully received packet, implying that E should emit enough amount of extra packets for the whole channel to compensate the loss and to make sure that D can reconstruct the message (Fig. 1a). This eventuates unnecessary traffic loads on the links closer to E , which is particularly painful when losses occur only on links far from E , and also increase latency.

Block codes in hop-by-hop manner (HbH): In this scheme we assume that relay nodes can also perform encoding and decoding that enables to generate extra packets per hop in a distributed way (Fig. 1b). This unburdens the network from the unnecessary packets but also infuse extra latency as every relay has to wait to start encoding until the full message is decoded.

Random Linear Network Coding: RLNC enables for relays to perform recoding, that is to create a coded packet from the received ones without decoding them first (Fig. 1c). This is far less complex than decode/encode procedure, hence eventuates immediate forwarding, furthermore, it is completely transparent, so decoding doesn't require extra effort. This greatly reduces latency and as it is carried out per hop requires the same number of packets as the HbH scheme. However, in order to use RLNC efficiently, first we have to deploy elements with *encoding*, *decoding* and *recoding* capabilities and we have to take care of steering the traffic over them.

In Section IV we provide an extensive comparison of RLNC and block codes supported both analytical and measurement results, but as the measurements were carried out on our SDN architecture first we show how SDN and virtualization can facilitate the integration process of RLNC in a seamless way.

III. SDN PROTOTYPE ARCHITECTURE

Here we give a brief introduction about SDN and Network Function Virtualization (NFV), followed by the implementation details of RLNC capable elements, finally we introduce the architecture which enables the definition, configuration and automated deployment of these novel elements implementing code centric operation in the network.

A. SDN and virtualization

The basic concept of SDN is to enable network innovation - realizing new capabilities and addressing persistent problems with networking -, which is almost impossible nowadays. The problem lies in the distributed and heterogen nature of current networks. There are closed, vendor specific hardwares, softwares and firmwares across the network managed by distributed control functions through different interfaces. This leads to difficult and extensive design and operation.

SDN aims to change this by creating well defined abstractions of different network layers, that each has its proper functionality and interfaces. In this sense the idea is somewhat similar to the ISO/OSI conception, but instead of individual devices it concerns the network as a whole with the following features: (i) maintains the separation of the data and control planes, (ii) uses uniform vendor-agnostic interface – one of the most commonly used is OpenFlow [7] – between control and data planes, (iii) treats the control plane in a logically, centralized way that is realized using a network operating system that constructs and presents a logical map of the entire network to services or control applications implemented on top of it, and (iv) slices and virtualises the underlying physical network.

During its two decades evolution [11] the concept of SDN inspired several novel technologies and turned out that it

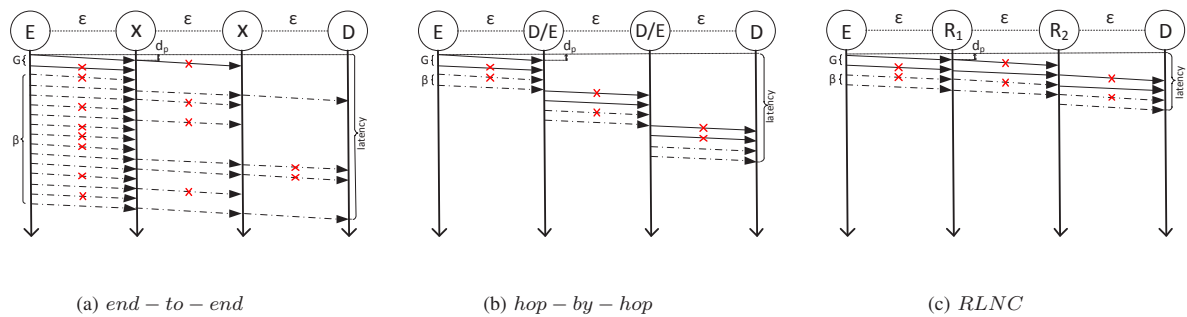


Fig. 1: Illustration of *end-to-end*, *hop-by-hop* and *RLNC* coding schemes for sending a message of 2 packets (G) through three hops with 50% probability loss on each link ($\varepsilon = 0.5$). β stands for redundancy (700%, 50% and 50% for E2E, HbH and RLNC, respectively) and d_p for propagation delay.

synergizes well with many existing ones. One that really shines out amongst them is Network Function Virtualization (NFV). NFV enables to implement any hardware middleboxes (a network device that manipulates traffic, e.g. firewall, network address translator, etc.) into software by creating Virtualized Network Functions (VNFs). These VNFs has exactly the same functionality but they don't require specific hardware and hundreds of them can be installed - even remotely - on a single device. This offers nice synergy with SDN as the control layer is capable to orchestrate the installation, configuration and traffic steering over VNFs in an automated way.

Such orchestration and steering is in perfect agreement with the current practice of Internet Service Providers (ISPs) that services are implemented in the form of appropriately concatenated middleboxes, also known as *service chains* [12]. However, today's service chains are usually built around special purpose networking hardware elements, configuring and operating these chains is a highly non-trivial task which still requires human interaction. SDN and virtualization can be a promising way out of this managerial trap as they enable flexible and automated deployment of service chains comprising our RLNC capable VNFs.

B. Implementation of RLNC Software Router Prototype

Since VNFs are run on NFV platforms the first design step is to choose one from the many existing ones ([13],[14],[15],[16]). Our design choice was ClickOS [17], as ClickOS virtual machines are extremely small (5 Mb), can boot very quickly (about 30 ms), add small delay (around 45 μ s) and hundreds of them can run concurrently with a throughput around 10 Gb/s. ClickOS requires VNFs created by the Click modular router platform [18], which enables to build custom routers by creating configurations pieced together from built-in or own-developed elements that implement atomic functionality like packet classifying, scheduling, queuing etc. Using the Kodo [19] network coding software library we have developed the RLNC encoder, recoder and decoder Click elements and using built-in modules we have created fully-fledged compute and forward software routers.

The Click interpreter reads configurations written in a Click-specific language. These config files describe a directed graph with *elements* at vertices and *edges* specifying possible paths

for the packets within the router. The behaviour of the elements are given by C++ code. At the code level each element is a subclass of the *Element* class, which has around 20 virtual functions and most subclasses have to override only up to six of them. The most simple subclass implementation, the *NullElement*, contains only 8 lines of code and overrides five *Element* class functions. Similarly, we have implemented our code-centric elements which encode, recode and decode the incoming packets using Kodo.

Kodo offers a number of different erasure correcting codes of which we chose Full Random Linear Network Code (Full RLNC), as it is one of the most common RLNC variants and provides several of the advantages that RLNCs have over traditional erasure correcting codes. Accordingly our three custom Click elements are *FullRLNCEncoder*, *FullRLNCDecoder* and *FullRLNCRecoder*. All of them take around 120-150 lines of C++ code (with no particular optimization) and override seven virtual functions of the *Element* class. They have one input and one output port and the coding parameters can be tuned through input arguments: *SYMBOLS*, *SYMBOL_SIZE*, *GF_SIZE*, *EXTRA*. The *SYMBOLS* argument stands for the generation size and tells the maximal number of symbols that can be combined into a coded symbol by the encoder. Increasing the generation size also increases the decoding delay, since the decoder has to receive at least *SYMBOLS* number of packets to be able to decode the whole generation. *SYMBOL_SIZE* represents the size of each symbol in bytes. Increasing this eventuates increased coding complexity. So the *SYMBOLS*SYMBOL_SIZE* product should be considered carefully and large data typically sent through multiple generations. The *GF_SIZE* argument stands for the size of the Galois Field, which has influence on the probability that an encoded packet doesn't carry any useful information. Finally the *EXTRA* parameter represents the ratio of redundancy, in other words tells how many extra packet should be generated. This parameter is required only for the encoder and the recoder.

Since other built-in Click elements can preprocess UDP¹ packets (i.e. strip IP and UDP headers) the general behaviour of our code-centric elements is quite simple: After a packet

¹Our current implementation can process UDP packets only. The handling of TCP flows is in our future work list.

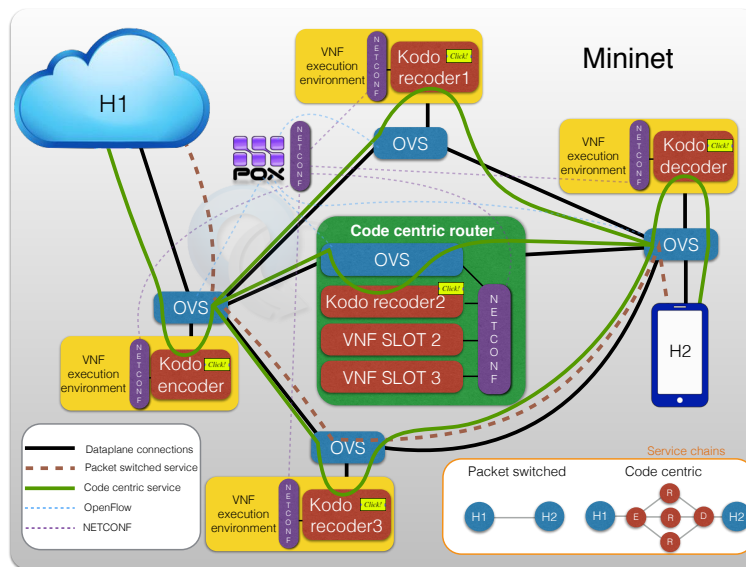


Fig. 2: The prototype architecture.

arrives extract the payload, encode/decode/decode it by calling the proper functions of Kodo, update IP and UDP headers (size and checksum fields as we slightly increase the packet size by adding the coding coefficients) and forward the packet. In this way our router configurations implement the compute and forward router as a VNF that performs code-centric operations on the packet going through and can easily be deployed into SDN environment.

C. Architecture

For showing the seamless integration of network coding and SDN we have built a prototype of the code centric network architecture. In a real network it would be a practical choice for operators to place NC encoder and decoder elements as close to the edge of the network as possible, while recoders operate in the most efficient way at intermediate nodes where they can aggregate traffic flows. To test our proof-of-concept we created a smaller network to model a similar topology where every packet between two users traverses an encoder a recoder and a decoder (in this order). To simulate such network we implemented our architecture in the ESCAPE prototyping environment. Well detailed description about it can be found in [20], however, here we recollect the most important information of the components.

ESCAPE is capable to simulate OpenFlow networks combining Mininet network virtualizer [21] using Open vSwitch (OVS) [22] instances and a POX network control prototyping software [23], which contains a steering module handling the flow tables according to the configuration of the running service chains. ESCAPE is designed in such way that it can initiate Mininet virtual containers which capable to run binaries or source codes written in Click language. To use these containers as VNFs ESCAPE configure OVS elements with POX in such way that all traffic between end users traverse them. Typically after an initial deployment process OVS configuration remains the same during the simulation. Since

the controller can automatically deploy VNFs implemented in Click and our software router in Sec. III-B is implemented in the Click platform too, our work here was to translate our Click configurations according to the templates used by ESCAPE and install all software required to run ESCAPE and Kodo. Note that the traffic steering in a real network with multiple users, diverse requirements and huge amount of independent flows raises several open questions. However, in this paper we restricted ourselves only to provide a proof of concept implementation which requires a minimalistic network with a few traffic flows.

Fig. 2 presents a scenario of our code-centric prototype. We build an OpenFlow 1.0 network of three Open vSwitch instances (OVS), two hosts (H1/H2) and three VNF containers. These containers (yellow boxes) are advanced Mininet hosts which can start a given VNF process. This solution stands for the case when we run VNFs outside the routers e.g. in a near OpenStack [24] data center. In these containers we deployed our compute and forward software router configured to encode/recode/decode packets similarly to our scenarios in Fig. 1 for implementing our coding schemes (E2E, HbH and RLNC). This solution may slightly increase latency but provides the possibility of scaling out in the presence of massive network loads combined with more complex coding schemes (e.g. more efficient random linear codes using larger GF field size).

Alternatively, we have also built a visionary prototype of the code centric router (green box). This router consists of a standard OVS (no modifications in OpenFlow) instance but has the capability to execute VNFs. Using code centric routers adds less delay but there is no way to scale out beyond the router’s hardware resources. The POX orchestrator module receives service chains as inputs (can be given by GUI), configure the switches and start the appropriate VNFs accordingly.

IV. COMPARING RLNC WITH BLOCK CODES

A comprehensive analysis can be found in [25] and [26] about the performance of difference coding schemes including complexity, delay, memory requirement, achievable rate, and adaptability. However, in order to facilitate understanding we recall the most important claims on the number of sent packets and latency adjusted to the communication scenarios described in Section II-B and provide measurements results for a wide range of parameter settings side-by-side.

For the measurements we realized all the three scenarios as service chains in our prototype architecture and besides the properties of the links (erasure probability and bitrate) we varied the number of hops, packet size and coding generation as well (Table I).

Parameter	Values
erasure probability ϵ	10%, 20%, 30%, 40%, 50%
packet size L	250 B, 500 B, 750 B, 1000 B, 1450 B
generation size G	16, 32, 64, 128
number of hops H	2, 3, 4, 5, 6, 7
channel rate	0.25, 0.5, 1, 2, 4, 8 Mbps

TABLE I: The parameter set for the measurements.

During the analysis we assume a *single path - multihop* channel (described in Section II), where the encoder E delivers a message of G packets through H number of links to a decoder D , we also assume error prone links with loss probability $0 \leq \epsilon \leq 1$.

A. Number of Sent Packets

Now we calculate the overall number of sent packets required D to successfully decode the message. In the case of E2E this is the sum of packets sent per hop - comprises extra packets for compensating losses - on the rest of the channel, which depends on generation size G , number of hops H and loss probability ϵ :

$$P_{E2E} = \sum_{h=1}^H G \prod_{i=h}^H \frac{1}{1 - \epsilon_i} \quad (1)$$

For HbH and RLNC it is again the sum of the packets sent individually but here losses have only local impact due to the decode/encode procedure carried out at each hop:

$$P_{HbH} = P_{RLNC} = G \cdot \sum_{i=h}^H \frac{1}{1 - \epsilon_i} \quad (2)$$

In Fig. 3 the number of overall packets conveyed in a three hop communication network versus the erasure probability per link for the three forwarding schemes is given for the theoretical (indicated by (T) in the figure) and for the measurement results. The figure show that the results of the theory and measurements are consistent with each other. HbH and RLNC use the same amount of packets, and while they increase the number of packets linearly with the loss probability, the E2E approach increases exponentially.

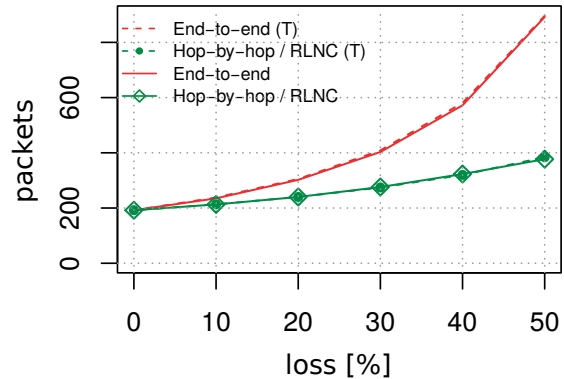


Fig. 3: Number of overall packets conveyed in the network versus channel loss probability (Packets 64 - Size 250 B - Hops 3)

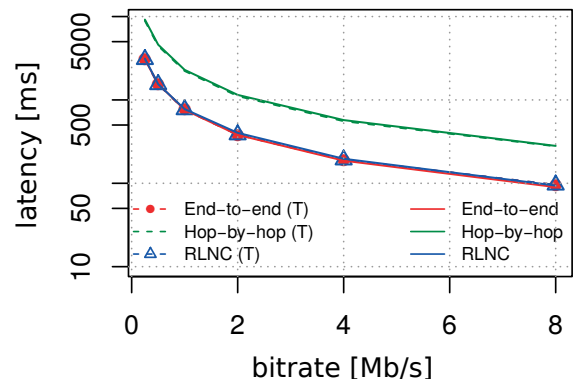


Fig. 4: Latency in the network versus channel rate for three coding approaches and no losses (Packets 64 - Size 1450 B - Loss 0% - Hops 3)

B. Latency

Based on packet numbers we can calculate the time required for decoding the message successfully. In other words, we are interested in the time that takes to deliver all packets of G from E to D and we also calculate with an inter packet time τ_P which is the multiplicative inverse of the packet sending rate and link delay τ_L that each packet suffers during forwarding (we assume the same delay for every H links).

In the case of E2E this is the sum of packets emitted at first hop - comprises extra packets as well - and an extra delay per hop (since packets are forwarded immediately and in parallel at each hop):

$$D_{E2E} = G \cdot \prod_{i=1}^H \frac{1}{1 - \epsilon_i} \cdot \tau_P + H \cdot \tau_L \quad (3)$$

For HbH this is the time for the first hop multiplied by the number of hops as every node has to perform decoding/encoding before forwarding even the first packet:

$$D_{HbH} = G \cdot \tau_P \cdot \sum_{i=1}^H \frac{1}{1 - \epsilon_i} + H \cdot \tau_L \quad (4)$$

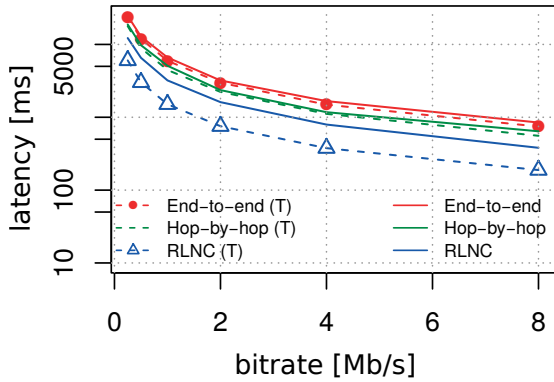


Fig. 5: Latency in the network versus channel rate for three coding approaches and high losses (Packets 64 - Size 1450 B - Loss 50% - Hops 3)

The case of RLNC scheme comprises the best part from both E2E and HbH, since packets are forwarded immediately and in parallel with the same number of packets per hop as in HbH:

$$D_{RLNC} = G \cdot \tau_P \cdot \frac{1}{1 - \max_{1 \leq i \leq H} \epsilon_i} + H \cdot \tau_L \quad (5)$$

Fig. 4 presents the latency in a three hop communication network versus channel rate without any losses for the three coding approaches. If there are no losses E2E and RLNC have the same latency values (since no extra packets are required to send, which would slow E2E), while the HbH ends up in higher latency values because each intermediate node needs to wait for all packet of G . The gain of RLNC over HbH remains constant for the higher values which means that the ratio of latency is independent from the bandwidth. Roughly, the ratio of the gain in latency equals to H , when G is significantly higher than H .

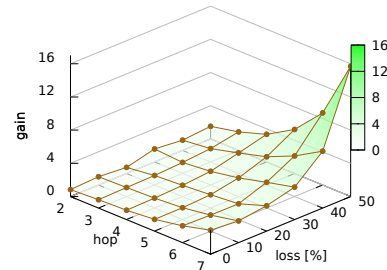
The latency results change a lot if the channel is error prone as given in Fig. 5 with an error probability of 50%. Now the advantage of RLNC over the other two schemes becomes evident and E2E is now even worse than HbH. After having a look again at Fig. 1 this is not so surprising, since E2E have to send through all redundancy on the whole channel. While HbH can unburden the network, as redundancy have to be

sent per hop, there the *store and forward* behaviour increases latency.

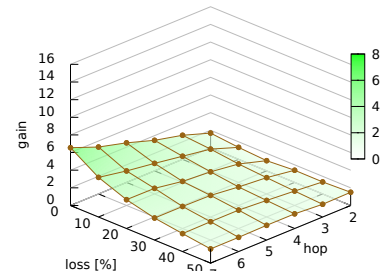
However, in Fig. 5 it can be observed that while measurement follows theory well for E2E and HbH we got much higher values for RLNC. In [25] authors already proved that in the case of a two-hop network with identical links the delay function grows as \sqrt{n} thus it does not follows the original formula in Eq. 5. We investigated this phenomenon further and discuss the reasons in Appendix A. Suffice it to say for now that RLNC performs a bit worse as theory would suggest when the error probabilities of the links are similar.

In the followings we extend the measurements for a wide variation of parameters and based on the fact that RLNC performs worse than expected when error probabilities are close to each other we set the values accordingly in order to show that even in this case RLNC outperforms the other coding schemes.

In Fig. 6 latency for the three transmission schemes depend-

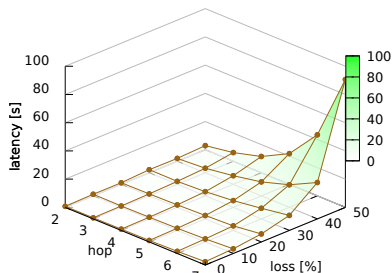


(a) Gain of RLNC over E2E

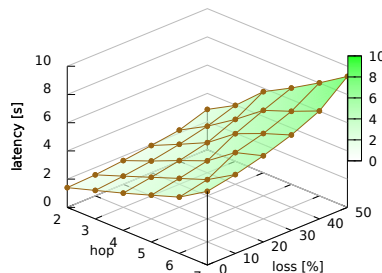


(b) Gain of RLNC over HbH

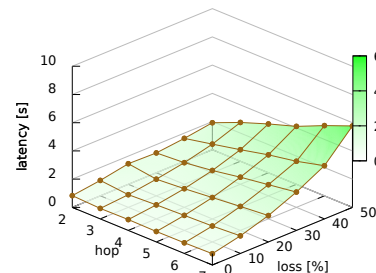
Fig. 7: Gains for the three transmission schemes (Packets 64 - Size 250 B - Bitrate 0.25 Mb/s).



(a) end-to-end



(b) hop-by-hop



(c) RLNC

Fig. 6: Latency for the three transmission schemes depending on number of hops and loss (Packets 64 - Size 250 B - Bitrate 0.25 Mb/s).

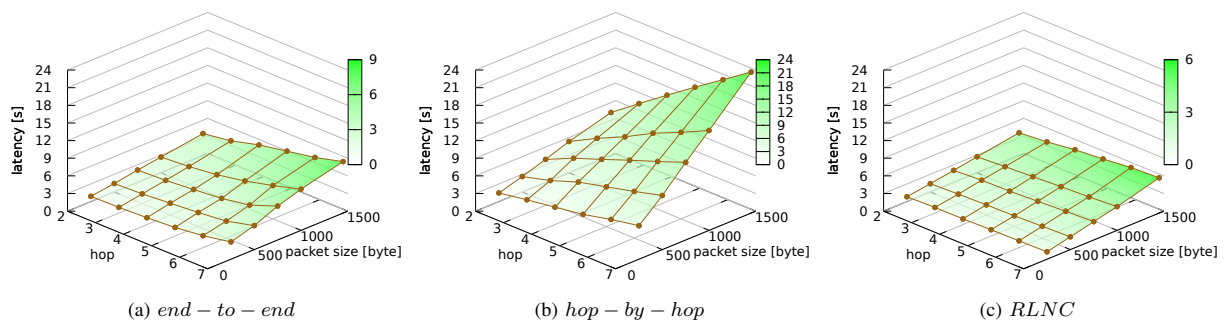


Fig. 8: Latency for the three transmission schemes depending on number of hops and packet size (Packets 64 - Loss 10% - Bitrate 0.25 Mb/s).

ing on number of hops and loss probabilities is given. In the case of small number of hops with low loss E2E can keep pace with RLNC, at the expense of more sent packets. However, the latency increases significantly for large number of hops that are highly error prone. For HbH it increases linearly with the number of hops and increases with the probability of losses as given in Equation 4. RLNC has a lower latency than the other two schemes over a wide range of parameters.

In Fig. 7 the gain of RLNC over the two schemes are given, namely E2E versus RLNC and HbH versus RLNC in Fig. 7a and Fig. 7b, respectively for a better comparison of the three schemes. The gain is calculated by the division of the latency either for E2E or HbH and RLNC. The plots in Fig. 7 show a clear gain of RLNC over the other schemes. The maximum gain over E2E and HbH for the given parameters is 16x and 6x, respectively. Note, in Fig. 7b the axes have been switched in order to increase visibility.

In Fig. 8 the loss probability is still set to 10% and the latency is plotted against the number of hops and the packet size. Most communication scenarios will use the maximum transfer unit (MTU) size of ~1500 bytes, but smaller packet size will probably come up in future. For all three forwarding schemes latency increases linearly with packet size but HbH suffers the most as it is slower up to 4 times – and E2E is up to 1.5 times – compared to RLNC. Considering that the rate of loss is small what really makes the difference here is the different packet forwarding mechanisms described in Fig. 1. So with very small losses E2E can operate almost as efficient as RLNC, because the few number of extra packets, but HbH still slow due to the decoding-encoding at the middle nodes. So summing up the cases observed RLNC does not resonate as much as the other two schemes and breaks new grounds for future networking systems.

V. CONCLUSION AND FUTURE WORK

In this paper we have investigated some of the most important advantages of RLNC, the modern form of network coding, and we have shed some light on its application possibilities. We have provided a detailed comparison of RLNC and other coding strategies in terms of latency and traffic imposed to the network. In order to facilitate the use of RLNC we have also presented a prototype architecture demonstrating a feasible integration in SDN environment by using Virtualized

Networking Functions. The VNFs implement RLNC functionality that enables us to leave all the management and traffic steering tasks on the SDN controller. This lead to flexible and automated deployment of service chains comprising network coding specific features, hereby introducing the code centric networking in SDN environment which is at same time compatible with the traditional packet switched networks.

According to our results - both analytical and measurement - RLNC not only outperforms the others, as efficiently decreasing latency and number of sent packets, but also introducing flexibility by enabling packet forwarding without a centralized scheduling logic. In the future we will extend the measurements and the SDN prototype with multi-path functionality, since multipath communication will not only increase the throughput and resilience, but also contribute to a further decreased latency. The need for RLNC over other coding techniques will become even more evident in the multipath context. Instead of the FullRLNC mode of Kodo, in the future we can use the sliding window approach that will reduce further the packet delay significantly.

APPENDIX A

RECURSIVE FORMULA FOR CALCULATING LATENCY IN A TWO HOP SYSTEM

To take a closer look on the difference between measurements and theory in Fig. 5 for RLNC we created a simulation environment for the most simple case of RLNC comprising only one encoder, one recoder and one decoder with two error prone links between them. For the sake of simplicity, in the simulation we calculated link delay as zero and used time slots as an analogy for inter packet time, so each node sends one packet per slot. Fig. 10 shows the latency as number of time slots required until the full message was decoded in dependency of the two channel error probabilities ϵ_1 and ϵ_2 . It can be seen that difference occurs between theory and simulation only when error probabilities are close to each other ($\epsilon_1 \approx \epsilon_2$), which suggests that Eq. 5 isn't precise but what actually happens is that due to the finite generation sizes the actual loss on the two channels during the simulation is not exactly ϵ_1 and ϵ_2 but slightly differs from them as a random variable. When the error rate on one channel is significantly higher than the rate on the other the impact of this effect is very small since there is very low chance that more packet

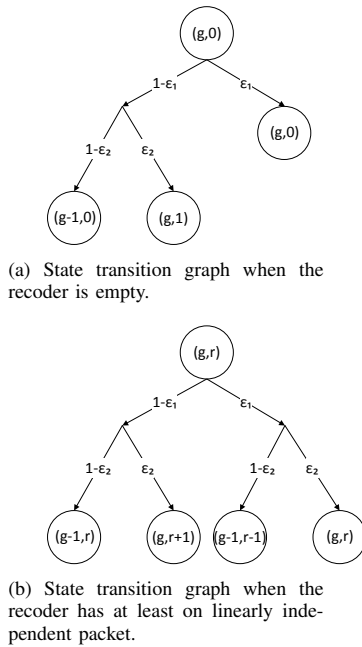


Fig. 9: Graphical representation of a two hop system: g is the number of packets that the decoder still needs in order to decode the full generation, r is the number of linearly independent packets in the recoder.

will be lost on the lower error rate channel (we can say that the higher error suppresses the lower). When the two error rates are close to each other we always have to calculate with the higher random value thus the result will be higher than expected from the theory.

To check our intuition we created a recursive formula based on the forwarding process that can calculate the latency in this 2 hop case. Since forwarding ends when the full generation comprising G packets is delivered to the decoder, let (g, r) be the state of the system, where g is the number of packets that has to be delivered to the decoder and r the number of linear independent – i.e. the useful – packets the recoder has and can send innovative packets based on them. This let us to distinguish two fundamentally different situations (Fig. 9), (i) when recoder is running dry (Fig. 9a) and (ii) when the recoder has useful packets to forward an innovative packet (Fig. 9a). When the recoder is running dry it means that if the packet from the encoder is lost the recoder can not send an innovative packet to the decoder thus the system stays in the same $(g, 0)$ state but one time slot wasted. In [25] authors present a similar model for delay calculation in RLNC and they state that a closed formula is too complex when g is larger than 4. After that they use a random variable for modelling the delay thus -due to our knowledge- we are the first ones to present a closed recursive formula for delay in RLNC using arbitrary generation number and link losses in a two hop network.

We differentiate three cases as follows.

- 1) If $r = g$: in case the recorer has enough number of

linearly independent packets to send the reminder of the generation to the decoder, it does not need any extra packet from the encoder. Thus it means that we have to send g number of packet through a single link with an error probability of ϵ_2 . In this case the expected number of time slots can be calculated as follows.

$$E(g, g) = g \cdot \frac{1}{1 - \epsilon_2} \tag{6}$$

- 2) If $r = 0$: in this situation if the packet from the encoder get lost the recoder can not send an innovative packet to the controller (see Fig. 9a). The expected number of time slot needed for sending the remaining packet can be calculated with the following recursive formula.

$$\begin{aligned} E(g, 0) &= 1 + (1 - \epsilon_1)(1 - \epsilon_2)E(g - 1, 0) \\ &\quad + (1 - \epsilon_1)\epsilon_2E(g, 1) + \epsilon_1E(g, 0) \\ &= \frac{1}{1 - \epsilon_1} + (1 - \epsilon_2)E(g - 1, 0) + \epsilon_2E(g, 1) \end{aligned} \tag{7}$$

- 3) If $0 < r < g$: in this case the recoder already has r number of linearly independent packets thus even when the packet from the encoder to the recoder get lost the recoder can send an innovative packet to the decoder (see Fig. 9b). The expected number of time slot needed for sending the remaining packet can be calculated with the following recursive formula.

$$\begin{aligned} E(g, r) &= 1 + (1 - \epsilon_1)(1 - \epsilon_2)E(g - 1, r) \\ &\quad + (1 - \epsilon_1)\epsilon_2E(g, r + 1) \\ &\quad + \epsilon_1(1 - \epsilon_2)E(g - 1, r - 1) \\ &\quad + \epsilon_1\epsilon_2E(g, r) \\ &= \frac{1}{1 - \epsilon_1\epsilon_2} \\ &\quad + \frac{(1 - \epsilon_1)(1 - \epsilon_2)}{1 - \epsilon_1\epsilon_2}E(g - 1, r) \\ &\quad + \frac{(1 - \epsilon_1)\epsilon_2}{1 - \epsilon_1\epsilon_2}E(g, r + 1) \\ &\quad + \frac{\epsilon_1(1 - \epsilon_2)}{1 - \epsilon_1\epsilon_2}E(g - 1, r - 1) \end{aligned} \tag{8}$$

On Fig. 11 we compared again the simulations with the values derived from the recursive formula and we get almost no difference, so this formula describes the process precisely. However, generalizing this recursive formula for H number of hops has exponential complexity since the state system can be described by H number of variables (the number of packets that the decoder still needs to decode the full generation and the linearly independent packets in every $H - 1$ recoders).

REFERENCES

- [1] R. Ahlswede, N. Cai, S.-Y. R. Li, and R. W. Yeung, "Network information flow," *Information Theory, IEEE Transactions on*, vol. 46, no. 4, pp. 1204–1216, 2000.
- [2] M. Medard, M.-J. Montpetit, C. Rosenberg, and F. Fitzek, "Network coding mythbusting: Why it is not about butterflies anymore," 2012.
- [3] R. Koetter and M. Médard, "An algebraic approach to network coding," *IEEE/ACM Transactions on Networking (TON)*, vol. 11, no. 5, pp. 782–795, 2003.

Network Coding as a Service

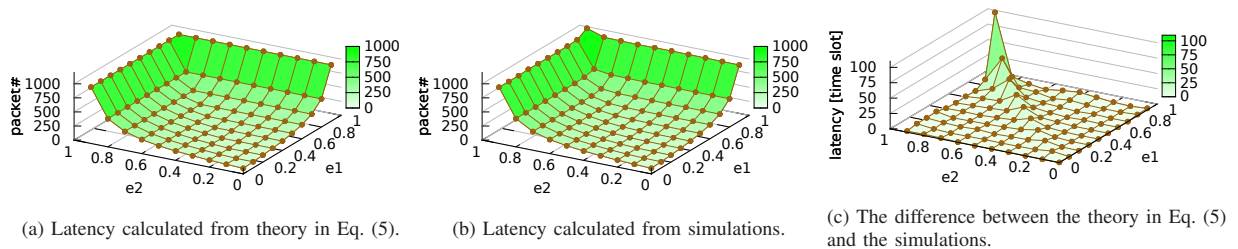


Fig. 10: Number of time slots required to successfully send one generation of packets using RLNC through a two channel network with loss probabilities of ϵ_1 and ϵ_2 .

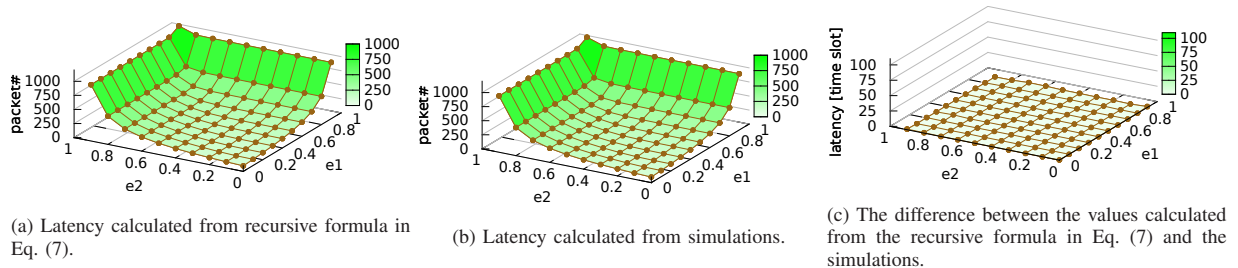


Fig. 11: Number of time slots required to successfully send one generation of packets using RLNC through a two channel network with loss probabilities of ϵ_1 and ϵ_2 .

[4] "Etsiportal, networkfunctionsvirtualisation: An introduction, benefits, enablers, challenges and call for action." October 2012. [Online]. Available: "http://portal.etsi.org/NFV/NFV_White_Paper.pdf"

[5] F. Németh, Á. Stipkovits, B. Sonkoly, and A. Gulyás, "Towards smart-flow: case studies on enhanced programmable forwarding in openflow switches," *ACM SIGCOMM Computer Communication Review*, vol. 42, no. 4, pp. 85–86, 2012.

[6] S. Liu and B. Hua, "Ncos: A framework for realizing network coding over software-defined network," in *Local Computer Networks (LCN), 2014 IEEE 39th Conference on*. IEEE, 2014, pp. 474–477.

[7] N. McKeown *et al.*, "OpenFlow: enabling innovation in campus networks," *SIGCOMM Comput. Commun. Rev.*, vol. 38, no. 2, pp. 69–74, 2008.

[8] A. Pašić and P. Babarčí, "Delay aware survivable routing with network coding in software defined networks," 2015.

[9] D. Szabó, A. Gulyás, F. Fitzek, and D. E. L. Roetter, "Towards the tactile internet: Decreasing communication latency with network coding and software defined networking."

[10] D. Szabó, F. Németh, B. Sonkoly, A. Gulyás, and F. H. Fitzek, "Towards the 5g revolution: A software defined network architecture exploiting network coding as a service," in *Proceedings of the 2015 ACM Conference on Special Interest Group on Data Communication*, ser. SIGCOMM '15, 2015, pp. 105–106.

[11] N. Feamster, J. Rexford, and E. Zegura, "The road to sdn," *Queue*, vol. 11, no. 12, p. 20, 2013.

[12] W. John, K. Pentikousis, G. Agapiou, E. Jacob, M. Kind, A. Manzalini, F. Risso, D. Staessens, R. Steinert, and C. Meirosu, "Research directions in network service chaining," in *Future Networks and Services (SDN4FNS), 2013 IEEE SDN for*. IEEE, 2013, pp. 1–7.

[13] V. Sekar, N. Egi, S. Ratnasamy, M. K. Reiter, and G. Shi, "Design and implementation of a consolidated middlebox architecture," in *Presented as part of the 9th USENIX Symposium on Networked Systems Design and Implementation (NSDI 12)*. San Jose, CA: USENIX, 2012, pp. 323–336. [Online]. Available: <https://www.usenix.org/conference/nsdi12/technical-sessions/presentation/sekar>

[14] J. Sherry, S. Hasan, C. Scott, A. Krishnamurthy, S. Ratnasamy, and V. Sekar, "Making middleboxes someone else's problem: Network processing as a cloud service," in *Proceedings of the ACM SIGCOMM 2012 Conference on Applications, Technologies, Architectures, and Protocols for Computer Communication*, ser. SIGCOMM '12. New York, NY, USA: ACM, 2012, pp. 13–24. [Online]. Available: <http://doi.acm.org/10.1145/2342356.2342359>

[15] "Cisco. cisco cloud services router 1000v data sheet," July 2012. [Online]. Available: "http://www.cisco.com/en/US/prod/collateral/routers/ps12558/ps12559/data_sheet_c78-705395.html"

[16] "Vyatta. the open source networking community," July 2012. [Online]. Available: "http://www.vyatta.org"

[17] J. Martins, M. Ahmed, C. Raiciu, V. Olteanu, M. Honda, R. Bifulco, and F. Huici, "Clickos and the art of network function virtualization," in *Proc. USENIX NSDI*, 2014, pp. 459–473.

[18] E. Kohler *et al.*, "The click modular router," *ACM Trans. Comput. Syst.*, vol. 18, no. 3, pp. 263–297, Aug. 2000.

[19] M. V. Pedersen, J. Heide, and F. H. Fitzek, "Kodo: An open and research oriented network coding library," in *NETWORKING 2011 Workshops*. Springer, 2011, pp. 145–152.

[20] A. Csoma, B. Sonkoly, L. Csikor, F. Németh, A. Gulyas, W. Tavernier, and S. Sahnaf, "Escape: Extensible service chain prototyping environment using mininet, click, netconf and pox," in *Proceedings of the 2014 ACM Conference on SIGCOMM*, ser. SIGCOMM '14. New York, NY, USA: ACM, 2014, pp. 125–126. [Online]. Available: <http://doi.acm.org/10.1145/2619239.2631448>

[21] B. Lantz *et al.*, "A network in a laptop: Rapid prototyping for software-defined networks," in *ACM HotNets 2010*.

[22] B. Pfaff, J. Pettit, K. Amidon, M. Casado, T. Koponen, and S. Shenker, "Extending networking into the virtualization layer," in *Honets*, 2009.

[23] "Pox wiki - open networking lab." [Online]. Available: "https://openflow.stanford.edu/display/ONL/POX+Wiki"

[24] O. Sefraoui, M. Aissaoui, and M. Eleuldj, "Openstack: toward an open-source solution for cloud computing," *International Journal of Computer Applications*, vol. 55, no. 3, pp. 38–42, 2012.

[25] T. K. Dikaliotis, A. G. Dimakis, T. Ho, and M. Effros, "On the delay of network coding over line networks," in *Information Theory, 2009. ISIT 2009. IEEE International Symposium on*. IEEE, 2009, pp. 1408–1412.

[26] P. Pakzad, C. Fragouli, and A. Shokrollahi, "Coding schemes for line networks," in *Information Theory, 2005. ISIT 2005. Proceedings. International Symposium on*. IEEE, 2005, pp. 1853–1857.



Dávid Szabó Received M.Sc. in Informatics at Budapest University of Technology and Economics (BME), Budapest, Hungary in 2010. Since 2012, he is a Ph.D. student at the High Speed Networks Laboratory at the Department of Telecommunications and Media Informatics, BME. His Ph.D. research is in the field of complex networks and routing protocols. His research interests also include network coding and future Internet technologies. Since 2013, Dávid is also enrolled in the Doctoral School on Innovation & Entrepreneurship organized by the EIT Digital of

the European Institute of Innovation and Technology.



Attila Csoma Received B.Sc. and M.Sc degree in Informatics at Budapest University of Technology and Economics (BME), Budapest, Hungary in 2010 and 2012 respectively. Since 2012, he is a Ph.D. student at the High Speed Networks Laboratory at the Department of Telecommunications and Media Informatics, BME. He conducts his Ph.D. research on network topology and complex networks. His research interests also include network coding and IoT.



Péter Megyesi Received his B.Sc. and M.Sc. in Electrical Engineering from the Budapest University of Technology and Economics (BME), Budapest, Hungary, in 2010 and 2012, respectively. Since 2012, he is a Ph.D. student at the High Speed Networks Laboratory at the Department of Telecommunications and Media Informatics, BME. His Ph.D. research is focused on synthetic network traffic generation. His research interests also include traffic measurements, traffic modeling and analysis and traffic identification. Since 2013, Péter is also

enrolled in the Doctoral School on Innovation & Entrepreneurship organized by the EIT Digital of the European Institute of Innovation and Technology.



András Gulyás Received M.Sc. and Ph.D. degree in Informatics at Budapest University of Technology and Economics, Budapest, Hungary in 2002 and 2008 respectively. Currently he is a research fellow at the Department of Telecommunications and Media Informatics. His research interests are complex and self-organizing networks and software defined networking.



Frank H. P. Fitzek Received his diploma (Dipl.-Ing.) degree in electrical engineering from the University of Technology - Rheinisch-Westfälische Technische Hochschule (RWTH) - Aachen, Germany, in 1997 and his Ph.D. (Dr.-Ing.) in Electrical Engineering from the Technical University Berlin, Germany in 2002 and became Adjunct Professor at the University of Ferrara, Italy in the same year. In 2003 he joined Aalborg University as Associate Professor and later became Professor. From 2014 he is the head of Chair of Communication Networks at

Technische Universität Dresden.

Increasing energy efficiency in WSNs using wakeup signal length optimization combined with payload aggregation and FEC

Ákos Milánkovich¹, Gergely Ill¹, Károly Lendvai¹, Sándor Imre¹ and Sándor Szabó¹

Abstract—Energy efficiency in wireless sensor networks is a vital question. There are several possibilities to achieve longer battery life in such devices. We investigated delay-tolerant wireless sensor networks with battery-operated nodes and use data-aggregation to lower the size of transmitted data overhead caused by packet headers.

In this paper a mathematical formula is presented to calculate the optimal wakeup signal (a special radio signal) length, which minimizes the energy consumed for waking up nodes in sleep mode. The demonstrated results and graphs are based on the investigation of an existing system. The contribution of this paper is a general method to improve the energy efficiency of wireless sensor networks by using the optimal length of the wakeup signal in case of different amounts of aggregated packet payloads and Forward Error Correction (FEC) schemes. The results presented can be applied to arbitrary packet-based wireless protocols and radio modules supporting wakeup signal listening.

Keywords—energy efficiency, wireless sensor networks, aggregation, sleep-wake cycle, wakeup signal length, WSN, FEC, DTN

I. INTRODUCTION

Wireless technologies drive the innovation in the telecommunication sector [1]. One of the key areas, wireless sensor networks is becoming popular in various scenarios such as environment, production and health care monitoring, intelligent home, precision agriculture, smart metering, etc. In the design and implementation phase of these systems, special attention should be paid to the energy consumption of the network nodes, since these in many cases operate on battery power. Moreover, in case of Delay-Tolerant Networks (DTN), it is possible that the nodes transmit the useful information in an application-specific predefined time T delay instead of real-time communication.

This paper focuses on the energy consumption of sensor networks with the restrictions defined by the operation of DTNs. Our goal is to minimize the energy consumption of network nodes, taking into account the BER (Bit Error Ratio) quality of the radio channel to maximize battery life. This paper aims to reach this goal by finding the optimal length of the wakeup signal. The method was developed for multi-hop wireless sensor networks with stationary nodes.

¹Department of Networked Systems and Services
Budapest University of Technology and Economics
Budapest, Hungary
Email: {milankovich, ill, lendvai, imre, szabos}@hit.bme.hu
Manuscript received: August 14, 2015. Revised: November 23, 2015

This paper is the extended version of [2]. In this paper solutions for sleep-wake optimization is presented. The problem is gaining attention nowadays as the popularity of sensor networks is rapidly increasing. Besides the solutions presented here, there are other approaches, but the basic idea behind them is similar to the discussed protocols. Among the published solutions there are synchronous and asynchronous scheduling methods and also low-energy MAC (Medium Access Control) protocols. The WSN (Wireless Sensor Network) community often refers to this problem as "low power listening".

This paper is organized as follows: Following the related work section, Section III. introduces the system model along with the considered parameters of the sensor network hardware and communication protocol. Section IV. shows the benefits of a better sleep-wake scheduling. Next, in Section V. the formulas for optimization and the results are presented. Finally, Section VI. concludes the paper.

II. RELATED WORK

The solution [3] employs relay nodes. These intermediate nodes can be installed easily and can be used to increase the reliability of the communication network. Moreover they can increase the energy efficiency of the network. In this solution the task is to select the relay node(s) to achieve the most energy-efficient routing. To optimize between energy efficiency and load balancing, authors determine the amount of energy required for the transmission and reception with proper QoS. Therefore the system can chose from multiple relays and energy levels combined with variable transmission power and cooperative sleep-wake scheduling.

S-MAC [4] handles the problem in the Medium Access Control layer. According to the protocol all nodes can be in one of these states: sleep, awake and listen. In sleep mode, the nodes turn their radios off and set a timer to wake up later. The length of listening and sleeping periods can be tuned for the applied scenario. The neighbor nodes are synchronized, so that they fall asleep and wake up at the same time. The nodes share their sleep-wake schedules with their neighbors, and store it in a table. Moreover, they can communicate with each other without perfect synchronization. Medium access is achieved by using RTS/CTS mechanism. Beside the advantages of S-MAC, there are also some disadvantages. The hop-by-hop delay may increase, which can be a problem in some applications. Also, every node has to maintain a scheduling table, which can consume a significant amount of memory in case of many

neighbors. To handle the scheduling the microcontroller has to stay awake continuously.

In case of the third method [5] the network consists of sensor nodes and sinks (data collectors). The sensor nodes are responsible for detecting events and sending packets to the sinks via multi-hop. The sinks are connected with wired links and have infinite power sources. For energy efficiency purposes, the nodes use asynchronous sleep-wake scheduling. The waking events are considered to be Poisson processes with parameter λ . Therefore the wake intensity means the frequency of switching to active state, and influences the energy spared during sleep state and also the bandwidth. The authors defined an overhead measure, which determines the amount of energy needed beyond the data transfer. The goal is to minimize this overhead by changing some variables, providing sufficient bandwidth according to the nodes data generation intensity, and to achieve, that in average a certain percent of nodes from the forwarding set should be awake to forward the data.

Another class of papers [6] [7] [8] [9] introduce a different approach to wakeup listening. They propose the use of an additional low-power radio module, which has the responsibility of receiving wakeup packets (in most cases out-of-band, and in rare cases they are even capable of addressing) and notify the microcontroller to switch on the main radio for the reception of the real packet. These papers suggest that the use of an additional low-power radio could significantly reduce the overall energy consumption compared to continuous idle listening. These papers sacrifice the radio range to achieve lower power. In this paper the authors preserve the radio range of the original radio module. Moreover the circuitry of the module is simpler, thus cheaper using only one radio module.

III. SYSTEM MODEL

A. Communication Protocol

In this section the operation of a communication protocol is presented as an example, which will be used in the formal mathematical model to show results. In the example communication protocol the header and trailer both have fixed length determined by the applied communication protocol, the types of encryption and error correction code. From the point of transmitted useful data, these are overhead. The combined length of the header and trailer is ω bits. The useful data consists of fix, predetermined length of elements and structure. The size of this payload data is φ bits. To maximize the energy efficiency of the system, the useful bits/all transmitted bits ratio has to be maximized. Assuming no error in the transmission the most possible useful data can be transmitted in one packet, which means, that aggregating the information into one packet is necessary, and guarantees that the overhead ratio in the packet is minimal. In a data packet, n pieces of data elements of φ bits length are transmitted, so the useful data amount is n times φ bits. Figure 1 shows the communication flow between a sender and a receiver node. The sender indicates its intention of sending a packet to the receiver node by broadcasting a wakeup signal, containing a special (longer) preamble which can be recognized by the RF chip. The application of such special preamble has to be supported by the RF chip hardware.

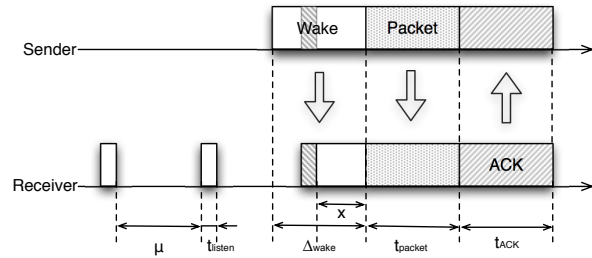


Fig. 1: Communication flow between two nodes

Some vendors refer to this functionality as WOR (Wake on Radio). Texas Instruments CC1101 [10] used in this paper supports this feature. The wake message contains the node ID of the destination node as well. Immediately after the wake message, the sender sends the packet, and then waits for acknowledgment. In case the ACK did not arrive in time, the packet is considered to be lost and will be resent later. Meanwhile the receiver nodes are listening for wakeup signals with μ periodicity. To successfully receive a wakeup signal, nodes need to listen for at least time t_{listen} . If the wakeup was successful, the receiver listens for the data packet. Otherwise the node was not awakened and the transmission was not successful. After the packet was successfully received, the receiver sends an ACK to the sender node.

In addition to the communication flow described above, some additional assumptions were made:

- The nodes in sensor networks usually have more states: sleeping, receiving and sending. In sleep mode the nodes turn their radio modules off, and set a timer to wake up later.
- The duration of signal propagation on the radio channel is considered to be zero,
- The wakeup signal always successfully wakes up the nodes,
- The radio channel is symmetrical for BER and PER,
- The packets never collide with other packets on the radio channel (to make the modeling easier),
- A node always receives one packet at once,
- The storage memory of the nodes is infinite, without restriction for packet length.

B. Model parameters

In this section, we introduce the parameters used in the following formulas. The parameters and their values are summarized in Table I. The demo system consists of an Atmel AVR XMEGA A3 microcontroller [11] and a TI CC1101 433 MHz radio module[10]. Both devices are extremely suitable for sensor networks, due to their low power consumption, reliability and low price.

B : 9.6 kbaud/sec. Using GFSK modulation, one symbol carries one bit, which equals 9.6 kbit/sec.

i_{tx} : 40 mA (at +10 dBm output power). This value should

Increasing energy efficiency in WSNs using wakeup signal length optimization combined with payload aggregation and FEC

TABLE I: Parameters for calculating optimal wake time

Symbol	Description	Value	Unit
ω_h	length of header	128	bit
ω_{MAC}	length of MAC	16	bit
B	transfer rate	9600	bit/s
n	aggregation number	1-100	pcs
φ	length of payload	80	bit
BER	bit error rate	4E-3,4E-4,4E-5	prob.
N	block size of FEC	depends on FEC	bit
K	code length of FEC	depends on FEC	bit
t	error correcting capability of FEC	depends on FEC	bit
r	number of retransmissions	depends on FEC and BER	pcs
i_{rx}	RX current	20	mA
i_{tx}	TX current	40	mA
i_{idle}	Current in SLEEP mode	0.031	mA
σ	Packet size	Depends on n	bit
$t_{WaitForACK}$	Expected waiting time for ACK (including processing and guard times)	1	s
t_{listen}	Listening time for successful awaking	0.073	s
T	Examined period length	1	h
λ_t	Number of sent packets during T	1-60	pcs
λ_r	Number of received packets during T	1-60	pcs
C_{src}	Battery stored energy	8500	mAh

be increased by the 1340 μA current draw of the microcontroller, but in case of transmission, the microcontroller encodes simultaneously, so this value is considered in I_{enc} . ([10] page 9, Table 4.)

i_{rx} : 20 mA (at sensitivity limit). This value should be increased by the 1340 μA current draw of the microcontroller, but similarly as the transmission, in case of receiving, the microcontroller simultaneously decodes, so this value is considered in I_{dec} . ([10] page 10, Table 4.)

C. Forward Error Correction schemes

In this article the authors use block codes for error correction, because their implementation requires fewer resources – from the limited computational capacity of microcontrollers - than other more advanced codes. The following three error correction codes were considered:

Hamming codes [12] are basic linear block codes [13] using parity checking as the added redundant information. They can only correct one bit per block and detect 2 incorrect bits. Hamming codes are perfect codes [13] and can be decoded using syndrome decoding [14]. They are often used in ECC memory modules.

Reed-Solomon [15], [16] codes are cyclic BCH codes. They are commonly used in CDs and DVDs.

BCH (Bose-Chaudhuri-Hocquenghem) [17] codes are also linear block codes, which can be defined by a generator polynomial.

To calculate the energy consumption of a Forward Error Correction (FEC) scheme, first the execution time of every FEC scheme on the same computer using Matlab simulation was measured. We chose this platform, as most of the FEC codes are already built-in. Then we implemented the selected code of each FEC scheme on the chosen microcontroller (Atmel

AVR Xmega128 A3 [11]) and measured the clock cycles of executing encoding and decoding. Using our simulation data, we could determine the proportion of each code and scaled the energy consumption according to the microcontrollers clock cycles. Table II shows the important parameters of the FEC codes, which are used in the following calculations, where N refers to the block length of the code K denotes the message length, t signifies the correctable symbols and κ_4 refers to the energy consumption of coding 1 bit using the particular FEC.

TABLE II: Summary of FEC code parameters

Code	Complexity	Type	N	K	t	κ_4
No FEC	none	none	1	1	0	0
Hamming (255,247)	low	block	255	247	1	5.0522E-9
Reed-Solomon (511,501)	high	block	511	501	5	5.4344E-7
BCH (511,502)	high	block	511	502	4	1.7619E-5

IV. OPTIMAL WAKEUP SIGNAL LENGTH

This section shows how to determine the optimal wakeup signal length to minimize the energy needed by one node, in order to maximize its lifetime. In case no aggregation is used, the nodes send as many separate packets (consisting of ω header and φ payload), as necessary to send the information. On the contrary, in case of aggregation the length of the packet depends on the number of φ payloads, the used n aggregation number and the $FEC(N, K)$ code applied. Formula (1) determines the packet length:

$$\sigma = \begin{cases} \omega + N \left\lceil \frac{n\varphi}{K} \right\rceil & , \text{ if aggregation is ON} \\ \omega + \varphi & , \text{ if aggregation is OFF} \end{cases} \quad (1)$$

According to the previous considerations, in case of aggregation only one packet is sent, otherwise as many as the n aggregation number. Therefore λ_t also depends on aggregation according to Formula (2):

$$\lambda_t = \begin{cases} 1 & , \text{ if aggregation is ON} \\ n & , \text{ if aggregation is OFF} \end{cases} \quad (2)$$

Equation (2) does not contain the case, when a node sends more aggregated packets in the same T period. The amount of time necessary for sending one normal packet is:

$$t_{packet} = \frac{\sigma}{B}. \quad (3)$$

The amount of time necessary for sending an ACK packet can be expressed as:

$$t_{ACK} = \frac{\omega_h}{B} = \frac{128 \text{ bit}}{9600 \text{ bit/s}} = 13.33 \text{ ms}. \quad (4)$$

The quality of the radio channel is modeled by the Bit Error Rate (BER), which gives the number of damaged bits per all sent bits ratio. In this paper we do not consider bit deletion errors in the channel.

In the calculation of PER we assume, that some kind of FEC is applied to correct statistically independent bits of the corrupted packet, and some kind of Message Authentication

Code (MAC) is used to recognize malicious modifications of the payload. This paper does not take correlated bit errors into account. We also assume that FEC is not applied to the header of the packets so that no unnecessary calculations are made in case the destination address was corrupted. In order to calculate the amount of Packet Error Rate (PER) of the channel in case of using FEC codes, we have to take into account the t error correction capabilities of the FEC codes, where β defines the amount of corrected bits in the payload:

$$\beta = \sum_{i=0}^t \binom{N}{i} BER^i (1 - BER)^{N-i}$$

$$PER = 1 - \left((1 - BER)^{\omega_h} \beta^{\lceil \frac{n\varphi + \omega_{MAC}}{K} \rceil} \right) \quad (5)$$

Without the use of FEC (5) is simplified to (6), as the values of the parameters are $N = 1$, $K = 1$ and $t = 0$ according to Table II.

$$PER_{NoFEC} = 1 - (1 - BER)^{\omega_h + n\varphi + \omega_{MAC}} \quad (6)$$

The packets transmitted are received successfully with probability $1 - PER$ on a channel characterized by a certain PER . The probability, that the number of retransmissions until success will be k , is given by probability variable X with geometric distribution and $p = 1 - PER$

$$P(X = k) = PER^{k-1} (1 - PER) \quad (7)$$

The expected value of X – which denotes that how many packets need to be sent for a successful reception in an average – can be expressed as (by geometric distribution):

$$E(X) = \sum_{k=1}^{\infty} k P(X = k) = \frac{1}{1 - PER} \quad (8)$$

Using (8), the average number of required retransmissions can be determined. The value of r should be a positive integer ($r \in \mathbb{Z}^+$), because every fraction of packet sent is considered to be a part of a new packet, therefore:

$$r = \left\lceil \frac{1}{1 - PER} \right\rceil \quad (9)$$

The total amount of time a node spends in transmission state is:

$$t_{tx} = \lambda_t (\Delta_{wake} + r t_{packet}) + r \lambda_r t_{ACK}. \quad (10)$$

To describe the total amount of time spent with receiving a packet a probability variable Y is introduced, which describes how much time is left from time interval Δ_{wake} at the moment the receiver node listens to the radio channel. Y is assumed to be uniformly distributed, because the amount of time left from Δ_{wake} can have any value from 0 to Δ_{wake} with equal probability. Therefore the expected value of Y probability variable is $E(Y) = \frac{\Delta_{wake}}{2}$. This is why the receiver node has to spend $E(Y)$ time (after a successful wake) in receiving state,

while the packet sending starts. According to the previous considerations the amount of time spent with receiving is:

$$t_{rx} = \lambda_r \left(\frac{\Delta_{wake}}{2} + r t_{packet} \right) + r \lambda_t (t_{WaitForACK} + t_{ACK}). \quad (11)$$

The time spent for listening to the wakeup signal in interval T becomes

$$t_{\sum listen} = \left\lfloor \frac{T - t_{tx} - t_{rx}}{\mu + t_{listen}} \right\rfloor t_{listen}. \quad (12)$$

To catch the wakeup signal every time the listening period is:

$$\mu = \Delta_{wake} - 2 t_{listen}. \quad (13)$$

The time spent in sleep state from period T is, what remains:

$$t_{sleep} = T - t_{rx} - t_{tx} - t_{\sum listen}. \quad (14)$$

The amount of electric charge used in a second can be calculated as:

$$C_{req} = \frac{t_{tx} i_{tx} + (t_{rx} + t_{\sum listen}) i_{rx} + t_{sleep} i_{idle}}{T}. \quad (15)$$

To compare the benefits due to the use of aggregation, FEC and the optimal wakeup signal length combined we propose to use the lifetime of the nodes expressed in days, calculated as:

$$\eta = \frac{C_{src}}{T C_{req}}. \quad (16)$$

To maximize the lifetime, it is equivalent to minimize the energy used in a second:

$$\max_{\Delta_{wake}} \{\eta\} \equiv \min_{\Delta_{wake}} \{C_{req}\}. \quad (17)$$

V. RESULTS

This section shows the results based on the calculations derived in the previous section. To be able to show some connections between the parameters, a sample scenario was chosen using the hardware and protocol introduced in the previous sections. The value of number of receptions λ_r was set to 1, and the channel was considered to be average quality with $BER = 4 \cdot 10^{-4}$.

Figure 2 depicts the change in expected lifetime (in days) as a function of Δ_{wake} (in seconds) with a fixed aggregation number of $n = 10$. Table III shows the optimal Δ_{wake} and maximal η for Figure 2. It can be observed, that the graphs from different scenarios have a maximum, therefore in every case the optimal Δ_{wake} , which maximizes the lifetime can be determined for every BER and aggregation number n . The value of the optimal Δ_{wake} is to the third decimal the same in case of different FEC codes, provided that the BER of the channel stays the same. In case of a lower quality channel (higher BER) the benefits of using the optimal wakeup signal length are more significant while enabling FEC as well. The benefit of using the optimal Δ_{wake} could result at least twofold increase in lifetime in case of no forward error correction used and over a fivefold increase in lifetime using RS or BCH FEC codes with the previously mentioned n and BER values.

Increasing energy efficiency in WSNs using wakeup signal length optimization combined with payload aggregation and FEC

Remark. In case of a poor channel, the value of Δ_{wake} depends more on the aggregation number, as the node is forced to resend the packets more times.

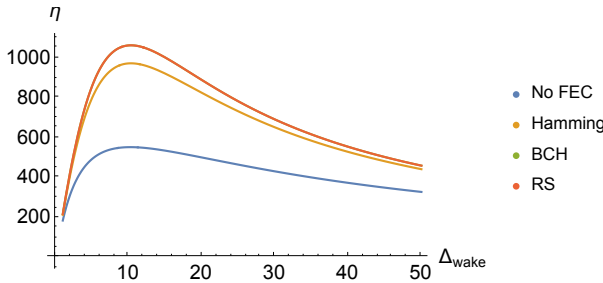


Fig. 2: The optimal value of Δ_{wake} is the same in case of different FEC codes with $BER = 4 \cdot 10^{-3}$

TABLE III: Optimal Δ_{wake} and maximal η for Figure 2

FEC	n	Δ_{wake}	η
No FEC	10	10.246	551.726
Hamming	10	10.312	971.346
BCH	10	10.319	1061.42
RS	10	10.319	1061.42

The optimal Δ_{wake} as a function of n in case of different BER channels can be seen in Figure 3. Δ_{wake} is not linearly depending on n , but the poorer the BER of the channel, the optimal Δ_{wake} decreases more rapidly as n grows.

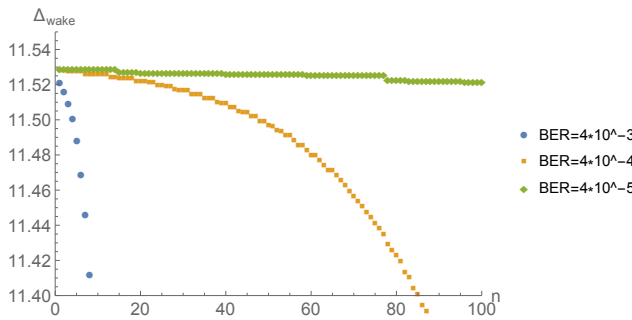


Fig. 3: Δ_{wake} as a function of n in case of different BER channels

Next we show that applying FEC code to the data increases the importance of choosing the optimal wakeup length beyond the significant energy benefits. Figure 4 shows that in case of no FEC is used, as the amount of aggregation is raised, the effect of the wakeup signal length increases as well. The lifetime scales very poorly in case the payload is increasing. Table IV shows the optimal Δ_{wake} and maximal η for Figure 4.

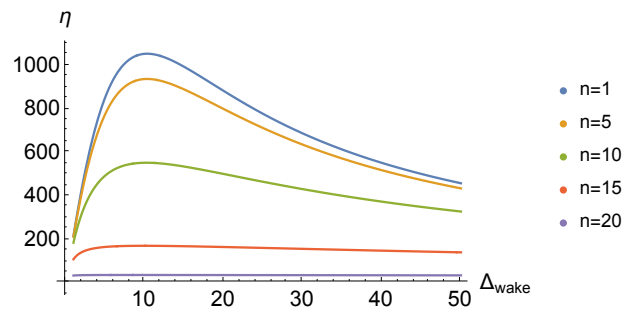


Fig. 4: η as a function of Δ_{wake} in case of different amounts of aggregation without FEC codes

TABLE IV: Optimal Δ_{wake} and maximal η for Figure 4

n	Δ_{wake}	η
1	10.318	1052.39
5	10.308	936.465
10	10.246	551.726
15	9.907	170.23
20	7.883	36.1383

Figure 5 and its corresponding Table V however, which shows the same aggregation values shows that as the benefits of using FEC as aggregation increases, the length of the wakeup signal determines the efficiency of the solution. In this case the lifetime scales significantly better as the amount of aggregated data is increasing.

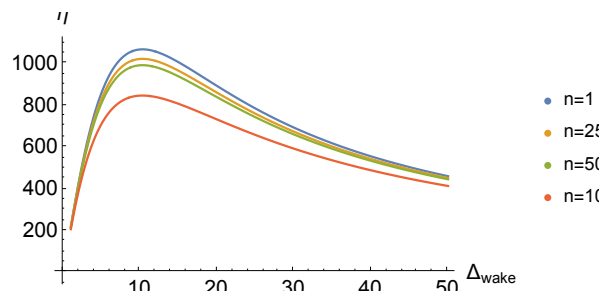


Fig. 5: η as a function of Δ_{wake} in case of different amounts of aggregation with BCH FEC code

TABLE V: Optimal Δ_{wake} and maximal η for Figure 5

n	Δ_{wake}	η
1	10.32	1067.07
25	10.317	1021.52
50	10.315	991.262
100	10.303	846.002

The same effect can be observed in case of Reed-Solomon and Hamming codes on Figure 6 and Figure 7 and their corresponding Table VI and Table VII.

Remark. Despite the magnitude of the effect on efficiency, the optimal wakeup signal length stayed the same in case of different amounts of aggregation or various FEC codes.

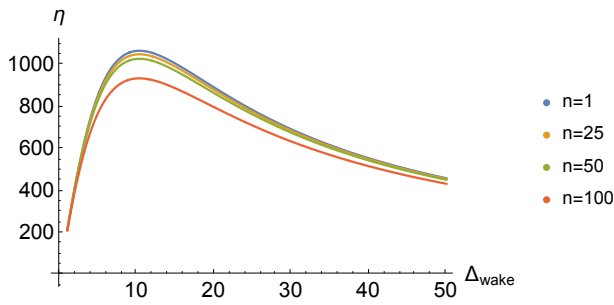


Fig. 6: η as a function of Δ_{wake} in case of different amounts of aggregation with Reed-Solomon FEC code

TABLE VI: Optimal Δ_{wake} and maximal η for Figure 6

n	Δ_{wake}	η
1	10.32	1067.07
25	10.319	1050.32
50	10.317	1028.79
100	10.311	935.817

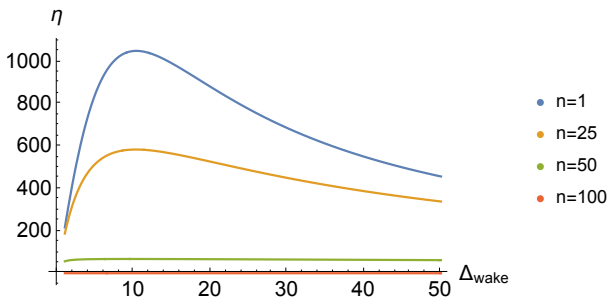


Fig. 7: η as a function of Δ_{wake} in case of different amounts of aggregation with Hamming FEC code

TABLE VII: Optimal Δ_{wake} and maximal η for Figure 7

n	Δ_{wake}	η
1	10.318	1049.57
25	10.259	584.053
50	9.245	67.553
100	1.001	0.313514

Let us examine how different FEC codes influence the lifetime without the use of aggregation. The results are shown

in Figure 8, which makes it clear, that not using FEC codes gives the shortest lifetime. Using any kind of FEC improves lifetime, but Reed-Solomon and BCH codes perform better. In this case n refers to the number of packets sent, because no aggregation was used. It can be seen, that in case of higher packet number, the result with the FEC codes do not differ much from the case with no FEC, since all of them converge to 0. This is because the packet number is so high, that due to repetitions necessary on the poor channel, the nodes are almost permanently awake. However, different FEC codes reach this state at distinct n values.

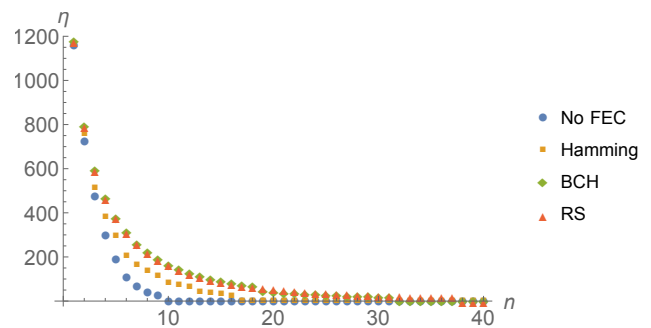


Fig. 8: Comparison of FEC codes without aggregation

Figure 9 investigates the benefits of using different FEC codes in case if aggregation enabled. The curves are decreasing, because longer packets need more energy. The worst results are in case we did not use FEC, and the best FEC code was Reed-Solomon. BCH is close to RS, but RS can correct one more bit, which explains its better values. The previous two graph shows clearly that the use of aggregation is very efficient, as it increases lifetime significantly. As the aggregation number n increases, the use of FEC codes is also more efficient.

Remark. We have investigated to include an RTS-CTS mechanism to our calculations, but the final results were not significantly affected by the use of RTS-CTS, therefore we omitted them to simplify the formulas.

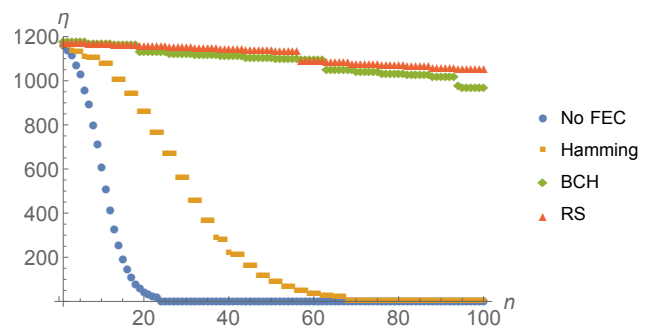


Fig. 9: Comparison of FEC codes with aggregation enabled

Increasing energy efficiency in WSNs using wakeup signal length optimization combined with payload aggregation and FEC

Combining all previous diagrams and the investigated phenomena Figure 10 shows the connection between η expected lifetime, n aggregation number, and Δ_{wake} optimal wakeup signal length in case of a poor $BER = 4 \cdot 10^{-3}$ channel. We can observe that the expected lifetime of a system without FEC stays much lower, than using FEC codes. The optimal length of the wakeup signal is depending on the type of FEC in use and the amount of aggregation.

Remark. The 3D plot should be continuous, as variable Δ_{wake} is not an integer, however it is easier to understand it on a discrete plot.

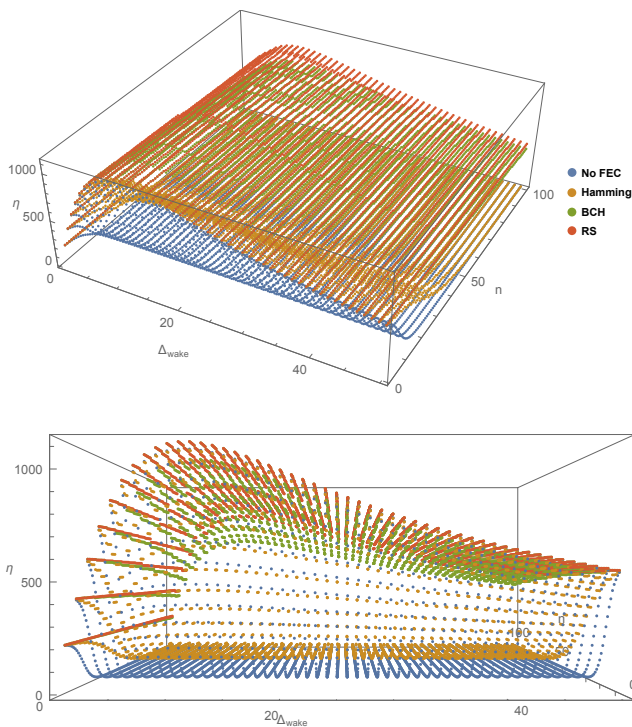


Fig. 10: The expected lifetime as a function of n and Δ_{wake}

VI. CONCLUSION

In this paper the authors presented the sleep-wake cycle optimization problem in WSNs. The authors showed, that (see Figure 3), the optimal value of Δ_{wake} wakeup signal length for minimal power consumption is not significantly affected by the length of the payload in case of a good quality channel. Besides the value of the optimal Δ_{wake} wakeup signal length is very similar in case of the presented block forward error correction codes, therefore it is considered independent. The results showed, that FEC codes and aggregation should be both combined with the optimal Δ_{wake} to significantly increase the lifetime of the devices. Solving both optimization problems gives the best results: first determine the optimal value of Δ_{wake} for a certain BER, because it is independent of the other

parameters; then calculate the optimal payload aggregation number according to the channel bit error rate (shown in [18]). Utilizing only the optimal wakeup signal length we can extend the battery life of a node more than twofold (depending on the BER of the channel and the amount of aggregation) without using FEC codes (as presented on Figure 4). In case the radio channel has poor quality, FEC codes combined with the optimal wakeup signal length can prolong lifetime of the nodes up to four times compared to baseline (as presented on Figure 5). Further investigations could dive into the problem of packet loss and collision with other packets on the radio channel to extend the presented results.

ACKNOWLEDGMENT

This research has been supported by BME-Infokom Innovator Nonprofit Ltd., <http://www.bme-infokom.hu>.

REFERENCES

- [1] L. Hanzo, H. Haas, S. Imre, D. O'Brien, M. Rupp, and L. Gyongyosi, "Wireless Myths, Realities, and Futures: From 3G/4G to Optical and Quantum Wireless," *Proceedings of the IEEE*, vol. 100, no. Special Centennial Issue, pp. 1853–1888, May 2012.
- [2] A. Milankovich, G. Ill, K. Lendvai, S. Imre, and S. Szabo, "Wakeup signal length optimization combined with payload aggregation and FEC in WSNs," in *European Wireless 2015; 21th European Wireless Conference; Proceedings of*, May 2015, pp. 1–6.
- [3] G. A. Elkheir, A. S. Lioumpas, and A. Alexiou, "Energy efficient cooperative scheduling based on sleep-wake mechanisms," in *Wireless Communications and Networking Conference Workshops (WCNCW), 2012 IEEE*. IEEE, 2012, pp. 238–242.
- [4] W. Ye, J. Heidemann, and D. Estrin, "An energy-efficient MAC protocol for wireless sensor networks," in *INFOCOM 2002. Twenty-First Annual Joint Conference of the IEEE Computer and Communications Societies. Proceedings. IEEE*. IEEE, 2002, pp. 1567–1576.
- [5] C.-C. Hsu, M.-S. Kuo, S.-C. Wang, and C.-F. Chou, "Joint Design of Asynchronous Sleep-Wake Scheduling and Opportunistic Routing in Wireless Sensor Networks," *Computers, IEEE Transactions on*, vol. 63, no. 7, pp. 1840–1846, 2014.
- [6] M. Magno and L. Benini, "An ultra low power high sensitivity wake-up radio receiver with addressing capability," pp. 92–99, 2014.
- [7] J. Ansari, D. Pankin, and P. Mähönen, *Radio-Triggered Wake-ups with Addressing Capabilities for extremely low power sensor network applications*. IEEE, 2008.
- [8] H. Karvonen, J. Petajajarvi, J. Iinatti, M. Hamalainen, and C. Pomalaza-Raez, "A generic wake-up radio based MAC protocol for energy efficient short range communication," in *Personal, Indoor, and Mobile Radio Communication (PIMRC), 2014 IEEE 25th Annual International Symposium on*. IEEE, 2014, pp. 2173–2177.
- [9] P. Kamalinejad, K. Keikhosravi, M. Magno, S. Mirabbasi, V. C. M. Leung, and L. Benini, "A high-sensitivity fully passive wake-up radio front-end for wireless sensor nodes," in *Consumer Electronics (ICCE), 2014 IEEE International Conference on*. IEEE, 2014, pp. 209–210.
- [10] Texas Instruments, Incorporated, *CC1101 Low-Power Sub-1 GHz RF Transceiver (Rev. 1)*, Nov. 2014.
- [11] Atmel, "8/16-bit XMEGA A3 Microcontroller," pp. 1–134, Jun. 2013.
- [12] S. Lin and D. J. Costello, *Error Control Coding, ser. Fundamentals and Applications*. Prentice Hall, 2004.
- [13] T. Etzion and A. Vardy, "Perfect binary codes: constructions, properties, and enumeration," *IEEE Transactions on Information Theory*, vol. 40, no. 3, pp. 754–763, May 1994.

- [14] M. P. C. Fossorier, S. Lin, and J. Snyders, "Reliability-based syndrome decoding of linear block codes," *IEEE Transactions on Information Theory*, vol. 44, no. 1, pp. 388–398, Jan. 1998.
- [15] D. V. Sarwate and N. R. Shanbhag, "High-speed architectures for Reed-Solomon decoders," *IEEE Transactions on Very Large Scale Integration (VLSI) Systems*, vol. 9, no. 5, pp. 641–655, Oct. 2001.
- [16] S. B. Wicker, V. K. Bhargava, I. C. Society, and I. I. T. Society, *Reed-Solomon codes and their applications*. Inst of Electrical &, Jun. 1994.
- [17] R. C. Bose and D. K. Ray-Chaudhuri, "Further results on error correcting binary group codes," *Information and Control*, vol. 3, no. 3, pp. 279–290, Sep. 1960.
- [18] Lendvai, K, Milánkovich, Á, Imre, S, and Szabo, S, "Optimized packet size for energy efficient delay-tolerant sensor networks with FEC," in *Proceedings of the 12th International Conference on Telecommunications (CONTEL '13)*.



Károly Lendvai received his degree in electrical engineering in 2008 at BUTE. At the Corvinus University of Budapest he graduated as engineer economist in 2011. He started his Ph.D. studies in 2008 at the Department of Telecommunications. His main research areas are optimization of transport protocols in wireless environment, wireless sensor networks and modeling of user movement in mobile networks.



Sándor Imre was born in Budapest in 1969. He received the M.Sc. degree in Electronic Engineering from the Budapest University of Technology (BME) in 1993. Next he started his Ph.D. studies at BME and obtained dr. univ. degree in 1996, Ph.D. degree in 1999 and D.Sc. degree in 2007. Currently he is carrying his teaching activities as Head of the Dept. of Networked Systems and Services of BME. His research interest includes mobile and wireless systems, quantum computing and communications. Especially he has contributions on different wireless

access technologies, mobility protocols and reconfigurable systems.



Gergely Ill received his M.Sc. degree in technical informatics from the Budapest University of Technology and Economics in 2012. He continued his Ph.D. studies at the Department of Networked Systems and Services. His research interests includes the energy efficiency of wireless sensor networks, wireless protocols and their security aspects.



Ákos Milánkovich received his M.Sc. degree in technical informatics in the field of networks and services from the Budapest University of Technology and Economics in 2012. He continued his Ph.D. studies at the Department of Networked Systems and Services. His research interests include wireless sensor networks, positioning technologies and UWB.



Sándor Szabó was born in 1977. He graduated in 2000 at the Faculty of Electrical Engineering and Informatics and received his Ph.D. degree in 2011. Currently he works as adjunct at the Dept. of Networked Systems and Services. He takes part in research projects at the university and he is the head of the Mobile Innovation Center. His research areas are integration of wired and wireless networks, mobility handling methods, IMS systems and sensor networks.

Modeling and Simulation of Mode Filtered Radio over Multimode Fiber Links

Tamás Cseh, Tibor Berceci, *Life Fellow, IEEE*

Abstract—In this paper mode filtered radio over multimode fiber systems are analyzed by simulations. Several mode filters are investigated such as mandrel wrap, air gap mode filter and single mode fiber patchcord. The multimode fibers and the mode filters are modeled, these models are implemented into VPI Transmission Maker and frequency responses are analyzed. According to the frequency responses, EVM analyses are also carried out, and the most advantageous mode filter is selected. All of these mode filters can reduce the effect of the modal dispersion however, their effect is different and their insertion loss is different too. The single mode fiber patchcord is the best choice when modal dispersion is the dominant effect. Mandrel and air gap filter provided better results if the noise is significant.

Index Terms—modal dispersion, mode filtering, multimode fiber, radio over fiber, radio over multimode fiber

I. INTRODUCTION

OPTICAL links are proper solutions for radio signal transmission and distribution, because of the large bandwidth and low attenuation of the optical fiber. The combined optical-radio system, called Radio over Fiber (RoF), is advantageous especially in indoor connections. In a RoF system a central office (CO) is connected to a high number of remote antenna units (RAUs) due to the high number of users. Therefore, the indoor RoF systems are cost sensitive, therefore low cost solutions are necessary. One of the most important ways to reduce the cost of the RoF link is the application of multimode fibers (MMFs). The large core of MMF can reduce the cost of installation, furthermore, older MMF connections could have been found in a lot of buildings and several government offices [1].

The MMFs are reasonable solutions for indoor RoF links, however, MMFs have higher linear distortion effects than single mode fibers (SMF). The main distorting effect is the modal dispersion, which causes bandwidth limitation in the link. The compensation of modal dispersion is an important task, and it is a relevant problem in Radio over Multimode Fiber (RoMMF) systems.

Several methods exist to reduce the effect of the modal dispersion and increase the modal bandwidth. The most important methods are mode filtering [2] and the offset launch

technique [3]. As it is mentioned above, RoMMF concept is cost sensitive, so simple and cheap solutions are preferred to reduce the effect of the modal dispersion. As the offset launch technique demands precise positioning of the light source, it makes the alignment complicated. Hence the mode filtering technique is more practical in RoMMF than the offset launch technique.

Several mode filters exist for different optical applications [4], but they have different effect on modal dispersion. In this paper the investigation of mode filters in RoMMF system is discussed. Three different mode filter types are investigated by simulations: mandrel wrap, air gap mode filter, and single mode fiber patchcord. They have different performance on modal dispersion and insertion loss, so they have different performance on the quality of the communication.

In this paper the performance utilizing mode filters is analyzed. First, the RoMMF link is modeled and this model focuses on modal dispersion. Then, a model of the mode filtered RoMMF with different mode filters is shown. After modeling, we analyze the frequency response of a radio over MMF link and a mode filtered RoMMF link with simulations to show the effects of the mode filters on our proposed system. After the simulation of the frequency responses, the quality of the link is analyzed with several simulation setups. The error vector magnitude (EVM) is investigated with different mode filters, and each mode filter are analyzed at different signal to noise ratios (SNR) and different modulation bandwidths.

II. SYSTEM MODEL

In this section the model of the RoMMF link is described. First, the total RoMMF link is investigated, then the model of MMF and mode filters are focused. Table I contains the main parameters of the proposed link.

A. Radio over multimode fiber link model

The radio over fiber system applies subcarrier optical modulation, hence a modulated radio frequency (RF) carrier modulates the light. The RoF systems apply intensity modulation in the optical domain, and direct detection. These systems are called IM-DD. The proposed RoF link applies multimode fiber. The block scheme of a radio over multimode fiber link (RoMMF) is shown in Fig. 1.

The RF signal modulates the intensity of the light. In the proposed model the intensity modulation (IM) is carried out by an external modulator. In order to neglect the nonlinear distortions of the link, the modulator is considered to be linear.

T. Cseh and T. Berceci are with the Department of Broadband Infocommunication and Electromagnetic Theory, Budapest University of Technology and Economics, H-1111 Budapest, Eötvös József u. 18., Hungary (email: tseh@mht.bme.hu, berceci@hvt.bme.hu)

Practically the external modulators are used in their linear region. Furthermore, in the RoMMF link model the modulator is considered to be chirpless.

Not only the modulator but also the fiber is linear in our system model. If the optical power of the laser is low enough, this consideration is also correct.

Beside the linearity of the link the noise characteristic is also important. Two components add Gaussian white noise to the link: the laser and the photodetector. The laser has relative intensity noise (RIN), and the photodetector generates thermal noise and shot noise. The RoMMF link can be modeled as a linear system with additional Gaussian noise. The block diagram of our RoMMF model is shown in Fig. 2.

The proposed mode filtered system is modeled like the non-mode filtered system. The block diagram of the mode filtered system, and the model of the mode filtered system can be seen in Fig. 3 and Fig. 4, respectively.

To describe the channel, the noise characteristic and the frequency response of the fiber have to be analyzed. In the next sections these two characteristics are modeled.

B. Frequency response of the RoMMF system

As it can be seen in Fig. 2, the frequency response of the multimode fiber is an important part of the model. According to [5], the frequency response of the fiber can be written as

$$H_{MMF}(f) = H_{Mod}(f) \cdot H_{Ch}(f), \tag{1}$$

where $H_{MMF}(f)$ is the frequency response of the MMF, $H_{Mod}(f)$ is the frequency response of the multimode behavior, and $H_{Ch}(f)$ is the frequency response of the chromatic behavior of the fiber. According to (1) the frequency response can be separated into two terms: one represents the modal dispersion and the other represents the chromatic dispersion. The chromatic dispersion is caused by the wavelength dependent group delay. The frequency response of the chromatic dispersion can be expressed as follows [6], [7]

$$H_{Ch}(f) = H_{LD}(f) \cdot H_{CS}(f). \tag{2}$$

The chromatic effects can also be separated to two terms: the first term ($H_{LD}(f)$) is caused by spectral linewidth of the laser, and the second term ($H_{CS}(f)$) is the carrier suppression effect which is caused by the optical double side band (ODSB) modulation [7]. These two terms can be written as the following according to [6], [7] and [8]

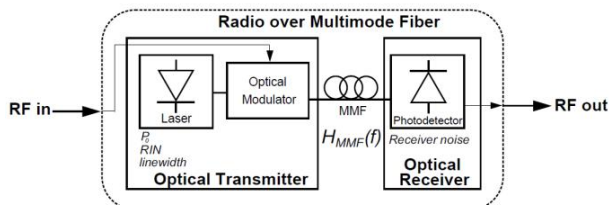


Fig. 1. Block diagram of the RoMMF link

$$H_{LD}(f) = e^{-\frac{1}{2}(D \cdot L \cdot \lambda_0 \cdot f)^2 \left(\frac{\Delta\nu}{f_{opt}}\right)^2}, \tag{3}$$

$$H_{CS}(f) = \cos\left(D \cdot L \cdot \lambda_0 \cdot \pi \cdot \frac{f^2}{f_{opt}^2}\right). \tag{4}$$

If we use the value of $\Delta\nu$ and f_{opt} from Table I, (3) can be approximated by one. Similarly, (4) can be also approximated by one, if we consider that the frequency does not exceed 10 GHz. These consideration are real in a RoMMF link. Hence, (3) and (4) can be rewritten as

$$H_{LD}(f) \approx 1, \tag{5}$$

$$H_{CS}(f) \approx 1. \tag{6}$$

As (3) and (4) are approximated by one, (2) leads to the following

$$H_{Ch}(f) \approx 1. \tag{7}$$

Hence, the effect of the chromatic dispersion can be neglected in our proposed system. This consideration is true in practical RoMMF systems, due to the relatively short the fiber length. As a conclusion (1) leads to

$$H_{MMF}(f) \approx H_{Mod}(f). \tag{8}$$

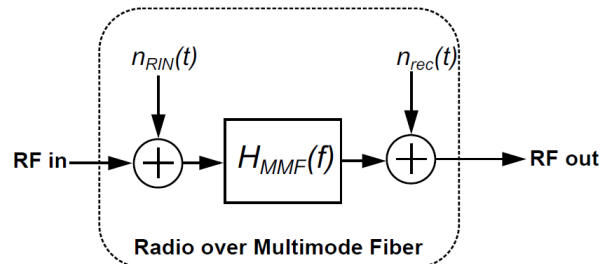


Fig. 2. Linear model of RoMMF.

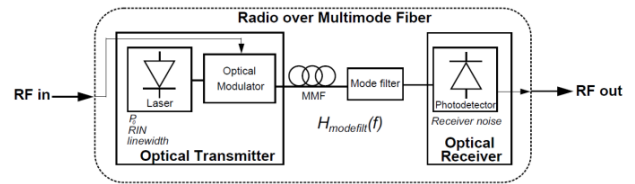


Fig. 3. Block diagram of mode filtered RoMMF

Modeling and Simulation of Mode Filtered Radio over Multimode Fiber Links

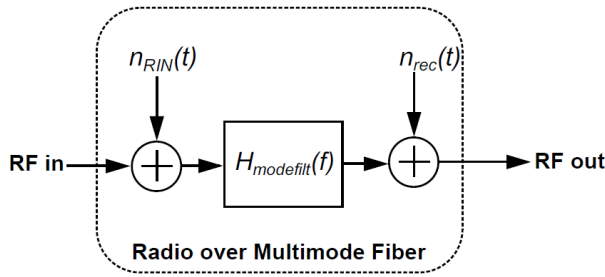


Fig. 4. Model of mode filtered RoMMF link

Therefore, in our proposed RoMMF connection, the modal dispersion is the most significant phenomenon. In the following, the frequency response of the modal behavior is described. The modal dispersion is caused by the different propagation velocity of the modes. In the MMF a lot of modes can propagate, however, several modes propagate with the same velocity and these modes constitute a mode group. The different mode groups propagate with different velocities, and that causes linear distortion, which is called modal dispersion. The total number of mode groups, the delay, the different attenuation of the mode groups, and the coupling between the mode groups influence the modal dispersion and the frequency response of the multimode fiber. The model of the MMF is described by Gloge [9] and Olshansky [10]. This model applies the power flow equation (PFE) [11].

 TABLE I
PARAMETERS OF THE PROPOSED LINK

Symbol	Parameter	Value	Units
n_{core}	refractive index of the core	1.45	-
$n_{cladding}$	refractive index of the cladding	1.44	-
Δ	refractive index contrast	0.0069	-
NA	numeric aperture of the fiber	0.17	-
λ_0	wavelength of the laser	1550	nm
$\Delta\nu$	linewidth of the laser	10	MHz
RIN	relative intensity noise	-135	dBc/Hz
f_{opt}	frequency of the optical carrier	193.55	THz
g	refractive index exponent	2	-
r_{core}	core radius	25	μm
$r_{cladding}$	cladding radius	62.5	μm
h	rms height of deformation	0.5	μm
γ_0	intrinsic fiber attenuation	0.2	dB/km
C_s	mode-coupling constant	6×10^{-5}	1/km
ρ, η	fitting constants for mode attenuation	9, 7.35	-
p	fitting parameter for mode coupling	2	-
ε	modal dispersion parameter	0	-
D	chromatic dispersion parameter	16	ps/nm·km
L	length of the fiber	3	km
r_{pD}	responsivity	1	A/W
R_L	load resistance	50	Ω
T	temperature	300	K

$$\frac{\partial P_m}{\partial z} + \tau_m \frac{\partial P_m}{\partial t} = -\gamma_m P_m + d_m (P_{m+1} - P_m) - \frac{m-1}{m} d_{m-1} (P_m - P_{m-1}). \quad (9)$$

In the PFE (9), z is the length of the fiber, t is time, P_m denotes the power of the m -th mode group, and τ_m , d_m and γ_m are group delay, attenuation and mode coupling coefficient of the m -th mode group respectively [11]. Equation (9) can be solved by several methods. In [11] a matrix exponential method is applied, and in this paper this effective calculation is applied. This method calculates the Fourier-transform of (9), and it leads to the following [11]

$$\underline{F}(z) = \exp(\underline{A} \cdot z) \cdot \underline{F}(0), \quad (10)$$

where z is the length of the fiber, $\underline{F}(z) = [F_1(z), F_2(z), \dots, F_M(z)]^T$, M is the total number of the mode groups, $F_m(z)$ is the average power of m th mode group which is calculated in frequency domain. \underline{A} is a tridiagonal matrix, which can be expressed as [11]

$$A_{m,m} = -(2\pi \cdot j \cdot f \cdot \tau_m + \gamma_m) - d_m - \frac{m-1}{m} d_{m-1}, \quad (11)$$

$$A_{m,m+1} = d_m, \quad (12)$$

$$A_{m,m-1} = d_{m-1} \frac{m-1}{m}. \quad (13)$$

The key parameters of (9), (11), (12) and (13) can be calculated according to [5] as the following

$$\tau_m = \frac{n_{core}}{c} \left(1 - \frac{\Delta[4 + \varepsilon]}{g + 2} \cdot \left(\frac{m}{M} \right)^{2g/g+2} \right) \times \quad (14)$$

$$\times \left(1 - 2\Delta \cdot \left(\frac{m}{M} \right)^{2g/g+2} \right)^{-1/2},$$

$$\gamma_m = \gamma_0 + \gamma_0 \cdot I_\rho \left(\eta \cdot \left(\frac{m-1}{M} \right)^{2g/g+2} \right), \quad (15)$$

$$d_m = C_s \left(\frac{h}{r_{cladding}} \right)^p \left(\frac{r_{core}}{r_{cladding}} \right)^{2p} \left[\frac{g+2}{g \cdot \Delta} \right]^{1+p} \left(\frac{m}{M} \right)^{-2q}, \quad (16)$$

with

$$q = \frac{[p(g-2)-2]}{g+2}. \quad (17)$$

By calculating d_m , τ_m and γ_m with substituting the values given in Table I to (14)-(17), we can conclude the following

$$d_m, d_{m-1} \ll \gamma_m, \quad (18)$$

therefore, d_m can be neglected in our proposed system. Hence \underline{A} is a diagonal matrix and (11)-(13) is the following

$$A_{m,m} \approx -(2\pi \cdot j \cdot f \cdot \tau_m + \gamma_m), \tag{19}$$

$$A_{m,m+1} \approx 0, \tag{20}$$

$$A_{m,m-1} \approx 0. \tag{21}$$

By replacing (19)-(21) to (10), we get the following expression

$$F_m(z, f) = F_m(0) \cdot e^{-(2\pi j f \tau_m + \gamma_m)z}, \tag{22}$$

and the frequency response of the multimode fiber can be calculated according to [11]

$$H_{Mod}(f) = \frac{\sum_{m=1}^M m \cdot F_m(z, f)}{\sum_{m=1}^M m \cdot F_m(0, f)}. \tag{23}$$

Equation (23) can be rewritten to another form, which contains the power of m -th mode group, and the total input power (P_0)

$$H_{MMF}(f) = \frac{1}{P_0} \sum_{m=1}^M P_m e^{-(2\pi j f \tau_m + \gamma_m)z}. \tag{24}$$

Equation (24) is the frequency response of radio over multimode fiber system, when the mode coupling can be neglected. As we have seen it above, this approximation is correct for our proposed system due to their parameters. Furthermore, (24) shows that the frequency response depends strongly on P_m , this way the influence of the input power distribution of the mode groups is very high. The input power distribution depends on the launch condition at the input of the fiber. Two types of launch conditions are tested in this paper: overfilled launch condition (OFL) and restricted mode launch (RML). The OFL is an important launch condition, because it shows a theoretically worst case of the modal behavior, and the launch condition of some practical RoMMF (which applies LEDs) connections can be considered as OFL as well. The OFL means that all of the modes are generated equally. If we know which modes belong to which mode group, the power distribution of the mode groups can be calculated. This calculation is well known [3], [4], [5].

The RML means that restricted number of modes are generated at the input. The RML is typical at laser-fiber interfaces. The power distribution which is caused by RML can be calculated by using overlap integral [3], [4], [12]. The overlap integral calculates the coupling between the laser modes and the modes of the MMF. To decide which modes belong to which mode group in the case of RML, the calculation which are mentioned in the case of OFL should be applied [3], [4], [5].

C. Frequency response of the mode filtered RoMMF system

The mode filters can reduce the number of the mode groups and this effect will cause reduction in the effect of the modal

dispersion. Each of the mode filters produces different attenuation for the mode groups, and the attenuation characteristics are also different for different mode filters. In this paper three mode filters are investigated in the RoMMF system: air gap filter, mandrel wrap, and SMF patchcord.

The air gap mode filter contains two multimode fibers coupled to each other with a small air gap. For the size of the gap 1 mm is taken in this paper. At the transmitter fiber end the light radiates out from the fiber. The diverged laser beam radiated out of the transmitter fiber, generates several modes in the other fiber at the receiver side. However, the diverged laser beam can generate restricted number of modes at the receiver fiber end of the air gap filter. Hence, the higher order modes are filtered off by the air gap [4], [12]. The mode filtering effect depends on the size of the gap: longer gap causes stronger filtering effect, but the attenuation will be higher as well. According to [4] the air gap filter with 1 mm gap size attenuates almost all of the mode groups except few lower order modes.

With a few turns of the fiber on a reel with small diameter, the higher order modes are filtered off [2]. This mode filter is called mandrel wrap. There is a radiation loss due to the turns on the reel, and the radiation loss is different for each mode group. The higher order modes are radiated stronger than the lower order ones. This effect depends on the reel diameter [4]. With a standard reel diameter of the mandrel wrap the half of the mode groups can be filtered off [2], [4].

The function of the SMF patchcord as a mode filter is the following: through the SMF patchcord only the fundamental mode can propagate due to its smaller core size. Except the fundamental mode all the modes are filtered off, but it cause relatively high insertion loss [2]. By applying a SMF patchcord as mode filter, the effect of the modal dispersion can be eliminated, and the frequency response of the mode filtered RoMMF could be perfectly flat. The mode filtering effect of the SMF patchcord is investigated in several papers such as [13], [14].

To describe the mode filtered RoMMF, the frequency response equation of RoMMF is used. As it was mentioned above, the mode filters can attenuate the different mode groups differently, so with some modifications in (24) the frequency response of the mode filtered RoMMF is given as the following

$$H_{Modfilt}(f) = \frac{1}{P_0} \sum_{m=1}^M \alpha_m P_m e^{-(2\pi j f \tau_m + \gamma_m)z}, \tag{25}$$

where α_m is the attenuation of a given mode filter on the m -th mode group. Equation (25) gives the frequency response of the mode filtered RoMMF and (24) gives the frequency response of the RoMMF without mode filtering. If the parameters of (24) and (25) are well known, the frequency responses can be calculated. In this paper the values of α_m are calculated by applying the results of [4].

Modeling and Simulation of Mode Filtered Radio over Multimode Fiber Links

D. Noise behavior of the proposed system

After the description of the frequency response of the RoMMF and the mode filtered RoMMF, the noise behavior should be analyzed. As it could be seen in Fig. 2 and Fig. 4, there are additive noise at both sides of the link. At the transmitter side the noise comes from the relative intensity noise (RIN) of the laser. The RIN can be calculated in the electrical domain as the following

$$\frac{\langle i_{RIN} \rangle}{\sqrt{B}} = P_0 \cdot r_{PD} \sqrt{RIN}, \quad (26)$$

where P_0 is the optical power of the laser r_{PD} is the responsivity of the photodetector, RIN is the relative intensity noise, B is the bandwidth, and $\langle i_{RIN} \rangle$ is the average noise current of the RIN at the photodetector.

At the receiver side of the link, the noise comes from the photodiode. The receiver noise has two components: the shot noise and thermal noise. If a PIN diode is applied as a receiver, the shot noise and thermal noise can be expressed, respectively [15]

$$\frac{\langle i_{shot} \rangle}{\sqrt{B}} = \sqrt{2 \cdot q \cdot P_0 \cdot r_{PD}}, \quad (27)$$

$$\frac{\langle i_{thermal} \rangle}{\sqrt{B}} = \sqrt{\frac{4 \cdot k \cdot T}{R_L}}, \quad (28)$$

where q is the elementary charge, T is the temperature, R_L is the load resistance, and k is the Boltzmann-constant. As RIN is relatively low in our proposed system (Table I) and P_0 is also low enough, the thermal noise will be the most dominant noise effect. In this paper the noise level is fixed, but the analysis is made at different signal power levels, so our proposed system is simulated at different signal to noise ratios (SNR).

After the description of the noise behavior and the frequency response of the RoMMF system, the linear model of the RoMMF link is determined. All of the parameters are given for the simulations of the RoMMF link in Table I.

TABLE II
CALCULATED PARAMETERS FOR SIMULATIONS

m	$\Delta\tau_m [ps]$	$\gamma_m [km^{-1}]$	P_m/P_0			α_m	
			OFL	RML	a)	b)	c)
1	0	4.61×10^{-2}	0.04	0.11	1	1	1
2	0.0043	4.61×10^{-2}	0.04	0	1	0.5	0
3	0.011	4.61×10^{-2}	0.08	0.35	1	0.44	0
4	0.021	4.61×10^{-2}	0.08	0	1	0.38	0
5	0.034	4.63×10^{-2}	0.12	0.34	0.5	0.31	0
6	0.05	4.86×10^{-2}	0.12	0	0	0.25	0
7	0.069	6.17×10^{-2}	0.16	0.16	0	0.18	0
8	0.09	12.05×10^{-2}	0.16	0	0	0.1	0
9	0.115	32.67×10^{-2}	0.2	0.04	0	0	0

a) mandrel wrap, b) air gap filter c) SMF patchcord.

III. SIMULATION RESULTS

In the former sections the model of the RoMMF and the calculations are described, hence, the calculated parameters are available for the simulation setup. Two parts of the simulation results are presented: in the first part the frequency responses are analyzed and in the second part EVM simulations are investigated. To simulate the frequency responses, the main parameters of (24) and (25) should be calculated. First the number of the mode groups (M) has to be determined. According to [5] the number of mode groups can be expressed as the following

$$M = 2\pi \cdot r_{core} \frac{n_{core}}{\lambda} \left(\frac{g \cdot \Delta}{g + 2} \right)^{1/2}. \quad (29)$$

By using (29) we got $M=9$. Hence, the main parameters of the MMF and mode filters should be calculated for nine mode groups. The calculated parameters are summarized in Table II.

A. Simulation of frequency responses

When the parameters are well known, the frequency response of RoMMF and mode filtered RoMMF can also be calculated. The frequency responses are obtained for both OFL and RML. These results are plotted in Fig. 5 and Fig. 6, respectively. The OFL frequency response without mode filtering has two notches up to 10 GHz at around 3 GHz and around 5.4 GHz. The mandrel shifts the latter notch, but this notch is also relatively strong. The air gap filter makes the frequency response smoother. The trace is not flat, however, the transmission level at the notches is smaller than in the case of the mandrel. Due to the smoother characteristics we expect better performance for air gap filter than mandrel. As the SMF patchcord filters off all of the mode groups except the fundamental mode, a totally flat characteristic is expected. The simulation results show totally flat frequency response with

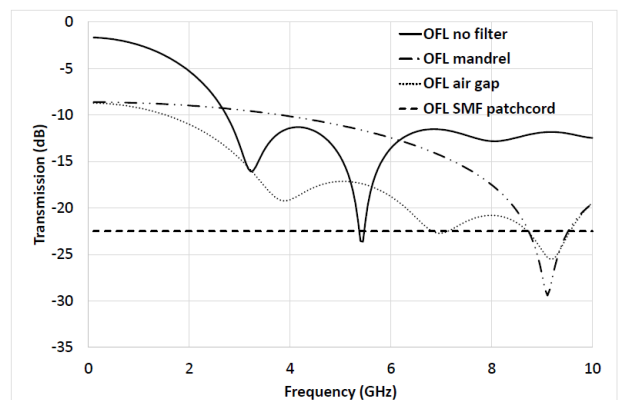


Fig. 5. Frequency responses of RoMMF with different mode filters for OFL

SMF patchcord for OFL condition.

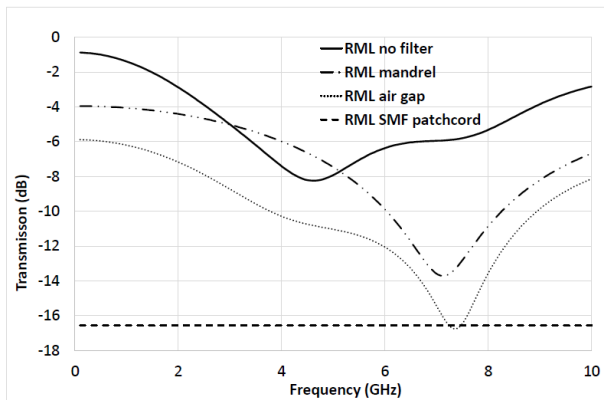


Fig. 6. Frequency responses of RoMMF with different mode filters with RML

For RML condition the frequency response without mode filtering has only one notch around 4.5 GHz, but the level of this notch is smaller than in the case of OFL condition. For RML the air gap and mandrel filtering show small difference. Both of the frequency response traces are almost the same, they have one notch, and the shape of the traces are really similar, hence, almost the same performance is expected for air gap and mandrel filter for RML condition.

The SMF patchcord has totally flat frequency response for both of the launch conditions, but its insertion loss is different for the two launch conditions. For OFL the insertion loss (IL) is around 22dB and for RML it is 16dB. Basically, the insertion losses of mandrel and air gap filter behave similarly to each other in case of both launch types. SMF patchcord has higher insertion losses compared to mandrel and air gap filter which is around 10dB. The insertion losses (IL) of the filters are summarized in Table III. The IL is very important, because of higher IL the signal to noise ratio (SNR) is more significant. Therefore, the SMF patchcord is the most sensitive for SNR, however, it can eliminate most of the modal dispersion effect, as the SMF patchcord can produce flat frequency response. As the efficiency of the mode filters depend on the frequency response and the SNR level together, in the following, the mode filters are compared to each other with different SNR. In order to compare the mode filters with different SNR, modulated signals are used, and the EVM is analyzed. The EVM analysis can show a better comparison for the performance of the mode filters, as a result, the best mode filters can be found for each of the RoMMF setups.

B. EVM analysis

For EVM analysis, a modulated signal is applied at a certain carrier frequency. In this paper QPSK modulation is used for EVM analysis, and the carrier frequency is set to notch frequencies: for OFL the carrier frequency is 5.42 GHz, and for RML it is 4.5 GHz. At the notch frequencies the effect of the modal dispersion is the strongest, so it is worth to analyze the mode filtering effect at these worst case frequencies. As it is mentioned in above, the EVM investigation is made at two different SNR to analyze the performance of the link. The higher SNR is 40dB and the lower SNR is 30dB. These SNR

TABLE III
INSERTION LOSS (IL) OF DIFFERENT MODE FILTERS

	OFL-IL(dB)	RML-IL(dB)
no filter	1.66	0.87
mandrel	8.61	3.95
air gap	8.7	5.85
SMF patchcord	22.5	16.56

values are considered at the transmitter side. Although, the performance of the link is usually determined by SNR at receiver side, however, the SNR at the receiver side can be different for different mode filtering setups. The mode filters have different insertion losses (Table III), furthermore, the insertion losses depend on the carrier frequencies (Fig. 5 and Fig. 6). Consequently, it is easier to use the SNR at the transmitter side.

The quality of the transmission depends on the modulation bandwidth. The effect of modal dispersion is higher for higher modulation bandwidth, therefore, the EVM is simulated at different modulation bandwidths as well. The simulations are carried out by using VPI Transmission Maker 9.2 [15]. The model of the mode filtered RoMMF links are implemented to VPI according to the calculations, which are described above. The EVM analysis is carried out for different SNR and for both OFL and RML. First, the EVM results are plotted for OFL at higher SNR in Fig 7.

In this case, the SNR is relatively high, so the dominant distortion effect is the modal dispersion. The best mode filter is the SMF patchcord, and its performance is especially impressive at higher modulation bandwidth. At 500MHz the effect of the SMF patchcord is improved to 1.5%. The air gap filter has worse performance than the SMF patchcord and better performance than the mandrel filter. This experiences are agreed with the results of frequency responses.

At lower SNR the modal dispersion is not the only significant distortion effect, the noise can also limit the quality of the channel. The EVM results are plotted for OFL at lower SNR in Fig 8.

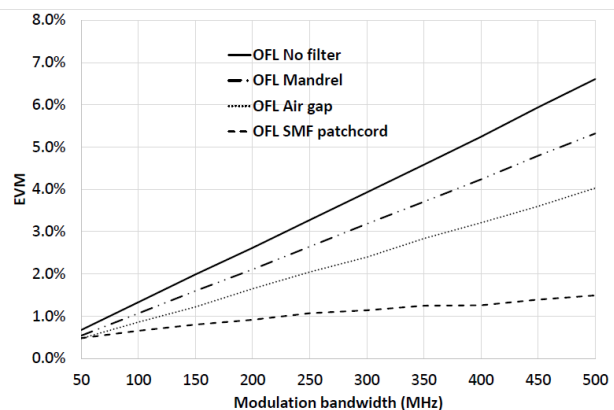


Fig. 7. Modulation bandwidth vs. EVM for OFL at higher SNR

Modeling and Simulation of Mode Filtered Radio over Multimode Fiber Links

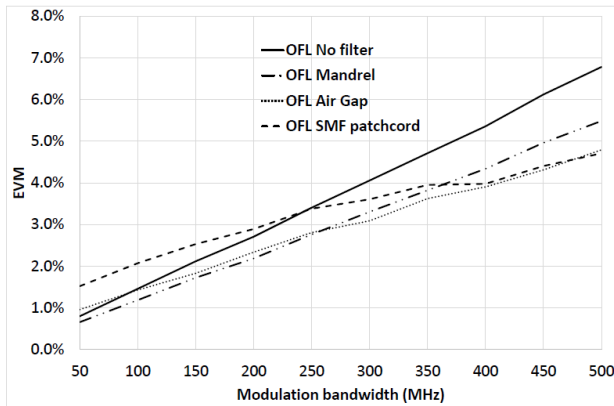


Fig. 8. Modulation bandwidth vs. EVM for OFL at lower SNR

In this case, the SMF patchcord is not effective enough especially at smaller bandwidth. When the modulation bandwidth is even higher, the modal dispersion affects the transmission more, so the performance of the SMF patchcord increases, but it is not as advantageous as at higher SNR. The air gap mode filter gives similar results: at higher modulation bandwidths, the air gap mode filter improves the quality of communication stronger than at lower modulation bandwidths. However, the mandrel have better performance at both lower and higher modulation bandwidths for OFL. As the mandrel is less sensitive to noise, due to its lower insertion loss, the mandrel can be a suitable type of mode filter at lower SNR for OFL.

When RML is applied the insertion losses of the mode filters are smaller (Table III), so the mode filters have different behavior. At higher SNR the results are shown in Fig. 9. As it can be seen, the mandrel and the air gap filter have almost the same performance. At 500 MHz modulation bandwidth the air gap improves the EVM from 5.5% to 5%, and the mandrel can improve the EVM to 4.5%. However, the SMF patchcord shows much better performance. When the link is mode filtered with SMF patchcord, the EVM is decreased to 0.9%. Hence, for RML at higher SNR the best mode filter is SMF patchcord.

At lower SNR the mode filters with higher insertion loss can be less advantageous. However, by applying RML launch

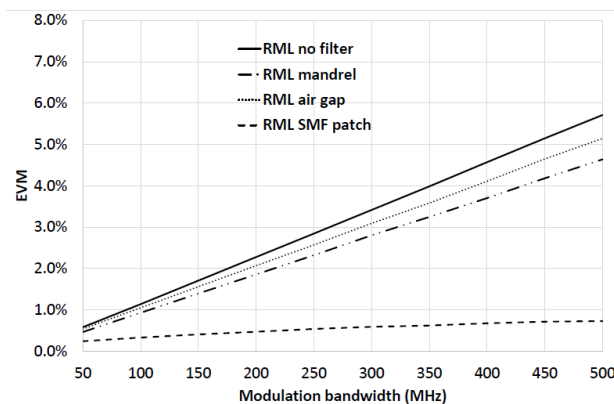


Fig. 9. Modulation bandwidth vs. EVM for RML at higher SNR

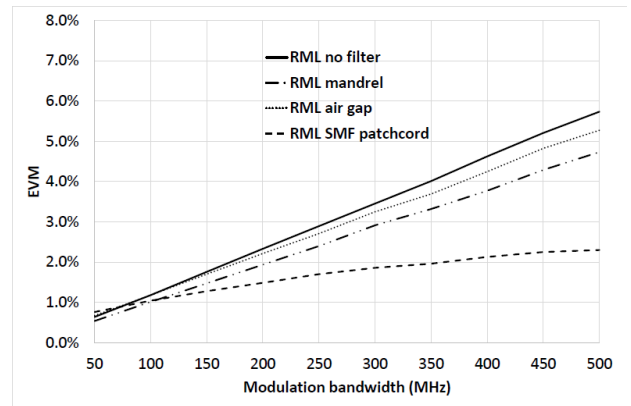


Fig. 10. Modulation bandwidth vs. EVM for RML at lower SNR

condition the insertion loss of the mode filters is much smaller than in the other case, when launch condition is OFL. At lower SNR with RML the results are shown in Fig. 10. In this case the SMF patchcord can reduce the EVM, but this improvement is smaller at lower SNR than at higher SNR. At lower SNR for RML the best mode filter is still SMF patchcord, because the mandrel and air gap filter cannot improve the quality of the communication as much as the SMF patchcord and the air gap mode filter and mandrel have almost the same performance. Thus, according to Fig. 10 the best mode filter for RML at lower SNR is the SMF patchcord, especially for higher modulation bandwidth.

By analyzing the EVM, the best mode filters for different RoMMF scenarios can be selected. These results are summarized in Table IV. It shows that for RML, the SMF patchcord is the best choice, however, for OFL the SMF patchcord shows better performance, when the SNR is high enough. On the other hand, at lower SNR, the mandrel and air gap filter could be a more advantageous choice than SMF patchcord.

TABLE IV
MODE FILTER SUMMARY

	OFL		RML	
	High SNR	Low SNR	High SNR	Low SNR
Low Modulation bandwidth	SMF patchcord	Mandrel/Air gap	SMF patchcord	SMF patchcord
High Modulation Bandwidth	SMF patchcord	Mandrel/Air gap	SMF patchcord	SMF patchcord

IV. CONCLUSION

To summarize, mode filtered radio over multimode fiber systems are investigated by simulations in this paper. The frequency response of the mode filtered RoMMF is modeled and simulated in order to find the most efficient mode filter at different RoMMF scenarios. Three different types of mode filters are analyzed in RoMMF: mandrel, air gap filter and SMF patchcord. Not only the frequency responses but also the EVM are simulated. The analysis is carried out for different launch conditions (OFL and RML) at different SNR level. The

frequency responses show that the SMF patchcord can eliminate the modal dispersion, but its insertion loss is also the highest. For OFL the insertion loss is higher than for RML, because for OFL the number of the mode groups are higher than for RML, and they do not propagate only around the center of the fiber, hence the mode filters can attenuate higher number of mode groups for OFL than for RML, which leads to higher insertion losses for the case of OFL.

The EVM analysis shows that SMF patchcord can be the best solution at higher SNR, and it could work fine at lower SNR as well, if the launch condition is RML. For OFL, at lower SNR, mandrel and air gap mode filter show better performance than the SMF patchcord. To conclude, if the launch condition is considered to be RML in a RoMMF system, the SMF patchcord is the best choice for mode filtering, especially at higher modulation bandwidth. At other scenarios mandrel or air gap filter can also shows advantageous behavior.

REFERENCES

[1] T. Cseh, E. Udvary, "Cost effective RoF with VCSELs and Multimode Fiber," in *16th European Conference on Networks and Optical Communications (NOC)*, Newcastle upon Tyne, UK, 2011, pp. 60-63.

[2] J. Siuzdak, G. Stepniak, "Influence of modal filtering on the bandwidth of multimode optical fibers," *Optica Applicata*, vol. 37, no. 1-2, pp. 31-39, 2007.

[3] L. Raddatz, I. H. White, D. G. Cunningham, M. C. Nowell, "An Experimental and Theoretical Study of the Offset Launch Technique for the Enhancement of the Bandwidth of the Multimode Fiber Links," *Journal of Lightwave Technology*, vol. 16, no. 3, pp. 324-331, March, 1998.

[4] A. G. Hallem, "Mode Control in Multimode Optical Fibre and its Applications," PhD dissertation, Aston University, 2007.

[5] G. Yabre, "Comprehensive Theory of Dispersion in Graded-Index Optical Fibers," *Journal of Lightwave Technology*, vol. 18, no. 2, pp. 166-177, February, 2000.

[6] I. Gasulla, J. Capmany, "RF transfer function of analogue multimode fiber using an electric field propagation model: Application to Broadband Radio over fiber systems," in *International Topical Meeting on Microwave Photonics*, Grenoble, France, 2006, pp. 1-4.

[7] D. S. Montero, I. Gasulla, I. Möllers, D. Jäger, J. Capmany, "Experimental Analysis of Temperature Dependence in Multimode Fiber Optical Links for Radio-over-Fiber Applications," in *17th International Conference on Transparent Optical Networks*, Sao Miguel, Azores, Portugal, 2009, pp. 1-4.

[8] L. A. Neto, D. Erasme, N. Genay, P. Chanclou, Q. Deniel, F. Traore, T. Anfray, R. Hmadou, C. Aupetit-Berthelemot, "Simple Estimation of Fiber Dispersion and Laser Chirp Parameters Using the Downhill Simplex Fitting Algorithm," *Journal of Lightwave Technology*, vol. 31, no. 2, pp. 334-342, January, 2013.

[9] D. Glöge, "Optical Powerflow in Multimode Fibers," *The Bell System Technical Journal*, vol. 51, no. 8, pp. 1767-1783, October, 1972.

[10] R. Olshansky, "Mode Coupling Effects in Graded-Index Optical Fiber," *Applied Optics*, vol. 14, no. 4, pp. 935-945, 1975.

[11] G. Stepniak, J. Siuzdak, "An efficient method for calculation of the MM Fiber frequency response in the presence of mode coupling" *Optical and Quantum Electronics*, vol. 38, no. 15, pp. 1195-1201, December, 2006

[12] P. Pepeljugoski, S. E. Golowich, A. J. Ritger, P. Kolesar, A. Risteski, "Modeling and Simulation of Next-Generation Multimode Fiber Links," *Journal of Lightwave Technology*, vol. 21, no.5, pp. 1242-1255, May, 2003.

[13] T. Cseh, T. Berceli: "Improved Receiver Techniques for Radio over Multimode Fiber Systems." *18th European Conference on Networks and Optical Communications (NOC)*, Graz, Austria, 2013, pp. 23-26.

[14] T. Cseh, T. Berceli: "Dispersion compensation in millimeter wave radio over fiber systems" *Microwave and Optical Technology Letters*, vol. 57, no. 1, pp. 204-207, January, 2015.

[15] VPI Transmission maker/VPI component maker, user's manual, May 2014



Tamás Cseh received the B.S. and M.S. degrees in electric engineering from the Budapest University of Technology and Economics. He started his Ph.D. studies in 2011, and he is currently a Research Assistant at Budapest University of Technology and Economics, Department of Broadband Infocommunication and Electromagnetic Theory. His interest includes optical communication with multimode fibers, and radio over fiber systems and dispersion compensation methods. He has authored and co-authored about 15 papers. Mr. Cseh is a member of Scientific Association for Infocommunications, Hungary (HTE)



Tibor Berceli graduated in electrical engineering at the Technical University of Budapest. He received the Doctor of Technical Science (D.Sc.) degree from the Hungarian Academy of Sciences. Dr. Berceli is Professor of Electrical Engineering at the Budapest University of Technology and Economics

As a researcher he worked on surface wave transmission lines, dielectric waveguides, several kinds of microwave semiconductor oscillators and amplifiers, parametric circuits, up- and down-converters, injection locked oscillators, etc.

His present field of interest is the combined optical-microwave circuits and systems. He initiated a new lightwave-microwave phase detector, and new mixing processes. He suggested new approaches for optical millimeter wave generation and sub-carrier optical transmission. Prof. Berceli is Life Fellow of IEEE. He is the author of 226 papers and 6 books published in English. He presented 96 papers at international conferences. Dr. Berceli was visiting professor at universities in the USA, UK, Germany, Japan, France, Finland and Australia

Fault-Tolerance Algorithm in Wireless Sensor Networks.

Nasser Al-Qadami and Andrey Koucheryavy

Abstract— In wireless sensor networks that rely on clustering hierarchical structure for routing and information exchange, some nodes are essential and have a pivotal role in the clustering process and data routing. Consequently, any failures of these important nodes may cause paralysis of the network and effect on the quality of services and the reliability of the network. In this paper, we proposed a fault tolerant routing TEEN (FT-TEEN) algorithm which is a modified version of the well-known TEEN protocol; FT-TEEN proposes vital solutions to some shortcomings of the pure TEEN. It provides fault detection, recovery process, reliability and quality of service. The simulation results showed a significant reliability in the amount of receiving data by the cluster heads and the base station compared to the amount of data in the reference TEEN protocol. The developed algorithm can be used in the ground fragments flying ubiquitous sensor networks.

Keywords — Wireless Sensor Networks (WSNs), Fault-Tolerance (FT), Fault Detection, Fault Recovery, Reliability, Clustering, TEEN protocol.

I. INTRODUCTION

A WIRELESS sensor network is made up of ultra-low-power consuming, low cost, distributed devices called sensor nodes that combine sensing, computation and communication [1]. Features such as low cost, low power, compact size and robustness of these sensor nodes aid them from being used for various applications [2]. One of the important sensor network applications is to detect, classify, and locate specific events, and track targets over a specific region. An example is to deploy a sensor network in battlefield to detect tanks [3]. A new application of sensor networks is flying ubiquitous sensor networks, which required high reliability and quality of service [11]. Data aggregation is a typical operation in many WSNs applications, especially, in hierarchical routing protocol for self-organizing WSNs manner is widely used for prolonging network lifetime, eliminate data redundancy and reduce the communication

load. One of the most important design issues and challenges for designing an effective and efficient wireless sensor network is adapting to changes in connectivity, scalability and fault tolerance.

A failure of some nodes in WSNs is almost unavoidable, due to a variety of reasons: energy depletion, hardware failure, software failure, communication link errors, malicious attack, etc. [4]. So the fault detection and recovery should be addressed in different applications of WSNs. Fault tolerance is the ability of a system to deliver a desired level of functionality in the presence of faults [5].

Actually, several works have been done that address one way or another fault tolerance in WSNs. In [6] the authors classified fault tolerance in WSNs into five levels, physical layer, hardware layer, system software layer, middleware layer, and application layer. Another research work on fault tolerance is fault management using cluster-based protocol in WSNs [7]. A priori methods for fault tolerance in wireless sensor networks were discussed in [8]. In hierarchical routing algorithm nodes organize themselves into clusters and cluster head is selected for each cluster. Cluster head nodes collect data from cluster members, produce processing and transmission of information on gateway or base station. This aggregation of data nodes in the head considerably reduces the energy consumption in the network and increases the life cycle duration. A typical example of the implied hierarchical clustering in WSNs is further illustrated in fig. 1.

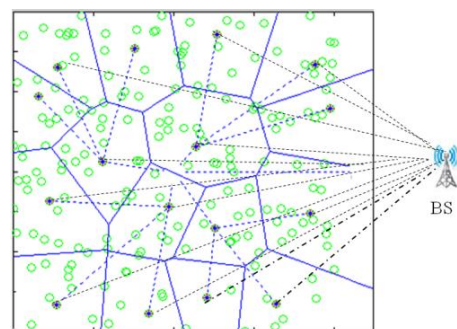


Fig. 1. Clustering Architecture

II. REVIEW OF TEEN PROTOCOL

TEEN [9] (Threshold sensitive Energy Efficient sensor Network protocol): is a reactive, event-driven protocol for time-critical applications, which uses randomization to

Submitted date paper for review 21.09.15. This study was supported by RFBR under the research project №15-07-09431a "Development of principles of construction and methods of self-organizing for flying sensor network".

Mr. Nasser Al-Qadami joined St. Petersburg University of Telecommunication, Russia, as a PhD student in the Department of Communications Networks in 2013. (E-mail: alkadami@spbgut.ru).

Dr. Sc. Andrey Koucheryavy is Chaired professor of the department of "Telecommunication Networks and Data Transmission" in the St. Petersburg State University of Telecommunication (SUT). pr.Bolshevikov22, St. Petersburg, Russia, 193232, (E-mail: akouch@mail.ru).

distribute the energy load evenly among the wireless sensor network [9]. A non-cluster head node senses the environment continuously, but turns the radio on and transmission only if the sensor value changes drastically and doesn't wait until the next period to transmit critical data.

Functioning of TEEN protocol:

At the beginning of each round each node in a cluster takes turns to become the cluster-head (CH) for a time interval called cluster period (cluster change time). The CH broadcasts in the following threshold values to its cluster members at every cluster setup phase (cluster change time):

- Hard Threshold (HT)
 - An absolute value for the sensed attribute.
 - A cluster member only reports/sends data to CH by switching on its transmitter, only if the node senses this value.
- Soft Threshold (ST)
 - It is a small change in the value of the sensed attribute which causes the node to turn on its transmitter.
 - A cluster member only reports/sends data to CH by switching on its transmitter, if its value changes by at least the soft threshold.

The operation is divided into rounds, each round contains two states:

A. Setup phase:

In TEEN protocol, cluster head formation process is based on LEACH [10] (Low Energy Adaptive clustering Hierarchy). Each sensor node generates a random number between 0 and 1. The node becomes a cluster head for the current round if the number is less than the following threshold:

$$T(n) = \begin{cases} \frac{P}{1 - P[r \bmod (1/P)]} & \text{if } n \in G \\ 0 & \text{otherwise,} \end{cases} \quad (1)$$

Where: P = Desired cluster head, percentage (e.g., P= 0.05), r = Current Round, G = Set of nodes which have not been cluster heads in 1/P rounds, 1/P is the expected number of nodes in one cluster. After a cluster head selection, each sensor node joins a cluster-head that requires the minimum communication energy.

B. Steady-state phase:

Once the cluster heads (CHs) are selected, the CH node creates a TDMA schedule and assigns each node a time slot when it can transmit. The members of the cluster sense their surroundings continuously. The first time a sensed data reaches its hard threshold value, the node transmits the sensed data. The sensed value is stored to a variable called the sensitive value (SV).

- Sensor nodes transmit data in the current cluster period only when the following conditions are true:
 - The current value of the sensed attribute is greater than the hard threshold.
 - The current value of the sensed attribute differs from the sensed value by an amount equal to or greater than the soft threshold.

In TEEN protocol, the hard threshold (HT) reduces the number of transmissions by sending only when the sensed data is in the range of interest. Also, the soft threshold reduces the number of transmissions by excluding from the transmissions which have little or no change in the sensed data.

III. ALGORITHM DESCRIPTION

Unexpected failure of CH may cause paralyzing the network or degrades application performance; therefore, CH node fault detection and recovery are very important.

For our proposed model, we adopt a few reasonable assumptions of the network model as follows:

- Sensor nodes are deployed densely and randomly in sensor field.
- The radio channel is symmetric.
- All the sensor nodes had an equal amount of energy.
- The proposed mechanism can be applied to many hierarchical routing protocols such as LEACH protocol.

The proposed algorithm is a modified version of the TEEN protocol, introduces a backup mechanism for cluster heads, providing fault recovery process and consists of two phases:

A. Advertising Phase (cluster formation)

In advertising phase, the clusters are organized and CHs are selected based on LEACH protocol mechanism. After selection the CHs advertise their selection to all other nodes. All nodes choose their nearest CH after receiving advertisements based on the received signal strength (RSS) and send to them join request including their current energies.

The CHs then find the node that has the max energy from cluster members, determine it as a sub-CH and send it to cluster members.

Fig. 2 shows the cluster formation in the proposed algorithm.

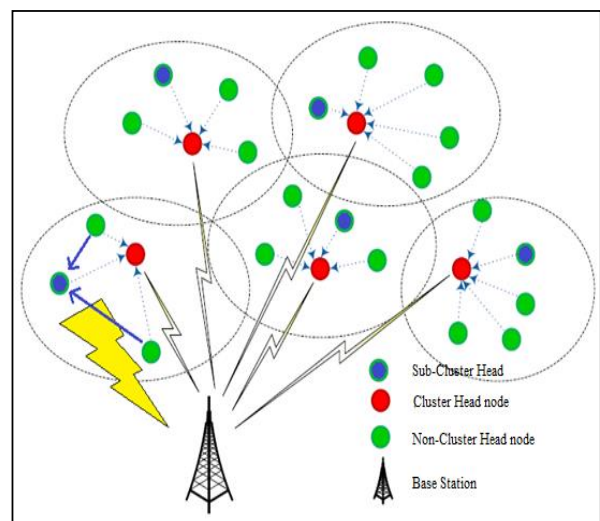


Fig. 2. Clustering in the proposed algorithm

The steps of advertising phase (cluster formation) procedure are described in Algorithm 1.

Algorithm 1 – Advertising Phase

```

1: do { //repeat for R rounds
2: if ( $E_{init}(s) > 0$  &  $s$  in  $G$ ) Then
3:    $r \leftarrow \text{random}(0, 1)$ ;
4:   Compute  $T(s)$ ; //given by (1)
5:   if ( $r < T(s)$ ) Then
6:      $CH\{s\} = \text{TRUE}$ ; //node  $s$  be a  $CH$ ;
7:   else
8:      $CH\{s\} = \text{FALSE}$ ; //node  $s$  not be a  $CH$ ;
9:   end if
10: end if
11: if ( $CH\{s\} = \text{TRUE}$ ) Then
12:    $BC(ADV)$  includes  $\leftarrow$  broadcast an advertisement message;
13:    $Join(IDi, \text{Residual energy})$ ; // non-cluster head node  $i$  join;
14:   Select the node with max energy as sub  $CH$ ;
15:    $Cluster(c)$ ; //form a cluster  $c$ ;
16: end if

```

R:	round
$E_{init}(s)$:	Initial energy
$T(s)$:	Threshold value
Msg :	Check message
ADV:	Advertisement message
BC:	Broadcast
PCK:	Packets
IDi :	Node Identification id

B. Data Transmission Phase

In data transmission phase the CH and sub CH exchange status message periodically and all normal nodes begin sensing and transmitting data to the cluster-head and sub cluster-head in their cluster. After receiving all the data, the cluster-head nodes aggregate it before sending it to the Base-Station (BS). Just like TEEN protocol the hard threshold (HT) reduces the number of transmissions by sending only when the sensed data is in the range of interest. Also, the soft threshold reduces the number of transmissions by excluding from the transmissions which have little or no change in the sensed data.

The steps of data transmission procedure are described in Algorithm 2.

Algorithm 2 – Data transmission

```

1: if (node is CH or sub) then
2:    $Receive(IDi, DataPCK)$  //receive data from members;
3:    $Aggregate(IDi, DataPCK)$  //aggregate received data;
4:    $Trans\ To\ BS(IDi, DataPCK)$ ; //transmit received data;
5: else
6:   if (node has data values are in the range of interest) then
7:      $Trans\ To\ CH\ and\ sub\ CH(IDi, DataPCK)$ ; //transmit sensed data to  $CH$  and sub  $CH$ ;
8:   else
9:      $SleepMode(i) = \text{TRUE}$ ; //node  $i$  at a sleep state;
10:  end if
11: end if
12: // one Round is completed.

```

IV. FAULT DETECTION & FAULT RECOVERY PROCESS

The proposed algorithm (FT-TEEN) detects and recovers the fault according to the following mechanism:

Step 1: Initialize CH & sub-CH in every cluster.

Step 2: IF no response comes from CH to sub CH within a time interval.

THEN

Step 3: Set CH as Faulty and sub-CH becomes CH in the cluster.

Step 4: IF no response comes from sub-CH to CH within a time interval.

THEN

Step 5: Set sub CH as Faulty and CH finds a new sub-CH from its cluster member.

Algorithm 3 – Fault Detection & Fault Response

```

Do { // For every cluster (c)
1:  $Exchange\ check\ Msg\ between\ CH\ and\ sub\ CH$ ;
2: if no response comes from  $CH$ ;
3:   Set  $CH$  as Faulty,  $CH \leftarrow sub\ CH$ ;
4: if no response comes from  $sub\ CH$ ;
5:  $Set\ sub\ CH$  as Faulty,  $CH$  find new sub  $CH$ 
}

```

The flow chart of the distributed cluster formation process is shown in fig. 5. While the flow chart of the steady state phase for the proposed algorithm shown in fig. 6.

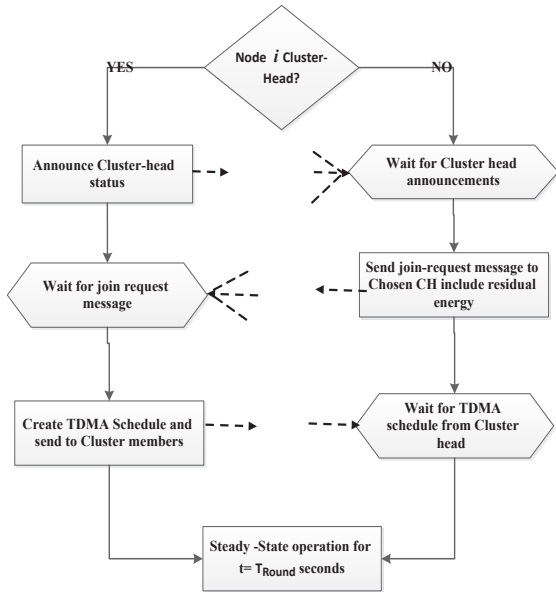


Fig. 5. Flow chart of the distributed cluster formation for the proposed algorithm

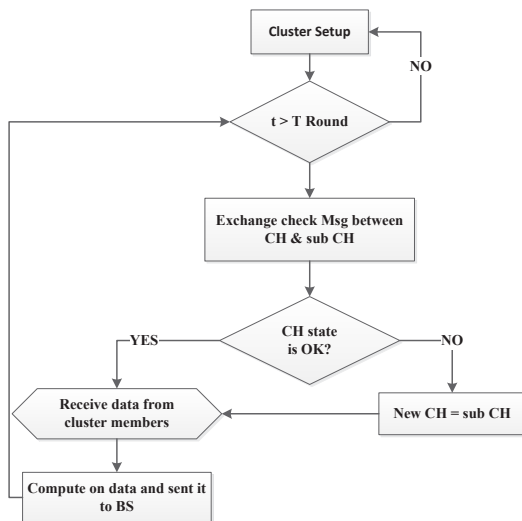


Fig. 6. Flow chart of the steady state phase for the proposed algorithm

V. SIMULATION/PERFORMANCE EVALUATION

In this section, for evaluating the performance of our proposed fault-tolerant algorithm through simulation results using MATLAB, we (compared) simulated FT-TEEN with TEEN protocol in terms of the number of data packets that are successful in reaching the base station from cluster heads and

cluster heads from their members every round and the cumulative average for the amount of data transferred over the network lifetime to the CHs and BS respectively. We have carried out these simulations with the same scenario presented in TEEN in order to illustrate the performance of our contribution. Hence, we considered a network topology with 100 sensor nodes placed randomly in a 100m*100m network region and a remote base station, which is located outside the area at (X=130, Y=50), with the radio model communication parameters shown in Table I.

The other values in the Table I selected based on [12]; the simulations were performed until all the sensors in the network consumed their energy. The data packet size was 512 and the number of frames in every round is 10.

TABLE I. SIMULATION PARAMETER

Parameter	Value
E_{elec}	50 nJ/bit
ϵ_{amp} friss-amp	10 pJ/bit
ϵ_{amp} two-ray-amp	0.0013 pJ/bit
DCrossover	87 m
P	5%
Initial energy	0.5 Joule
Packet size	512 bits
Soft Threshold(ST)	2
Hard Threshold(HT)	100

Fig. 7, 8 show the average of packets received at the CHs and the BS in TEEN and FT-TEEN per round when the fault probability in the CHs at 10 % and desired cluster head percentage is p=5%.

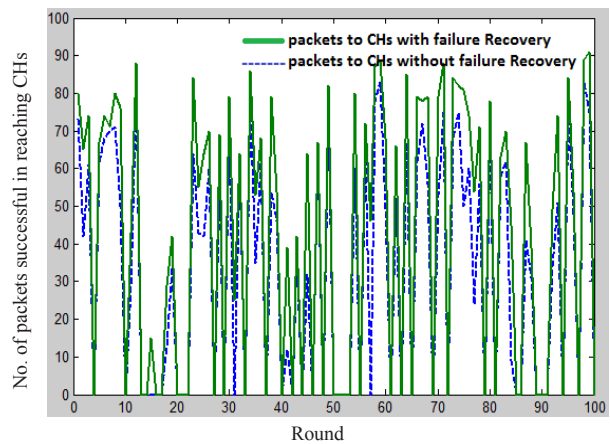


Fig. 7. No. of data packets those are successful in reaching the CHs in TEEN & proposed protocol every round (Pf=10%)

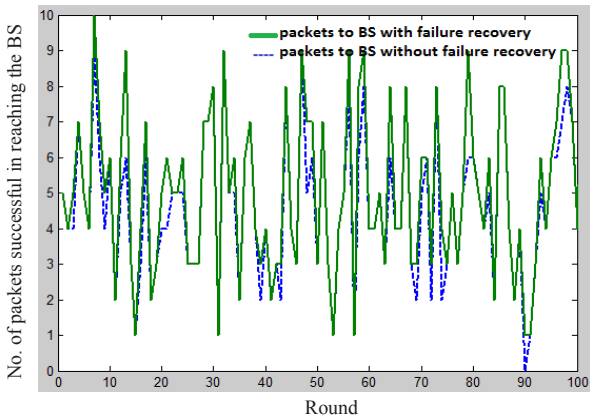


Fig. 8. No. of data packets those are successful in reaching the base station in TEEN & proposed protocol every round (Pf=10%)

In this scenario, to test the performance of the proposed protocol when the fault Probability is bigger, we set the fault probability in the CHs at 20 %, $p=5\%$.

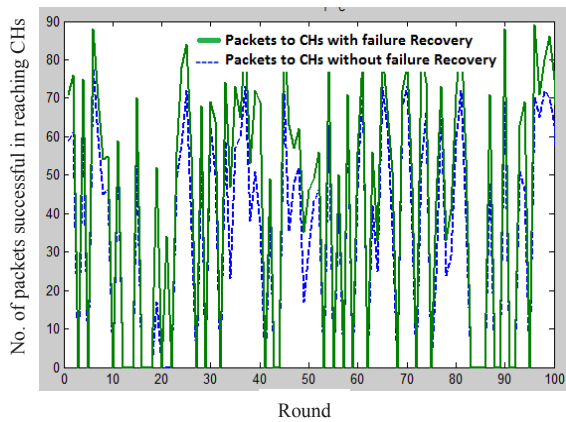


Fig. 9. No. of data packets those are successful in reaching CHs in TEEN & proposed protocol every round (Pf=20%)

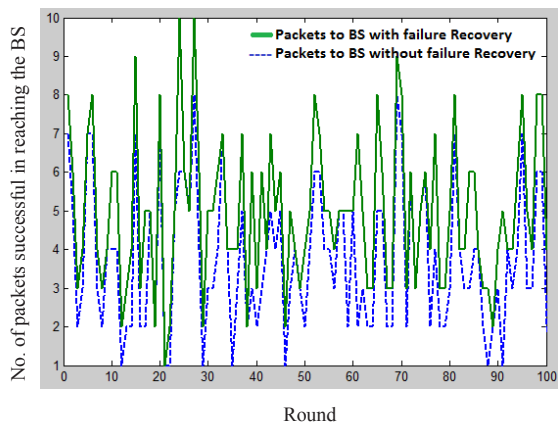


Fig. 10. No. of data packets those are successful in reaching the base station in TEEN & proposed protocol every round (Pf=20%)

It is clear from the simulation results shown in Fig. 7, 8, 9, 10 that, the average packets received at the CHs and the sink in TEEN protocol is less compared to the new mechanism (with failure recovery). The result show also, whenever the fault probability is bigger, the feasibility and efficiency of the proposed protocol is better. Here it should be noted that the fluctuations in the number of receiving packets caused by the fluctuation in the number of elected CHs in TEEN protocol every round.

The cumulative average of the amount of data transferred over the network lifetime to the CHs and BS with failure detection (FT-TEEN) and without failure detection (normal TEEN) at different fault probability is shown in the cumulative graphs 11, 12. Where the loss of transferring data, increasing when the fault probability increasing for TEEN, while the amount of data transferred by the proposed algorithm is constant and much more than TEEN, because the proposed algorithm detecting and recovering any fault in the CHs.

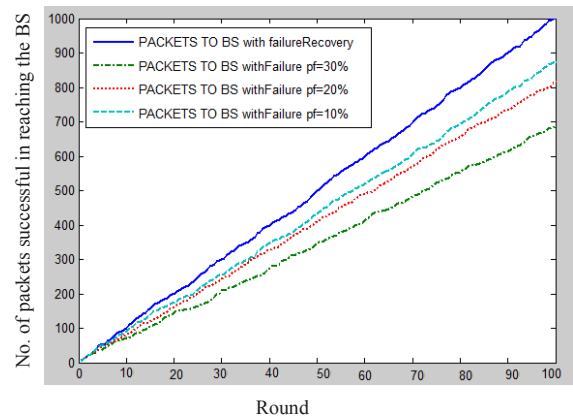


Fig. 11. Transferred data over the network lifetime to BS

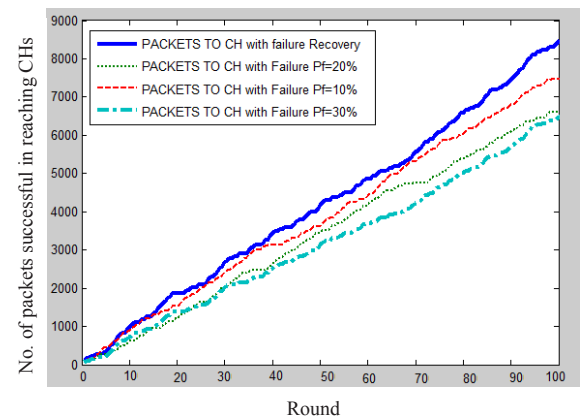


Fig. 12. Transferred data over the network lifetime to CHs

These results are shown in numbers in Table II besides, the improvement ratio of the amount of data transferred over the network lifetime to the CHs and BS with failure detection (FT-TEEN) and without failure detection (normal TEEN).

TABLE II. SIMULATION RESULTS

Head Failure Rate	Head Failure Rate					
	TEEN		Proposed Algorithm		Improvement Ratio	
	Without Failure detection and Recovery		With Failure detection and Recovery			
	No. Packets in CHs	No. Packets in BS	No. Packets in CHs	No. Packets in BS	In CHs	In BS
Pf=10%	7500	876	8409	1005	12%	15%
Pf=20%	6655	822	8409	1005	26%	22%
Pf=30%	6405	692	8409	1005	30%	45%

VI. CONCLUSION

In this paper, we proposed an innovative, scalable way to avoid the fault-tolerance in WSNs (FT-TEEN) which is a modified version of the well-known TEEN protocol, simulation results showed that:

- 1) The proposed mechanism out performs TEEN protocol and has improved the performance of TEEN in terms of number of packets successfully received at the base station with 12% and the number of packets successfully received at cluster heads with 15% if cluster heads failure percent is 10% and with 26% & 22% if the failure probability is 20%.
- 2) TEEN is not an efficient in data transferred to CHs as in data transferred to BS, because CHs may be failed for all rounds. The proposed algorithm delivers more data to CHs and to BS because it uses many steps to detect CHs failure and use alternative CHs.
- 3) The proposed algorithm detecting and recovering any fault in the CHs so, the amount of data transferred by the proposed algorithm is constant and much more than TEEN while, the loss of data transferring data increasing when the fault probability increasing in teen protocol.
- 4) The proposed algorithm enables the network to maintain maximum network connectivity and quality of service under failure conditions.
- 5) The drawback of this algorithm is the overhead communication that caused by exchanging status messages between the CH and sub CH at the beginning of each frame and also caused by advertising a new cluster head to the members of the cluster in the event of failure.

FUTURE WORK

In the future work we are going to quantify the communication overhead between CH and sub-CH and applied this mechanism to others hierarchical routing protocols.

REFERENCES

- [1] Michael May. "Design of a Wireless Sensor Node Platform," University of Waikato 2012.
- [2] Sudip Misraa, Manikonda Pavan Kumara, Mohammad S. Obaidatb, "Connectivity preserving localized coverage algorithm for area monitoring using wireless sensor networks," Kharagpur, India, Monmouth University, New Jersey, USA 2011.
- [3] Hai Liu, Amiya Nayak, and Ivan Stojmenovi' "Fault-Tolerant Algorithms/Protocols in Wireless Sensor Networks," Chapter 10 Guide to Wireless Sensor Networks, Computer Communications 261 and Networks, DOI: 10.1007/978-1-84882-218-410, Springer-Verlag London Limited 2009.
- [4] Meenakshi Panda and P. M. Khilar "Energy Efficient Distributed Fault Identification Algorithm in Wireless Sensor Networks,," Journal of Computer Networks and Communications, Volume 2014 (2014), Article ID 323754, 16 pages.
- [5] Doo-Soon Park, "Fault Tolerance and Energy Consumption Scheme of a Wireless Sensor Network," International Journal of Distributed Sensor Networks, Volume 2013 (2013), Article ID 396850, 7 pages.
- [6] F. Koushanfar, M. Potkonjak, and A. Sangiovanni-Vincentelli, "Fault Tolerance in Wireless Sensor Networks," in Handbook of Sensor Networks, I. Mahgoub and M. Ilyas (Eds.), CRC press, Section VIII, no. 36, 2004.
- [7] M. Hla Yin and Z. Win, "Fault Management Using Cluster-Based Protocol in Wireless Sensor Networks," International Journal of Future Computer and Communication vol. 2, no. 6, pp. 36-39, 2014.
- [8] Bellalouna, M.; Ghabri, A., "A priori methods for fault tolerance in wireless sensor networks," Computer and Information Technology (WCCIT), 2013 World Congress on, vol., no., pp.1,6, 22-24 June 2013.
- [9] M. Arati and P. A. Dharma, "TEEN: a routing protocol for enhanced efficiency in wireless sensor networks," in Proceedings of the 15th International Parallel & Distributed Processing Symposium, pp. 2009–2015, San Francisco, Calif, USA, April 2001.
- [10] Heinzelman, W. R. Chandrakasan, A.; Balakrishnan, H. "Energy-efficient communication protocol for wireless microsensor networks." In Proceedings of the Hawaii International Conference on System Sciences, Maui, Hawaii, Jan 2000.
- [11] Ruslan Kirichek, Alexandr Paramonov, Andrey Koucheryavy "Flying Ubiquitous Sensor Networks as a Queueing System," Phoenix Park, PyeongChang, Korea ICACT2015, Jun. 2015.
- [12] Heinzelman, W.R, " Application Specific Protocol Architectures for Wireless Sensor Networks," Massachusetts Institute of Technology. June 2000.



Mr. Nasser Al-Qadami joined St. Petersburg University of Telecommunication, Russia, as a PhD student in the Department of Communications Networks in 2013. He was born in May 1983 in Sana'a, Yemen. He received his BSc and MSc degree from Odessa National Academy of Telecommunications A.S Popov (ONAT), Odessa, Ukraine in 2009 and 2011, respectively. He had worked as a lecturer at Sheba 'a University and Cisco Academy in Sana'a until 2013. His research interests

include Communication Systems, Networks Systems and Wireless Sensor Networks.



Dr. Sc. Andrey Koucheryavy was born in Leningrad 02.02.1952. After graduated from Leningrad University of Telecommunication in 1974 he going to Telecommunication Research Institute named LONIIS, where A. Koucheryavy working up to October 2003 (from 1986 up to 2003 as the First Deputy Director). He became the Ph.D. and D.Sc. in 1982 and 1994 respectively. A. Koucheryavy is the St. Petersburg State University of Telecommunication (SUT) professor from 1998. He is Chaired professor

of the department "Telecommunication Networks and Data Transmission" from 2011. He is honorary member of A.S.Popov's society. Prof. A. Koucheryavy was the vice-chairman Study Group 11 ITU-T (Study periods 2005-2008, 2009-2012). His scientific areas of interest are the network planning, tele-traffic theory, IoT and its enablers.

On Measuring the Geographic Diversity of Internet Routes

Attila Csoma, András Gulyás and László Toka

Abstract—Route diversity in networks is elemental for establishing reliable, high-capacity connections with appropriate security between endpoints. As for the Internet, route diversity has already been studied at both Autonomous System- and router-level topologies by means of graph theoretical disjoint paths. In this paper we complement these approaches by proposing a method for measuring the diversity of Internet paths in a geographical sense. By leveraging the recent developments in IP geolocation we show how to map the paths discovered by traceroute into geographically equivalent classes. This allows us to identify the geographical footprints of the major transmission paths between end-hosts, and building on our observations, we propose a quantitative measure for geographical diversity of Internet routes between any two hosts.

Index Terms—geodiversity; traceroute; geolocation; disjoint routes

I. INTRODUCTION

The value of knowledge of the Internet topology is arguably immense. In the last decades we have witnessed a myriad of stories in which topology-related information about the Internet was directly compiled into more efficient architectures, services and more appropriate business decisions. Content Delivery Networks (CDNs) [1], in which global topological peculiarities are highly exploited for e.g. surrogate server and cache placement strategies or request routing mechanism, are just a narrow segment of the whole spectrum. Peer-to-peer networks [2, 3], data center placement [4], traffic engineering [5], business-based AS peering strategies [6], just to mention a few, are all receivers of Internet topology related knowledge. With this non-comprehensive list of receivers in mind, it should come at no surprise that many researchers have contributed to our current understanding of the topology of the Internet.

An elemental metric of Internet topology is the diversity of routes between end-hosts, as multiple uncorrelated routes can provide better throughput, resiliency and security. In [7], [8] and [9] authors describe how to increase the resiliency of

future networks and the role of multipath communication in it. A detailed description about network security can be found in [10] and authors in [11] propose a method which improves network security; however it requires multiple path between end-hosts.

Existing studies of IP-level route diversity usually focus on extracting routes between end-hosts, e.g. by using `traceroute`, and on computing their diversity by means of edge or node disjointness in a graph theoretical sense [12, 13, 14]. Such analysis provides an interpretation of route diversity in a microscopic level where each node in the route is a router interface having a particular IP address. In [15] the authors propose to interpret route diversity at a higher level, namely at the level of PoP's (Point of Presence): the interfaces residing in the same building or campus are grouped together, forming a PoP, and finally route diversity is computed at the level of these PoP's. In this paper we interpret route diversity at an even higher, geographical level. We propose grouping routers in a given geographic vicinity and compute route diversity at the level of geographical regions (e.g. the level of cities) independently from ASes. Our contribution is threefold: *first we describe a method for identifying the geographically equivalent routes in traceroute outputs; second, we show the efficiency of the method in terms of successfully merged traceroute routes and present their possible applications; finally we define a metric which can capture the geo-diversity of Internet routes between endpoints and compute this metric for our measurement dataset.* Such characterization of routes' "geo-diversity" is clearly beneficial if one is curious about connectivity between end-hosts in case of e.g. power outages affecting larger geographical areas. is also given about how

The rest of the paper is organized as follows. In Sec. II we overview the corresponding related work. Sec. III describes our `traceroute` measurements and our algorithms for extracting geographically equivalent routes from those. In Sec. IV we define and evaluate a metric called Geographic Diversity Index (GDI) that captures how Internet routes differ from each other. In Sec. V we validate our framework and present its performance. Finally we draw the conclusions and list the possible applications and future work in Sec. VI.

II. RELATED WORK

Numerous existing studies apply geographical information to uncover non-trivial aspects of the Internet topology. In [16] the authors use the geographical positions of routers to estimate route circuitousness, route length distribution and

Manuscript received October 7, 2015, revised December 21, 2015.

A. Csoma is with Budapest University of Technology and Economics, Hungary and with HSNLab, Dept. of Telecommunications and Media Informatics. e-mail: csoma@tmit.bme.hu

A. Gulyás is with Budapest University of Technology and Economics, Hungary, with HSNLab, Dept. of Telecommunications and Media Informatics and with MTA-BME Information Systems Research Group. e-mail: gulyas@tmit.bme.hu

L. Toka is with Budapest University of Technology and Economics, Hungary, with HSNLab, Dept. of Telecommunications and Media Informatics and with MTA-BME Information Systems Research Group. e-mail: toka@tmit.bme.hu

The work of László Toka was supported by the János Bolyai Research Scholarship of the Hungarian Academy of Sciences (MTA).

geographic fault tolerance from an end-to-end and from an ISP perspective. However, the DNS name-based geolocation method used in their work has its own limitations and may create a false spatial distribution as described in [17]. The distance and angle between consecutive IP hops are investigated in [18]. In [19] the authors use geographic information to construct the hyperbolic map of the Internet and prove the navigability of the AS level topology using greedy algorithms. Points of presence are detected using delay constraints on an IP interface graph and the distribution of PoPs around the globe is visualized in [15]. Authors of [20] used PoP detection to evaluate the accuracy of some IP geolocation database. Inter-AS route diversity is examined through the network of Sprint in [14]. In [21] the authors study the route diversity of multi-homed and overlay networks as seen from multiple vantage points using graph theoretical methods exclusively. However none of these works capture route diversity in the pure geographical sense on the router-level.

III. MEASUREMENT FRAMEWORK

We built a framework that determines the extent of geographical heterogeneity of end-to-end routes that are being used to carry traffic between any two points in the Internet. The method that we implemented is the following: first, we run `traceroute` measurements to collect the IP-level routes between the selected endpoints; second, we use *MaxMind* [22], a localization tool that determines the geographical position of the recorded IP addresses; third, we group those IP-level routes that we consider equivalent from a geographical perspective; finally, we calculate a route diversity index for the selected endpoints. In this section we present these steps in details.

A. Route measurements with `traceroute`

Usually `traceroute` is used to discover end-to-end routes between two endpoints in the Internet. Network operators use it for detecting network errors, researchers use it to build Internet topology models. Although most in-network routers and endpoints support its operation, `traceroute` has a number of well-known shortcomings. On one hand it can be easily deceived by load-balancers, on the other hand it is an active measurement tool and due to the extra data traffic it generates, certain network equipment are configured to disable reactions to `traceroute` (and `ping`).

Several projects exist that collect `traceroute` measurements and make them publicly available. These data sources differ significantly based on their vantage point types, their vantage point location, the `traceroute` implementation they run and their endpoint selection methods. Two such projects are IPlane [23] and CAIDA's ITDK (Internet Topology Data Kit) [24]. IPlane offers a route performance prediction service and periodically runs `traceroute` measurements from PlanetLab [25] nodes to a set of endpoints changed bi-weekly. ITDK data sets are produced from measurements collected by CAIDA's Archipelago project: `paris-traceroute` [26] is run from 89 vantage points spread over 37 countries to randomly selected endpoints. In order to measure route diversity between two endpoints, we need to detect as many

routes between those two endpoints as possible. Although the `paris-traceroute` output of ITDK is more reliable than that of IPlane's `traceroute`, the random selection of endpoints implemented by CAIDA hinders the collection of routes between the same vantage- and endpoints. Therefore we used the data of IPlane's `traceroute` measurements.

B. IP localization and filtering of routes

Once we have the IP-level routes, we determine the geographic position of each node appearing in them. Naturally the accuracy of the positioning is of paramount importance. As it is also noted in [27, 17], the use of DNS names and contents of various registries leads to unacceptable inaccuracy. Instead, we use the freely available geolocation tool MaxMind GeoLite [22] in order to establish the position for the IP addresses recorded in the measurements. As pointed out in [28], it is one of the most reliable, freely available geolocation database.

We filter the `traceroute` dataset from IPlane in order to remove measurements of vantage- and endpoint pairs between which only 1 IP-level route was observed. After localizing the IP hops, we further removed those vantage- and endpoint pairs between which only 1 geographic path was observed. With this second filter we eliminated traces differing only due to IP-aliasing and load balancing. The remaining set of traces contained ~ 0.5 million discovered routes; interestingly $\sim 80\%$ of vantage- and endpoint pairs had only 1 geographic path in the measurements.

C. Clustering of routes

After establishing *geo-paths* for the remaining routes by localizing their IP hops, we set out to decide which routes can be considered to be the same and which ones are different in a geographical sense. We make this decision by clustering the geo-paths on a hop-by-hop basis and by defining geodiversity, a mutual metric, between geo-paths. Iterating through all the geo-paths from a given vantage point to a given endpoint, we choose an appropriate cluster for each geo-path: if the geo-path satisfies the geographical equality with all cluster members then it is assigned to that cluster if not, then a new cluster is created for it. At the end, all geo-paths in each cluster are considered to be geographically the same.

Two geo-paths are geographically equal if they are not farther from each other than 50 km: the distance between any of their nodes and the closest one of the straight lines determined by consecutive nodes of the other geo-path is not larger than 50 km. We used the arbitrary threshold of 50 km to reflect a large city's diameter [29]. Note, that this threshold also allows for fiber duct curves in the physical network, alleviating the mismatch between the location of IP-level nodes of `traceroute` measurements and the actual trail of the underlying physical links.

As a demonstrative example, we drew two geo-paths that are grouped in the same cluster in Fig. 1. Those routes differ at the IP-level and their geo-paths are also different, but since the distance (marked with dashed blue line) of the intermediate node of one route from the geo-path of the other route is smaller than 50 km, our clustering algorithm rules the geographic difference between these two routes negligible.



Fig. 1: Route merging example

IV. CALCULATION OF GEOGRAPHIC ROUTE DIVERSITY

Our final step to capture the geographic route diversity is to define and evaluate a Geographic Diversity Index (GDI). We require GDI to produce values to a given route set between a source and destination pair such that multiple geo-paths spanning over large geographical areas get a higher GDI.

A. Requirements

Before describing the computation of GDI in details we highlight the key attributes which make a route set "more" diverse in a geographical sense against an other. Let us assume a source (S) and a target (T) node as endpoints and two "cover" routes S-A-B-C-T (R1) and S-F-G-H-I-T (R3) as shown in Fig. 2¹. Let us assume that nodes are positioned according to their geographic positions. Let us also assume that the GDI for this setting is \hat{r} . Our first goal is to reward higher route count. Therefore a route set with two routes must achieve lower GDI than the same route set extended with another arbitrary route. That is if we add R2 to our theoretical example and obtain \hat{r}_2 as the GDI for this amended route set, then we expect $\hat{r} < \hat{r}_2$. Our second goal is to reward higher geographic distance between routes. Therefore if we modify the route set by reducing the distance between the routes, then the GDI of the new route set must be lower: by replacing R2 with R4

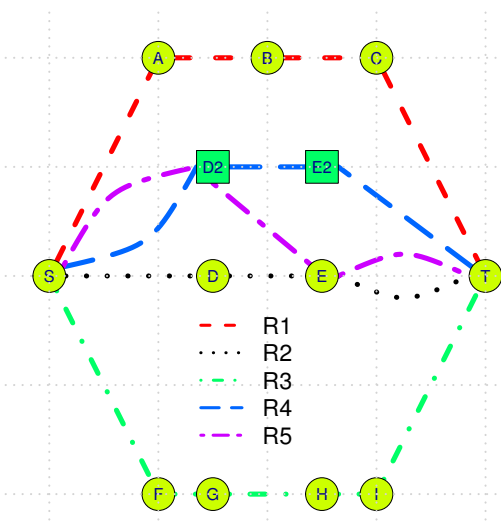


Fig. 2: Geo-diversity example

¹Lines are curved to distinguish different routes using the same link.

(new GDI is \hat{r}_4), we require the GDI to fall. It follows that geo-paths with varying distances (from other routes) increase more the GDI (e.g. R5 and \hat{r}_5) than parallel geo-paths (e.g. R4 and \hat{r}_4) closer than R2. Therefore we require the order between GDI values as:

$$\hat{r} < \hat{r}_4 < \hat{r}_5 < \hat{r}_2 \quad (1)$$

B. Geographic Diversity Index (GDI)

We model geo-paths of Internet routes as collections of sections between their consecutive nodes. Let us assume two routes defined by their nodes: $P = \{a, b, c, d\}$ and $L = \{e, f, g\}$. Naturally, the distance $\delta(a, L)$ between node a and route L translates to the distance between a and the closest point (not necessarily a node) of route L to a . Let $\Delta(P, L) = \{\forall u \in P | \delta(u, L), \forall u \in L | \delta(u, P)\}$ be a vector containing all possible node distances between P and L . In the toy example of Fig. 3 $\Delta(P, L) = \{\delta(a, L), \delta(b, L), \delta(c, L), \delta(d, L), \delta(e, P), \delta(f, P), \delta(g, P)\}$.

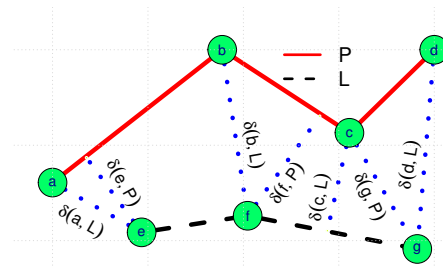


Fig. 3: Distance example

In order to satisfy the requirements listed in Sec. IV-A we define GDI for a given set of routes as follows. First, we define a diversity index between two routes as:

$$d(P, L) = \left(1 - \text{Var}'(\Delta(P, L))\right) \text{Mean}(\Delta(P, L)), \quad (2)$$

where Var' denotes the variance of its arguments normalized to the interval $[0..1]$. Second, we define the diversity between a single route P and a set of routes \mathbb{V} as:

$$\mathcal{D}(P, \mathbb{V}) = \min_{L \in \mathbb{V}} d(P, L) \quad (3)$$

Finally, we quantify the overall GDI for a given set of routes. In order to calculate this, we use a step-by-step method. Let us assume a set \mathbb{V} containing the routes. The process starts from an empty set $\mathbb{U} = \{\}$. In the 0. step we search in set \mathbb{V} for the two routes having the highest diversity score $d_0 = \max_{P, L \in \mathbb{V}} (d(P, L))$ and move paths $\text{argmax}_{P, L \in \mathbb{V}} (d(P, L))$ to \mathbb{U} . In the i -th step we compute $\mathcal{D}_i = \max_{P \in \mathbb{V}} (\mathcal{D}(P, \mathbb{U}))$ and move the path $\text{argmax}_{P \in \mathbb{V}} (\mathcal{D}(P, \mathbb{U}))$ to \mathbb{U} . The process terminates when \mathbb{V} is empty. Finally we compute GDI as:

$$\text{GDI} = d_0 + \sum \mathcal{D}_i. \quad (4)$$

To demonstrate that the proposed method of GDI calculation satisfies the requirements we set, we show the GDIs of the route sets defined in Sec. IV-A (with a grid cell size is ~ 84 km in Fig. 2) in Table I. Note, that the produced GDI values fulfill Eq. 1.

r	2182
\hat{r}_4	3299
\hat{r}_5	3467
\hat{r}_2	3729

TABLE I: GDI values for the geo-diversity example

V. RESULTS

In this section we show the geodiversity results we achieved from the measurement data set. First we show through an illustrative example the difference between the raw `traceroute` outputs and the geographically equivalent routes achievable after applying our route clustering algorithm. Second, we present the compression rates that we were able to attain on the whole measurement set. Finally, we show the GDI results that we calculated for the already clustered route set.

A. An example for route clustering

An example of the results of our route clustering algorithm is shown in Fig. 4. Arcs represent hops between the localized IP nodes obtained from `traceroute` output. Note, that arcs do not indicate a real link trajectories, merely distinguish routes on the same intermediate links. On the left-hand side one can observe all the routes that the `traceroute` measurements yielded between a source node located in Poland and a destination node located in India (Fig. 4a). Between these two hosts there exist 7 different routes on the IP-level, but only 3 geographically different routes, i.e., geo-paths (Fig. 4b).

B. Compression ratio of route counts

Stepping up from one example, here we show the overall results in terms of route clustering on the whole measurement data set. We call the ratio of the number of original routes and the resulting clusters as the geo-compression ratio. In Fig. 5 we plot the empirical distribution of this geo-compression ratio for all source and destination host pairs in our data set.

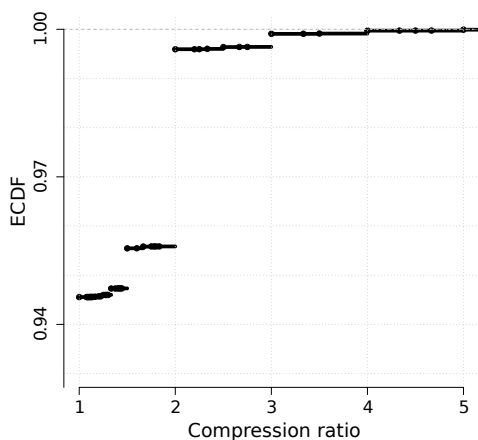


Fig. 5: ECDF of compression ratios for all source-destination pairs

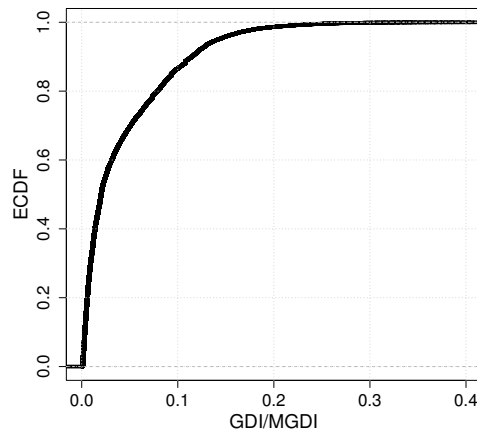


Fig. 6: Geo-diversity results given by GDI/MGDI

The fraction of source-destination pairs for which the route clustering does not decrease the number of geographically equivalent routes is large (around 80%). In these cases the main reason for the poor compression performance is the fact that only one route is yielded by `traceroute`. Another reason, in less significant number of cases, is that the multiple recorded routes run through nodes at exactly the same locations (Sec. III-B). On the remaining 20% of source-destination pairs we applied our clustering algorithm with remarkable results: this is shown in Fig. 5. In more than 4% of the all cases we could obtain a geo-compression ratio higher than 2.

C. Geo-diversity results

Using the GDI metric that we defined in Sec. IV to characterize the geo-diversity of routes between a source and a destination pairs we show how the calculated values compare to the theoretical maximum of the same metric, taking only the number of geographically equivalent routes and the length of the longest one into account (not their actual trajectories). For this hypothetical maximal value, denoted as MGDI, we place a number of routes forming triangle shapes, the longest one reaching to the highest, so that their GDI would be the largest. In Fig. 6 we plot the distribution of the ratios of GDI over MGDI for those source-destination pairs between which we found at least 2 geographically different routes (20% of all pairs, as mentioned above). The results show that for 80% of these cases the GDI of routes is less than 10% of their MGDI, i.e., the theoretically maximum diversity given the number of routes and the length of the longest route.

VI. CONCLUSION

Our goal was to find out where on Earth the packets travel exactly when traffic is carried over the Internet. We discovered that between two given points packet flows are not so scattered as the diversity of `traceroute` results suggest. We actually saw very few host pairs between which more than 1 geographically different routes exist. We showed that 80% of endpoints with

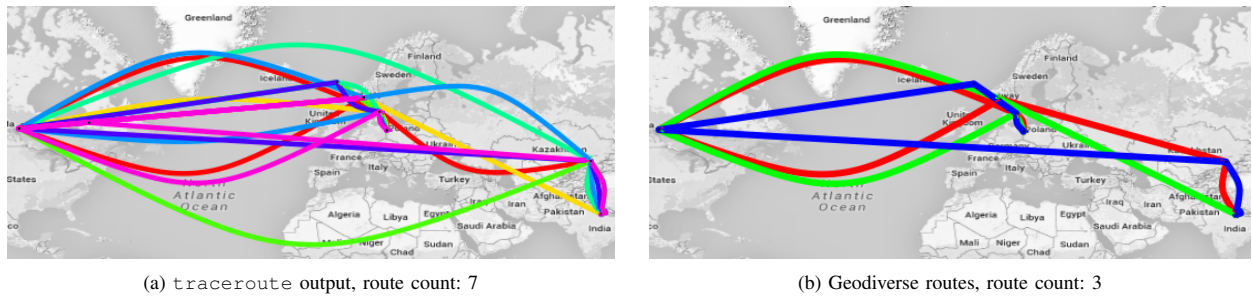


Fig. 4: Route count comparison

more than one route has less than a 10% MGDI value which indicates low diversity in terms of geographic distance. The knowledge we gained from this study about the geographical diversity of Internet routes is useful for several applications. In this section we give a few examples of these, and we discuss the weaknesses of our method.

A. Applications

Estimating bufferbloat: In order to measure Internet delay correctly one must fight many sources of inaccuracy: if one-way latency measurement is possible between two hosts, their clocks must be synchronized, if not, several issues come up: misleading *traceroute* results due to load balancing and MPLS tunnels, different return path of the ICMP_REPLY when using *ping*, etc. Indeed, even if the topology is correctly discovered, many aspects of the actual operation of the network equipment pieces affect the measured delay. In order to somehow infer the impact of bufferbloat from the total delay, a very hot topic nowadays, it is important to have an idea about the propagation delay of the packets. Since the propagation delay is closely related to the traveled geographic distance, the sets of geographically equivalent paths, discovered by our method, provide important input to the analysis of the bufferbloat phenomenon.

Network resilience: Network resilience, in its classical sense, is a well-studied research domain [30]. When network links are not going down individually, but instead are affected en masse due to a regional catastrophe, let it be a natural disaster, a power blackout or an EMP attack, then the geographic topology of the Internet suffers correlated link failures. In order to be ready for this, planning geographic redundancy of Internet paths can use the results of our method as an input.

B. Discussion

After discussing the potential role of our method in various use cases, we turn to the weaknesses of it that we are aware of. First, by applying measurements created by the relatively simple tool *traceroute*, we do not tackle IP-aliasing when building the paths before clustering nodes close-by to each other. One could argue that performing an already documented merging method targeting IP aliases might yield the same result as the geomerging we do. Second, one might question the accuracy of MaxMind, the tool we use to position the nodes. However its accuracy is explored in details in [28] and

in long run measurements, we plan to use active measurement based geolocation tools, such as Spotter [31]. Third, it can be argued that estimating geo-paths using straight lines between IP-level nodes may be misleading. However, our city-sized threshold ensures that as long as there are IP-level nodes in close proximity of fiber ducts' ends, this is avoided with high probability. Finally, the proposed GDI and MGDI metrics might seem simplistic, but we argue that to define a diversity metric between routes, many key attributes must be taken into account, and a trade-off between various features and scenarios must be accepted.

REFERENCES

- [1] M. Pathan *et al.*, *A taxonomy of CDNs*. Springer, 2008.
- [2] M. Castro *et al.*, "Topology-aware routing in structured peer-to-peer overlay networks," in *Future directions in distributed computing*. Springer, 2003.
- [3] E.-K. Lua *et al.*, "A survey and comparison of peer-to-peer overlay network schemes," *IEEE Communications Surveys and Tutorials*, vol. 7, no. 1-4, pp. 72-93, 2005.
- [4] A. Greenberg *et al.*, "The cost of a cloud: research problems in data center networks," *ACM SIGCOMM CCR*, vol. 39, no. 1, pp. 68-73, 2008.
- [5] D. Awduche *et al.*, "Overview and principles of internet traffic engineering," RFC 3272, Tech. Rep., 2002.
- [6] D. Clark *et al.*, "Interconnection in the internet: the policy challenge," in *Research Conference on Communication, Information and Internet Policy*, 2011.
- [7] J. P. Sterbenz, D. Hutchison, E. K. Cetinkaya, A. Jabbar, J. P. Rohrer, M. Schöller, and P. Smith, "Resilience and survivability in communication networks: Strategies, principles, and survey of disciplines," *Computer Networks*, vol. 54, no. 8, pp. 1245-1265, 2010.
- [8] J. P. Sterbenz, E. K. Cetinkaya, M. A. Hameed, A. Jabbar, S. Qian, and J. P. Rohrer, "Evaluation of network resilience, survivability, and disruption tolerance: analysis, topology generation, simulation, and experimentation," *Telecommunication systems*, vol. 52, no. 2, pp. 705-736, 2013.
- [9] J. Rak, *Resilient Routing in Communication Networks*. Springer, Computer Communications and Networks series, 2015.
- [10] C. Kaufman, R. Perlman, and M. Speciner, *Network security: private communication in a public world*. Prentice Hall Press, 2002.
- [11] W. Lou, W. Liu, and Y. Fang, "Spread: Improving network security by multipath routing," in *Military Communications Conference, 2003. MILCOM'03. 2003 IEEE*, vol. 2. IEEE, 2003, pp. 808-813.
- [12] Y. Schwartz *et al.*, "On the diversity, stability and symmetry of end-to-end internet routes," in *INFOCOM Workshops*. IEEE, 2010.
- [13] W. Mühlbauer *et al.*, "Building an AS-topology model that captures route diversity," *ACM SIGCOMM CCR*, vol. 36, no. 4, pp. 195-206, 2006.
- [14] R. Teixeira *et al.*, "In search of path diversity in ISP networks," in *SIGCOMM IMC*. ACM, 2003.
- [15] Y. Shavitt *et al.*, "Geographical internet pop level maps," in *Traffic Monitoring and Analysis*. Springer, 2012, pp. 121-124.
- [16] L. Subramanian *et al.*, "Geographic properties of internet routing," in *Annual Technical Conference*. USENIX, 2002.

[17] M. Zhang, Y. Ruan, V. S. Pai, and J. Rexford, "How dns misnaming distorts internet topology mapping," in *USENIX Annual Technical Conference, General Track*, 2006, pp. 369–374.

[18] S. Laki *et al.*, "A detailed path-latency model for router geolocation," in *TridentCom*. IEEE, 2009. [Online]. Available: http://ieeexplore.ieee.org/xpls/abs_all.jsp?arnumber=4976258

[19] M. Boguná, F. Papadopoulos, and D. Krioukov, "Sustaining the internet with hyperbolic mapping," *Nature Communications*, vol. 1, p. 62, 2010.

[20] Y. Shavitt *et al.*, "A structural approach for PoP geo-location," in *INFOCOM Workshops*. IEEE, 2010.

[21] J. Han *et al.*, "An experimental study of internet path diversity," *IEEE Transactions on Dependable and Secure Computing*, vol. 3, no. 4, pp. 273–288, 2006.

[22] "Geolocation and online fraud prevention from MaxMind," <http://www.maxmind.com/>, accessed: 2014-12-22.

[23] H. V. Madhyastha, T. Isdal, M. Piatek, C. Dixon, T. Anderson, A. Krishnamurthy, and A. Venkataramani, "iplane: An information plane for distributed services," in *Proceedings of the 7th symposium on Operating systems design and implementation*. USENIX Association, 2006, pp. 367–380.

[24] CAIDA, "Macroscopic Internet Topology Data Kit (ITDK)," <http://www.caida.org/data/internet-topology-data-kit>.

[25] B. Chun, D. Culler, T. Roscoe, A. Bavier, L. Peterson, M. Wawrzoniak, and M. Bowman, "Planetlab: an overlay testbed for broad-coverage services," *ACM SIGCOMM Computer Communication Review*, vol. 33, no. 3, pp. 3–12, 2003.

[26] B. Augustin *et al.*, "Avoiding traceroute anomalies with Paris traceroute," in *IMC*. ACM, 2006. [Online]. Available: <http://dl.acm.org/citation.cfm?id=1177100>

[27] S. Laki *et al.*, "Spotter: A model based active geolocation service," in *INFOCOM*. IEEE, 2011. [Online]. Available: http://ieeexplore.ieee.org/xpls/abs_all.jsp?arnumber=5935165

[28] B. Huffaker *et al.*, "Geocompare: a comparison of public and commercial geolocation databases - Technical Report," Cooperative Association for Internet Data Analysis (CAIDA), Tech. Rep., May 2011.

[29] Y. Shavitt and N. Zilberman, "A study of geolocation databases," *CoRR*, vol. abs/1005.5674, 2010. [Online]. Available: <http://arxiv.org/abs/1005.5674>

[30] W. Najjar *et al.*, "Network resilience: a measure of network fault tolerance," *IEEE Transactions on Computers*, vol. 39, no. 2, pp. 174–181, 1990.

[31] P. Mátray *et al.*, "On the spatial properties of internet routes," *Computer Networks*, vol. 56, no. 9, pp. 2237–2248, 2012. [Online]. Available: <http://linkinghub.elsevier.com/retrieve/pii/S1389128612000989>



Attila Csoma Received B.Sc. and M.Sc degree in Informatics at Budapest University of Technology and Economics (BME), Budapest, Hungary in 2010 and 2012 respectively. Since 2012, he is a Ph.D. student at the High Speed Networks Laboratory at the Department of Telecommunications and Media Informatics, BME. He conducts his Ph.D. research on network topology and complex networks. His research interests also include network coding and IoT.



László Toka László Toka is currently a post doc researcher at the Hungarian Academy of Sciences, and works as an assistant professor at the Department of Telecommunications at the Budapest University of Technology and Economics. He received his PhD in 2011 at Telecom Paris, and afterwards worked at Ericsson Research for 3 years before rejoining academia. His main research topics lie within software defined networking, data analytics, and economic modeling of distributed systems.



András Gulyás Received M.Sc. and Ph.D. degree in Informatics at Budapest University of Technology and Economics, Budapest, Hungary in 2002 and 2008 respectively. Currently he is a research fellow at the Department of Telecommunications and Media Informatics. His research interests are complex and self-organizing networks and software defined networking.

Our reviewers in 2015

The quality of a research journal depends largely on its reviewing process and, first of all, on the professional service of its reviewers. It is my pleasure to publish the list of our reviewers in 2015 and would like to express my gratitude to them for their devoted work.

Your Editor-in-Chief

Cedric Adjih

INRIA, France

Özgür B. Akan

Koc University, Turkey

Márton Bérces

Budapest University of Technology and Economics (BME), Hungary

József Bíró

BME, Hungary

János Bitó

BME, Hungary

Gábor Borbély

István Széchenyi University of Győr, Hungary

Vesna Crnojević-Bengin

University of Belgrade, Serbia

Milos Drutarovsky

Technical University of Kosice, Slovakia

Károly Farkas

BME, Hungary

Péter Fazekas

BME, Hungary

Gábor Fehér

BME, Hungary

Győző Gódor

BME, Hungary

László Gyarmati

Qatar Computing Research Institute, HBKU

András Hajdu

University of Debrecen, Hungary

Evangelos Haleplidis

University of Patras, Greece

Thomas Heistracher

Salzburg University of Applied Sciences, Austria

Zhang Hongming

University of Southampton, UK

Jukka Huhtamäki

Tampere University, Finland

Andrea Huszti

University of Debrecen, Hungary

Ebroul Izgueirdo

Queen Mary University of London, UK

Chirag Jain

Drexel University, USA

Frantisek Jakab

University of Kosice, Slovakia

Zoltán Jakó

BME, Hungary

Dóra Maros

Óbuda University, Budapest, Hungary

Vaclav Matyas Masaryk

University, Brno, Czech Republic

Vjekoslav Matic

Infineon, Croatia

Miklós Máté

BME, Hungary

Zeljka Mihajlovic

University of Zagreb, Croatia

Ádám Knapp

BME, Hungary

Caglar Koca

Koc University, Turkey

Ivan Korobko

Technical University of Sofia, Bulgaria

Imre Lendák

University of Novi Sad, Serbia

Lajos Nagy

BME, Hungary

Szilvia Nagy

István Széchenyi University of Győr, Hungary

Mehdi Nikkhah

Drexel University, USA

Ossi Nykanen

Tampere University, Finland

Péter Odry

University of Subotica, Serbia

István Oniga

University of Debrecen, Hungary

Géza Paksy

BME, Hungary

László Pap

BME, Hungary

Ármin Petkovics

BME, Hungary

Joan Lluís Pijoan

Ramon Llull University, Barcelona, Spain

Michał Piore

Warsaw University of Technology, Poland and Lund University, Sweden

Gyula Simon

University of Veszprém, Hungary

Marek Sys

Masaryk University, Brno, Czech Republic

Ta Vinh Tong

University of Central Lancashire, UK

János Tóth

University of Debrecen, Hungary

Eszter Udvary

BME, Hungary

Lóránt Vajda

BME, Hungary

Rolland Vida

BME, Hungary

László Zömbik

Ericsson Research, Budapest, Hungary

BME* Budapest University of Technology and Economics



39th INTERNATIONAL CONFERENCE ON TELECOMMUNICATIONS AND SIGNAL PROCESSING

June 27-29, 2016, Vienna, Austria



The 2016 39th International Conference on Telecommunications and Signal Processing (TSP) will be held during **June 27-29, 2016** in **Vienna, Austria**. In cooperation with the IEEE Austria Section, IEEE Czechoslovakia Section, IEEE Czechoslovakia Section SP/CAS/COM Joint Chapter, and IEEE Croatia Section Communications Chapter, it is organized by twelve European universities from Austria, Bulgaria, Croatia, Czech Republic, Hungary, Poland, Romania, Slovak Republic, Slovenia, and Turkey, for academics, researchers, and developers and it serves as a forum to promote the exchange of the latest advances in telecommunication technology and signal processing. The aim of the TSP 2016 Conference is to bring together both novice and experienced scientists, developers, and specialists, to meet new colleagues, collect new ideas, and establish new cooperation between research groups from universities, research centers, and private sectors.

TOPICS

Telecommunications:

- Information Systems
- Network Services
- Network Technologies
- Telecommunication Systems
- Modelling, Simulation and Measurement

Signal Processing:

- Analog Signal Processing
- Audio, Speech and Language Processing
- Biomedical Signal Processing
- Digital Signal Processing
- Image and Video Signal Processing

PROCEEDINGS

All accepted papers will be published in the TSP 2016 Conference Proceedings issued on USB drive. The Proceedings with presented papers will be submitted for indexing in all relevant databases.

INDEXED BY



IMPORTANT DATES

Paper Submission: February 15, 2016
Notification of Acceptance: April 5, 2016
Authors' Registration: May 15, 2016

CONTACTS

E-mail: tsp@feec.vutbr.cz
Web: <http://tsp.vutbr.cz/>

ORGANIZERS



FOLLOW US





SPECOM 2016

18th International Conference on Speech and Computer
August 23-27, 2016 | Budapest, Hungary

PROGRAMME COMMITTEE

Rodmonga Potapova
Moscow State Linguistic University, Russia
General Conference Co-Chair

Andrey Ronzhin
SPIIRAS, Saint-Petersburg, Russia,
General Conference Co-Chair

Géza Németh
Budapest University of Technology and Economics, Hungary
Organising Committee Chair

Etienne Barnard, North-West University, South Africa
Laurent Besacier, Laboratory of Informatics of Grenoble, France

Vlado Delic, University of Novi Sad, Serbia
Olivier Deroo, Acapela Group, Belgium
Christoph Draxler, Institute of Phonetics and Speech Communication, Germany

Thierry Dutoit, University of Mons, Belgium
Nikos Fakotakis, University of Patras, Greece
Peter French, University of York, UK
Hiroya Fujisaki, University of Tokyo, Japan
Todor Ganchev, Technical University of Varna, Bulgaria
Ruediger Hoffmann, Dresden University of Technology, Germany

Oliver Jokisch, Leipzig University of Telecommunication, Germany
Slobodan Jovicic, University of Belgrade, Serbia
Dimitri Kanevsky, IBM Thomas J. Watson Research Center, USA

Alexey Karpov, SPIIRAS, Saint-Petersburg, Russia
Heysem Kaya, Bogazici University, Turkey
Irina Kipyatkova, SPIIRAS, Russia
Daniil Kocharov, St. Petersburg State University, Russia
George Kokkinakis, University of Patras, Greece
Steven Krauwer, Utrecht University, The Netherlands
Lin-shan Lee, National Taiwan University, Taiwan
Boris Lobanov, United Institute of Informatics Problems, Belarus

Elena Lyakso, St. Petersburg State University, Russia
Konstantin Markov, The University of Aizu, Japan
Yuri Matveev, ITMO University, Russia
Péter Mihálik, Budapest University of Technology and Economics, Hungary
Konstantinos Moustakas, University of Patras, Greece
Iosif Mporas, University of Patras, Greece
Heinrich Niemann, University of Erlangen-Nuremberg, Germany

Alexander Petrovsky, Belarusian State University of Informatics and Radioelectronics, Belarus
Dimitar Popov, Bologna University, Italy
Elias Potamitis, University of Patras, Greece
Lawrence Rabiner, Rutgers University, USA
Gerhard Rigoll, Munich University of Technology, Germany
Murat Saraclar, Bogazici University, Turkey
Jesus Savage, University of Mexico, Mexico
Tanja Schultz, University of Karlsruhe, Germany
Milan Secujski, University of Novi Sad, Serbia
Pavel Skrelin, St. Petersburg State University, Russia
Viktor Sorokin, Institute for Information Transmission Problems, Russia

Yannis Stylianou, University of Crete, Greece
György Szaszák, Budapest University of Technology and Economics, Hungary
Klára Vicsi, Budapest University of Technology and Economics, Hungary
Christian Wellekens, EURECOM, France
Csaba Zainkó, Budapest University of Technology and Economics, Hungary
Milos Zelezny, University of West Bohemia, Czech Republic



THE CONFERENCE

The International Conference on Speech and Computer – SPECOM is a regular event organized since 1996 and attracts researchers in the area of computer speech processing, multimodal interfaces and applied systems for telecommunication, robotics, intelligent and cyberphysical environments.

ORGANIZERS

The conference is organized by Budapest University of Technology and Economics (Budapest, Hungary) and Scientific Association for Infocommunications (HTE, Hungary), in cooperation with **Moscow State Linguistic University (MSLU, Moscow, Russia)**, **St. Petersburg Institute for Informatics and Automation of the Russian Academy of Science (SPIIRAS, St. Petersburg, Russia)** and **St. Petersburg National Research University of Information Technologies, Mechanics and Optics (ITMO University, St. Petersburg, Russia)**

TOPICS

The SPECOM conference is devoted to issues of human-machine interaction, particularly:

- Applications for human-computer interaction
- Audio-visual speech processing
- Automatic language identification
- Corpus linguistics and linguistic processing
- Forensic speech investigations and security systems
- Multichannel signal processing
- Multimedia processing
- Multimodal analysis and synthesis
- Signal processing and feature extraction
- Speaker identification and diarization
- Speaker verification systems
- Speech and language resources
- Speech analytics and audio mining
- Speech dereverberation
- Speech driving systems in robotics
- Speech enhancement
- Speech perception and speech disorders
- Speech recognition and understanding
- Speech translation automatic systems
- Spoken dialogue systems
- Spoken language processing
- Text-to-speech and Speech-to-text systems
- Virtual and augmented reality

FORMAT OF THE CONFERENCE

The conference program will include presentation of invited papers, oral presentations, and poster/demonstration sessions. Papers will be presented in plenary or topic oriented sessions.

Details about the social events will be available on the web page.

SUBMISSION OF PAPERS

Authors are invited to submit a full paper not exceeding 8 pages formatted in the LNCS style (see below). Those accepted will be presented either orally or as posters. The decision on the presentation format will be based upon the recommendation of three independent reviewers. The authors are asked to submit their papers using the on-line submission form accessible from the conference web site.

Papers submitted to SPECOM 2016 must not be under review by any other conference or publication during the SPECOM review cycle, and must not be previously published or accepted for publication elsewhere.

The paper format for the review has to be the PDF file with all required fonts included. Upon notification of acceptance, speakers will receive further information on submitting their camera-ready and electronic sources (for detailed instructions on the final paper format see <http://www.springer.com/computer/lncs?SGWID=0-164-6-793341-0>).

PROCEEDINGS

SPECOM Proceedings will be published by Springer as a book in the Lecture Notes in Artificial Intelligence (LNAI) series listed in all major citation databases such as DBLP, SCOPUS, EI, INSPEC, COMPENDEX. SPECOM Proceedings are included in the list of forthcoming proceedings for August 2016.

IMPORTANT DATES

- | | |
|--------------------|--|
| April 15, 2016 | Submission of full papers |
| May 15, 2016 | Notification of acceptance |
| June 01, 2016 | Final papers (camera ready) and registration |
| August 23-27, 2016 | Conference date |

The contributions to the conference will be published in proceedings that will be made available to participants at the time of the conference.

VENUE

The conference will be organized in at the campus of Budapest University of Technology and Economics, Budapest, Hungary (<http://www.bme.hu>).

Budapest, "the pearl of the Danube" is one of the truly historic European capitals with its past stretching back over one thousand years. The picturesque bridges spanning the river Danube, the Castle Hill, the churches and architecture, the sculptures, the wooded hills, the Hungarian cuisine and wine, and the warm hospitality of Hungarian people all ensure that no guest can leave here without longing to return.

ACCOMMODATION

The organising committee has arranged accommodation for reasonable prices in hotels, which are situated near the city center. The rooms with sufficient discount are reserved for the conference days.

CONTACT

All correspondence regarding the conference should be addressed to:

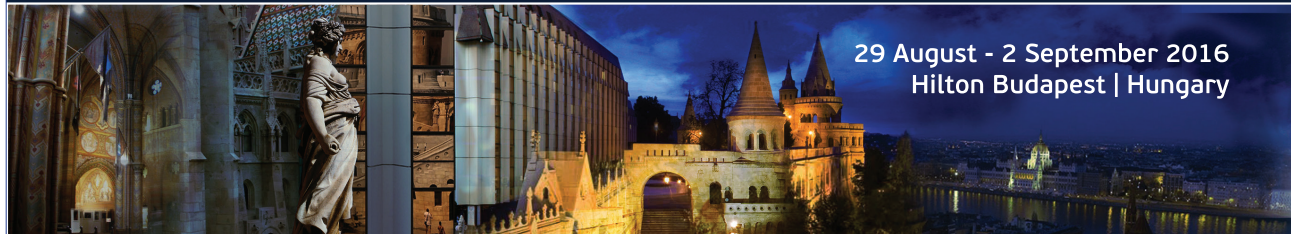
SPECOM 2016 Secretariat

Scientific Association for Infocommunications, HTE, Hungary
E-mail: specom@hte.hu
Phone: +36 1 353 1027

SPECOM 2016 conference web site: <http://www.hte.hu/specom2016>

EUSIPCO2016

EUROPEAN SIGNAL PROCESSING CONFERENCE



29 August - 2 September 2016
Hilton Budapest | Hungary

CALL FOR PAPERS

General Chair

Lajos Hanzo
University of Southampton, UK

Technical Co-Chairs

Andrea Conti
University of Ferrara, Italy
Saeid Sanei
University of Surrey, UK

Plenary Sessions Chair

Gerhard Bauch
TU Hamburg-Harburg, Germany

Tutorial Sessions Co-Chairs

Pier Luigi Draghotti
Imperial College London, UK
Gan Woon-Seng
Nanyang Technological University, Singapore

Special Sessions Chair

Alberto Rabbachin
European Commission

Operations Chair

Rolland Vida
Budapest Univ. of Tech. and Econ., Hungary

Publication Chair

Peter Müller
IBM Zurich, Switzerland

Student Activities

Tommaso Melodia
Northeastern University, USA

International Liaisons

Chong-Yung Chi
National Tsing Hua Univ., Taiwan

Moeness Amin
Villanova University, USA

Local Arrangements Chair

Nandor Matrai
Asszisztencia, Hungary

Finance Chair

Peter Nagy
HTE, Hungary



The 2016 European Signal Processing Conference will be held in the vibrant city of Budapest, Hungary from 29 August – 02 September 2016. This flagship conference of the European Association for Signal Processing (EURASIP, www.eurasip.org) will feature a comprehensive technical program addressing all the latest developments in research and technology for signal processing. EUSIPCO 2016 will feature world-class speakers, oral and poster sessions, keynotes, exhibitions, demonstrations and tutorials and is expected to attract many leading researchers and industry figures from all over the world.

TECHNICAL SCOPE

The focus will be on signal processing theory, algorithms, and applications. We invite the submission of original, unpublished technical papers on topics including but not limited to:

- ▶ Audio and acoustic signal processing
- ▶ Speech processing
- ▶ Language processing
- ▶ Image and video processing
- ▶ Multimedia signal processing
- ▶ Signal processing theory and methods
- ▶ Sensor array, multichannel and communications signal processing
- ▶ Radar and sonar array signal processing
- ▶ Estimation theory and applications
- ▶ Nonlinear signal processing and adaptive filters
- ▶ Cooperative networking
- ▶ Compressive sensing, dictionary learning, and sparse reconstruction
- ▶ Machine learning
- ▶ Signal processing for education
- ▶ Design and implementation of signal processing systems
- ▶ Information forensics and security
- ▶ Bio-inspired modelling and signal processing
- ▶ Medical image and signal processing
- ▶ Signal processing applications
- ▶ Signal processing for Quantum

Accepted papers will be included in IEEE Xplore®.

IMPORTANT DATES

- Special session proposals: **15th December 2015**
- Tutorial proposals: **8th February 2016**
- Full paper submissions: **8th February 2016**
- Notification of acceptance: **25th May 2016**
- Camera-ready papers: **17th June 2016**

Full details of submission procedures are available at <http://www.eusipco2016.org>

Guidelines for our Authors

Format of the manuscripts

Original manuscripts and final versions of papers should be submitted in IEEE format according to the formatting instructions available on

http://www.ieee.org/publications_standards/publications/authors/authors_journals.html#sect2,

“Template and Instructions on How to Create Your Paper”.

Length of the manuscripts

The length of papers in the aforementioned format should be 6-8 journal pages.

Wherever appropriate, include 1-2 figures or tables per journal page.

Paper structure

Papers should follow the standard structure, consisting of *Introduction* (the part of paper numbered by “1”), and *Conclusion* (the last numbered part) and several *Sections* in between.

The Introduction should introduce the topic, tell why the subject of the paper is important, summarize the state of the art with references to existing works and underline the main innovative results of the paper. The Introduction should conclude with outlining the structure of the paper.

Accompanying parts

Papers should be accompanied by an *Abstract* and a few *index terms (Keywords)*. For the final version of accepted papers, please send the *short cvs* and *photos* of the authors as well.

Authors

In the title of the paper, authors are listed in the order given in the submitted manuscript. Their full affiliations and e-mail addresses will be given in a footnote on the first page as shown in the template. No degrees or other titles of the authors are given. Memberships of IEEE, HTE and other professional societies will be indicated so please supply this information. When submitting the manuscript, one of the authors should be indicated as corresponding author providing his/her postal address, fax number and telephone number for eventual correspondence and communication with the Editorial Board.

References

References should be listed at the end of the paper in the IEEE format, see below:

- a) Last name of author or authors and first name or initials, or name of organization
- b) Title of article in quotation marks
- c) Title of periodical in full and set in italics
- d) Volume, number, and, if available, part
- e) First and last pages of article
- f) Date of issue

[11] Boggs, S.A. and Fujimoto, N., “Techniques and instrumentation for measurement of transients in gas-insulated switchgear,” *IEEE Transactions on Electrical Installation*, vol. ET-19, no. 2, pp.87–92, April 1984.

Format of a book reference:

[26] Peck, R.B., Hanson, W.E., and Thornburn, T.H., *Foundation Engineering*, 2nd ed. New York: McGraw-Hill, 1972, pp.230–292.

All references should be referred by the corresponding numbers in the text.

Figures

Figures should be black-and-white, clear, and drawn by the authors. Do not use figures or pictures downloaded from the Internet. Figures and pictures should be submitted also as separate files. Captions are obligatory. Within the text, references should be made by figure numbers, e.g. “see Fig. 2.”

When using figures from other printed materials, exact references and note on copyright should be included. Obtaining the copyright is the responsibility of authors.

Contact address

Authors are requested to send their manuscripts via electronic mail or on an electronic medium such as a CD by mail to the Editor-in-Chief:

Csaba A. Szabo
 Department of Networked Systems and Services
 Budapest University of Technology and Economics
 2 Magyar Tudosok krt.
 Budapest, 1117 Hungary
 szabo@hit.bme.hu



LEGRAND

UNINTERRUPTED POWER SUPPLIES

Redundant modular systems:

- Single phase modular ups's in tower and rack version with unique architecture. Expandable power and backup time without external accessories.
- Three-phase, expandable modular ups's with a unique, single phase redundant architecture. Configurable in/out phases: 3:3, 3:1, 1:1, 1:3.

Stand-alone systems:

- Wide range of line interactive and online double-conversion products in tower and rack version
- Wide range of three-phase online double conversion devices upto 800kVA.

The range of the products contains network interfaces, softwares and licenses. Please visit the webpage of Legrand (www.legrand.hu) or call Legrand Technical Assistance for further information.

Legrand Technical Assistance: 06-80/204-186

THE GLOBAL SPECIALIST
IN ELECTRICAL AND DIGITAL BUILDING INFRASTRUCTURE



 **legrand**[®]

SCIENTIFIC ASSOCIATION FOR INFOCOMMUNICATIONS



Who we are

Founded in 1949, the Scientific Association for Infocommunications (formerly known as Scientific Society for Telecommunications) is a voluntary and autonomous professional society of engineers and economists, researchers and businessmen, managers and educational, regulatory and other professionals working in the fields of telecommunications, broadcasting, electronics, information and media technologies in Hungary.

Besides its 1000 individual members, the Scientific Association for Infocommunications (in Hungarian: HÍRKÖZLÉSI ÉS INFORMATIKAI TUDOMÁNYOS EGYESÜLET, HTE) has more than 60 corporate members as well. Among them there are large companies and small-and-medium enterprises with industrial, trade, service-providing, research and development activities, as well as educational institutions and research centers.

HTE is a Sister Society of the Institute of Electrical and Electronics Engineers, Inc. (IEEE) and the IEEE Communications Society.

What we do

HTE has a broad range of activities that aim to promote the convergence of information and communication technologies and the deployment of synergic applications and services, to broaden the knowledge and skills of our members, to facilitate the exchange of ideas and experiences, as well as to integrate and

harmonize the professional opinions and standpoints derived from various group interests and market dynamics.

To achieve these goals, we...

- contribute to the analysis of technical, economic, and social questions related to our field of competence, and forward the synthesized opinion of our experts to scientific, legislative, industrial and educational organizations and institutions;
- follow the national and international trends and results related to our field of competence, foster the professional and business relations between foreign and Hungarian companies and institutes;
- organize an extensive range of lectures, seminars, debates, conferences, exhibitions, company presentations, and club events in order to transfer and deploy scientific, technical and economic knowledge and skills;
- promote professional secondary and higher education and take active part in the development of professional education, teaching and training;
- establish and maintain relations with other domestic and foreign fellow associations, IEEE sister societies;
- award prizes for outstanding scientific, educational, managerial, commercial and/or societal activities and achievements in the fields of infocommunication.

Contact information

President: **GÁBOR MAGYAR, PhD** • elnok@hte.hu

Secretary-General: **ISTVÁN BARTOLITS** • bartolits@nmhh.hu

Operations Director: **PÉTER NAGY** • nagy.peter@hte.hu

International Affairs: **ROLLAND VIDA, PhD** • vida@tmit.bme.hu

Address: H-1051 Budapest, Bajcsy-Zsilinszky str. 12, HUNGARY, Room: 502

Phone: +36 1 353 1027, Fax: +36 1 353 0451

E-mail: info@hte.hu, Web: www.hte.hu